Dissertation

submitted to the
Combined Faculties for the Natural Sciences and for Mathematics
of the Ruperto-Carola University of Heidelberg, Germany
for the degree of

Doctor of Natural Sciences

presented by

Julian David Langer, Diplom-Chemiker
born in Heidelberg

Oral examination: .

Conformational dynamics of coatomer: functional and structural studies.

Referees: Prof. Dr. Felix Wieland

Prof. Dr. Irmgard Sinning

Table of contents

Abstract

In my PhD thesis I have investigated molecular mechanisms in the biogenesis of membrane vesicles.

Formation of transport vesicles involves polymerization of cytoplasmic coat proteins. In COPI vesicle biogenesis, the heptameric complex coatomer is recruited to donor membranes by the interaction of multiple coatomer subunits with the budding machinery. Specific binding to the trunk domain of coatomer's subunit γ-COP of the Golgi membrane protein p23 induces a conformational change in the γ-subunit, leading to polymerization of the complex in vitro.

Using a combination of biochemical assays and an assay based on single-molecule, single-pair fluorescence resonance energy transfer, we find that this conformational change is only induced by dimers of the p24-family proteins p23 and p24, and neither by the other p24-family members nor by cargo proteins. This conformational change takes place in individual coatomer complexes, independent of each other, and the rearrangement induced in γ-COP is transmitted within the complex to its α-subunit. α-COP is one of coatomer's subunits capable of binding to dibasic cargo motifs, and also shows analogy to the Clathrin molecule. We propose a model in which capture of membrane protein machinery triggers cage formation in the COPI system.

At the nanometer resolution I started investigating the structure of the lattice of conformationally changed coatomer on COPI vesicles generated in vitro from purified Golgi membranes and coating machinery, using cryo electron tomography. Initial data on coated vesicles and coated buds is presented.

Zusammenfassung

In meiner Doktorarbeit habe ich die molekularen Mechanismen der Biogenese von COPI-Vesikeln untersucht.

Der Transport von Proteinen und Membranen in einer eukaryotischen Zelle erfolgt über vesikuläre Träger. Zur Bildung dieser Vesikel polymerisieren Hüllproteine, die sowohl in einer löslichen, cytosolischen Form als auch in einer membrangebundenen Form vorliegen. In der Biogenese eines COPI Vesikels bindet der heptamere Hüllkomplex Coatomer an die Donormemrbanen über multiple Interaktionen mit der Maschinerie zur Abknospung der Vesikel. Die Interaktion der γ-Untereinheit von Coatomer (γ-COP) mit dem transmembran-Protein p23 induziert einen Konformationswechsel in γ-COP, der zur Polymerisation des Komplexes in vitro führt.

In dieser Arbeit wurden biochemische und biophysikalische Methoden verwendet, um diesen Konformationswechsel in Coatomer zu untersuchen. Dabei wurde ein Verfahren zur Untersuchung der Konformation individueller Coatomer-Komplexe mit Einzelmolekül-Fluoreszenz-Resonanz-Energie-Transfer etabliert. Der beschriebene Konformationswechsel in γ-COP wird nur durch dimere der Proteine p23 und p24 induziert, und nicht durch andere Mitglieder der p24-Familie oder Frachtproteine. Er findet in einzelnen Coatomer-Komplexen statt, und wird in die periphere Untereinheit α-COP weitergeleitet. α-COP ist eine der beiden Untereinheiten von Coatomer, die Frachtmoleküle mit dibasischen Signalsequenzen binden; zudem zeigt α-COP Analogien zu Clathrin über α-solenoide und β-Propeller-Domänen. In dieser Arbeit wird ein Modell vorgeschlagen, in dem die Bindung von spezifischen Transmembranproteinen die Polymerisierung der Hüllproteine und die Ausbildung der COPI-Vesikelhülle induziert.

In einem zweiten Projekt wurde die Struktur von Coatomer in der COPI-Hülle auf in vitro generierten COPI Vesikeln durch cryo-Elektronenmikroskopie und Tomographie untersucht. Erste tomographische Rekonstruktionen von Vesikeln und COPI-Knospen an Donormembranen werden gezeigt.

Abbreviations

AA (aa)	Amino Acids
AP	Adaptor protein
APD	Avalanche photo diode
APS	Ammonium persulfate
Arf	ADP-ribosylation factor
ATP	Adenosin tri-phosphate
BFA	Brefeldin A
BSA	Bovine serum albumin
COP	Coat protein
DMMA	Dimethylmaleic acid anhydride
DMSO	Dimethyl sulfoxide
DNA	Desoxyribonucleic acid
DTT	Dithiothreitol
E_{App}	Approximated energy transfer efficiency
EDTA	Ethylendiaminetetra-acetic acid
ER	Endoplasmic reticulum
ERGIC	ER-Golgi intermediate compartment
FRET	Fluorescence Resonance Energy Transfer
GAP	GTPase activating protein
GDP	Guanosine diphosphate
GEF	Guanosine nucleotide exchange factor
GST	Glutathione-S-transferase
GTP	Guanosine tri-phosphate
h	hour
Hepes	4-(2-hydroxyethyl)-1-piperazin-ethansulfonic acid
HPLC	High pressure liquid chromatography
HRP	Horse radish peroxidase
IgG	Immunoglobulin class G
IMAC	Immobilized metal affinity chromatography
IP	Immunoprecipitation
IPTG	Isopropyl-1-thio-β-D-galactopyranoside
K_D	Dissociation constant
kDa	kilo-Dalton
kHz	kilo-Hertz
MALDI	Matrix assisted laser desorption/ionization
min	minute
NP-40	Nonidet® P40 (Nonylphenylpolyethylene glycol)
nt	Nucleotides
OD	Optical density
PBS	Phosphate buffer saline
PBS-T	Phosphate buffer saline + Tween 20
PCR	Polymerase chain reaction
PMSF	Phenylmethulsulfonyl fluoride
PVDF	Polyvinyldifluoride
rpm	Revolutions per minute
s	second
SDS-PAGE	Sodium dodecyl sulfate-polyacrylamide gel electrophoresis
SNARE	Soluble N-ethylmaleimide sensitive factor attachment protein receptor
TCA	Trichloroacetic acid
TEMED	N, N, N', N'-Tetramethylethylenediamine
TGN	Trans Golgi network
TMB	Tetramethylbenzidin
wt	wild type

List of figures

List of tables

Declaration of primary authorship

I hereby declare that I have completed this thesis independently and without any assistance from third parties. Furthermore, I confirm that no sources have been used in the preparation of this manuscript other than those indicated in the thesis itself.

Heidelberg, 28. 07. 2008

1. Introduction

Eukaryotic cells are highly specialized and compartimentalized systems, generating different intracellular micro-environments. By their individual protein and lipid composition, each compartment allows for specific, characteristic reactions (i.e. disulfide bond formation, glycosylation or protein degradation). These compartments ("organelles") have to continuously exchange proteins and lipids to maintain the specific composition required for the individual reactions, in order to both replenish lipids, proteins and substrates required for the reaction, and to transport products to their destination within or outside the cell. The bulk of this cargo is transported via small vesicles with a diameter of 60-100nm.

1.1. The Secretory Pathway

In Eukaryotic cells, the majority of the proteins synthesized in the Endoplasmic Reticulum is transported to their respective destinations via an intracellular route comprising several organelles (Figure 1). This pathway, termed the Secretory Pathway, was described first in exocrine pancreatic cells (Caro and Palade, 1964).

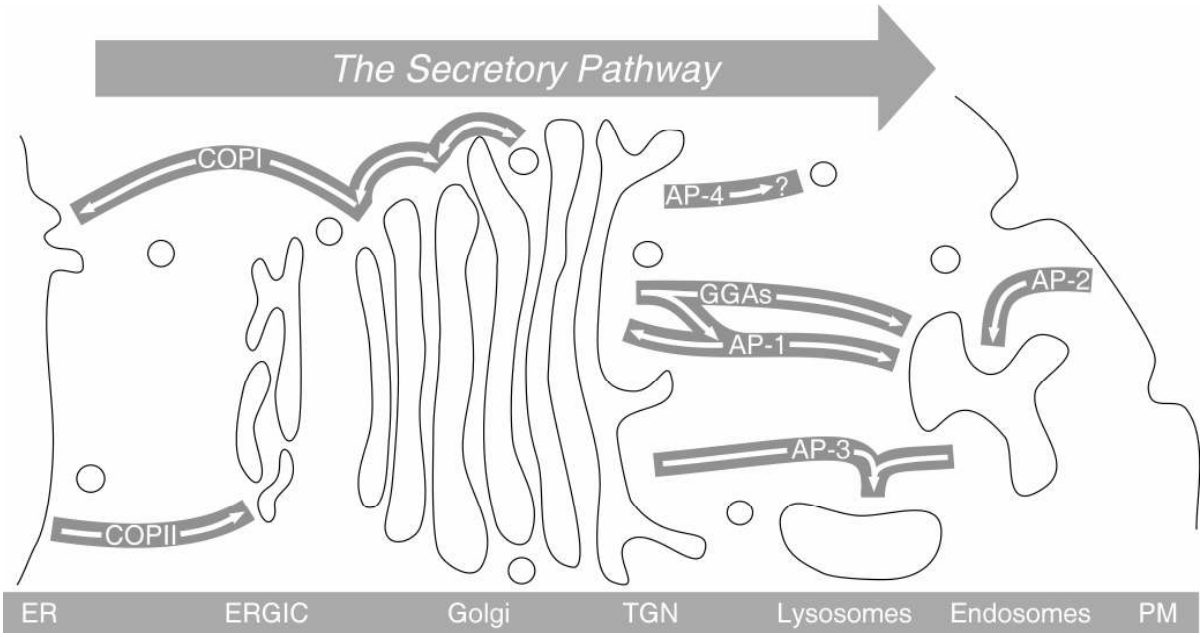

Figure 1: Schematic representation of the Secretory Pathway. Some of the pathways indicated are still under debate.

Unlike cytosolic proteins or proteins targeted to compartments like the nucleus or mitochondria, proteins transported along the Secretory Pathway bear distinct signal sequences, targeting them initially to the ER (Blobel and Dobberstein, 1975a; Blobel and

Dobberstein, 1975b). They are comprised of secreted proteins, lysosomal/vacuolar proteins and membrane proteins. During their transition through the Secretory Pathway leading to their respective destinations, these proteins also undergo post-translational modifications (i.e. disulfide bond formation (Freedman, 1989), N-glycosylation (Kornfeld and Kornfeld, 1985), prolin-hydroxylation and attachment of GPI-anchors (Caras and Weddell, 1989)).

Proteins that travel along the Secretory Pathway begin their journey in the ER. As soon as the nascent protein chain bearing the signal sequence leaves the ribosome, further translation is arrested (Walter and Blobel, 1981a; Walter and Blobel, 1981b; Walter et al., 1981). The signal sequence then binds to the signal recognition particle (SRP), and this complex, in turn, binds to the ER-bound SRP receptor (Ganoth et al., 1988; Gilmore et al., 1982a; Gilmore et al., 1982b; Walter and Blobel, 1980). Here, translocation through the ER membrane is mediated by the "translocon", a trimeric protein complex comprising the proteins Sec61$\alpha/\beta/\gamma$ (Deshaies et al., 1991; Deshaies and Schekman, 1989).
In the ER, two independent housekeeping systems exist that target un- and misfolded proteins (Friedlander et al., 2000; Travers et al., 2000): The unfolded-protein-response-system (UPR) and the ER-associated-degradation-system (ERAD). Proteins identified as un- or misfolded (for example by free thiol groups or incorrect N-glycosylations) are re-translocated into the cytoplasm (Plemper and Wolf, 1999), polyubiquitinated (Hershko et al., 1979) and subjected to proteasome-mediated proteolysis (Haass and Kloetzel, 1989).

Proteins that have successfully folded and have passed ER quality control are exported from the ER by COPII vesicles (Barlowe et al., 1994). The COPII coat is comprised of the small GTPase Sar1p, that governs the coating process by its nucleotide state, and the coating protein complexes Sec23/24 and Sec13/31 (Salama et al., 1993), that sequentially bind to Sar1p once it has been activated by GDP-to-GTP exchange on the donor membrane to form the COPII coat (see also: 1.2.2. COPII-coated vesicles).
Two classes of proteins transported via COPII vesicles have been characterized: First, membrane proteins with exposed, cytosolic domains that typically bear diacidic (DxE) or diaromatic signal sequences have been identified (Barlowe, 2003). Both motifs bind to one member of the cytosolic coating protein complex Sec24 on two distinct sites (Miller et al., 2003; Mossessova et al., 2003). The second class of cargo proteins is comprised of soluble cargo proteins and GPI-anchored proteins that cannot access the cytosolic coating machinery. Two different models describing anterograde transport are currently discussed: The bulk-flow model and the receptor-induced-transport model.
In the bulk-flow model, no signal sequences are required for uptake of these proteins into COPII vesicles, and all soluble proteins are transported from the ER to the Golgi. Proteins

destined for the ER bear distinct ER-retrieval signals that allow them to recycle to the ER via COPI-mediated transport (Karrenbauer et al., 1990; Wieland et al., 1987). This model was supported by studies analysing the secretion rate of glycosylated acyltripeptides (Wieland et al., 1987) and that of amylase and chymotrypsinogen by quantitative EM (Martinez-Menarguez et al., 1999).

The receptor-induced-transport model postulates binding of soluble, lumenal cargo proteins to transmembrane receptors as a key step in ER-to-Golgi transport. These transmembrane receptors would, in turn, via their cytoplasmic domains, bind to the COPII machinery and sort cargo into the vesicles. Supporting this hypothesis, deletion of the yeast membrane protein Erv29 resulted in reduced uptake of the soluble pheromone α-factor into COPII vesicles (Malkus et al., 2002). However, direct interaction of soluble cargo with a transmembrane receptor has not been proven to date.

On their route to the Golgi, proteins exiting the ER pass through the ERGIC (ER-Golgi Intermediate Compartment) that is defined by the presence of the protein ERGIC-53 (Hauri et al., 2000). It is yet unclear if the ERGIC is formed by homotypic fusion of COPII vesicles or if it is a distinct compartment that binds COPII vesicles by heterotypic fusion (Bannykh and Balch, 1998; Bannykh et al., 1998). The ERGIC presumably acts as an interface between COPII- and COPI-mediated transport, as it can be decorated with markers specific for both COPII and COPI (Scales et al., 1997). These markers localize to distinct regions: Those that can be decorated with markers for proteins cycling between the ER and the Golgi and for COPI, and regions that can be decorated with markers for secreted proteins. Thus, the ERGIC has been put forward as the location where the first sorting steps take place (Martinez-Menarguez et al., 1999). This hypothesis was further strengthened by in vivo studies showing a differential behaviour of ERGIC-53 and anterograde cargo (Ben-Tekaya et al., 2005). Transport from the ERGIC to the Golgi is COPI-independent, as structures with anterograde cargo leaving the ERGIC are both negative for COPI (Martinez-Menarguez et al., 1999) and are significantly larger than typical COPI vesicles (Presley et al., 1997; Scales et al., 1997).

The next step for proteins in the Secretory Pathway consists of intra-Golgi transport from the cis-side to the trans-side. In eukaryotic cells, a Golgi stack consists of four to six cisternae, that differ in both protein and lipid composition, and form a gradient from the cis-side (the entry point from the ERGIC), the cis-Golgi-network (Rambourg and Clermont, 1990) to the trans side, the trans-Golgi-network (Griffiths and Simons, 1986).

Transport within the Golgi is mediated by COPI vesicles. The coating process is, again, governed by a small GTPase, Arf1. The proteinous coat of COPI vesicles is formed by the heptameric protein complex coatomer that is recruited to the donor membrane en bloc (see

also: 1.2.3. COPI-coated vesicles, (Hara-Kuge et al., 1994)). COPI vesicles mediate transport in both the anterograde and in the retrograde direction within the Golgi, and take up proteins bearing specific ER-retrieval signals (Cosson and Letourneur, 1994; Letourneur et al., 1994), and transfer them back to the ER. Thus, in contrast to COPII vesicles, that transfer cargo in an anterograde direction only, COPI vesicles mediate bidirectional transport (Orci et al., 1997; Pelham and Rothman, 2000).

Two of coatomer's subunits, γ- and ζ-COP, were found to be isotypic (Blagitko et al., 1999; Futatsumori et al., 2000; Wegmann et al., 2004). The two isotypes of each subunit were termed γ1 (ζ1) and γ2 (ζ2), respectively. The different isotype combinations are present in diverging amounts within the cell: γ1ζ1 (53%), γ1ζ2 (16%), γ2ζ1 (26%) and γ2ζ2 (5%), and localize differentially within the Golgi (Moelleken et al., 2007). These findings strongly suggest that the different isotypes mediate specific transport steps within the Golgi, however, no distinct binding partners interacting with one of the isotypes have been characterized to date.

Proteins following the Secretoy Pathway through the Golgi undergo repetitive shuttling processes, and, in each cisterna, are sorted for their respective destination. This model was first described in the "Destillation-hypothesis" (Dunphy et al., 1981; Rothman, 1981), that implied that in each step, anterograde cargo is preferentially incorporated in COPI vesicles moving in direction of the TGN, and retrograde cargo is transported back in direction of the ER. Thus, in each transport step from one cisterna to the next on the route through the Golgi, cargo is further enriched by selective uptake into the vesicles going in the correct direction.

Thus, proteins traversing the Golgi via the Secretory Pathway are both modified by the corresponding enzymes in the different cisternae, and sorted for their corresponding destinations.

At the next station, the Trans Golgi Network (TGN), transport is mediated mainly by clathrin-coated vesicles (CCVs), that are made up from three core components: A small GTPase, an adaptor protein complex and the scaffolding protein clathrin (see 1.2.1 Clathrin-coated vesicles). The TGN comprises the second big sorting station in intracellular trafficking. Here, on one hand, endocytic cargo is transported from the plasma membrane via CCVs. On the other hand, anterograde cargo is distributed to its respective destinations by two different types of transport: regulated exocytic transport via secretory granules, and constitutive transport via clathrin-coated vesicles.

Constitutive transport is mediated by various forms of clathrin-coated vesicles. Cargo destined for organelles or the plasma membrane is sorted by different adaptor protein complexes. Two classes of these complexes take part in this process: First, adaptor protein complexes that recognize cargo by distinct peptide sequences or monoubiquitination (i.e.

AP-complexes, GGAs or β-Arrestins), and second, lipid binding complexes (AP180/CALM, Epsins and Amphiphysins).
For example, lysosomal hydrolases are recognized via attached mannose-6-phosphate (M6P) groups by M6P-receptors, and incorporated into vesicles destined for endosomes and subsequently lysosomes. Monoubiquitinated proteins are taken up into vesicles that are targeted towards late endosomes, and lysosomes. Mis- or unfolded proteins are targeted to the lysosomes for degradation.

Regulated exocytic transport only takes place in endocrine or neuroendocrine cells. Here, prohormones are taken up into secretory granules that allow release of the mature hormones after an extracellular stimulus (Tooze et al., 2001). In the formation of secretory granules no coating proteins have been described to date. However, clathrin-coated vesicles are involved in the removal of mislocalized proteins (i.e. secretory proteins) from the secretory granules.

1.2. Vesicular Transport: The three coating systems

As described above, three types of transport vesicles have been characterized in eukaryotic cells so far:
Clathrin-coated vesicles (CCVs) that shuttle between the trans-Golgi network, endosomes, lysosomes and the plasma membrane; COPII-coated vesicles that mediate exit from the ER; and COPI-coated vesicles that function within the early Secretory Pathway (reviewed by (McMahon and Mills, 2004)). All intracellular vesiculation systems share certain homologies and the following chapter focuses on the characteristics of each system.

1.2.1. Clathrin-coated vesicles

Clathrin-coated vesicles are structured in three layers. The innermost layer is comprised of the membrane bilayer containing the transmembrane cargo proteins. It is linked to the outer, scaffolding clathrin layer by a middle layer of adaptor proteins. These adaptor proteins are a disparate group of proteins with no obvious sequence homology (see 1.2.1.1 Structural studies on clathrin-coated vesicles). They are termed adaptor proteins as they bind to both transmembrane components and clathrin, and hereby mediate a link ("adaptor") between the cargo in the innermost layer and the scaffolding on the outside.

Clathrin-coated vesicles were first described by Roth and Porter in 1964 (Roth and Porter, 1964), studying the yolk uptake of mosquito oocytes. First electron microscopy images of the soccerball-like structure of a clathrin-coated vesicle were obtained by Kanaseki and Kadota

1969 (Kanaseki and Kadota, 1969), and the outer scaffolding protein, clathrin, was subsequently discovered by Pearse (Pearse, 1975).
At the same time, the adaptor proteins, the middle layer of CCVs, were identified (Keen et al., 1979). Further biochemical characterization revealed that there are at least two classes of these proteins (Keen et al., 1987): The tetrameric adaptor protein complex 1 (AP-1), localized to the trans-Golgi network and the tetrameric adaptor protein complex 2 (AP-2), localized on the plasma membrane (Ahle et al., 1988). As different kinds of cargo are transported at the TGN and the plasma membrane, it was speculated that not clathrin, but the adaptor protein complexes confer specificity for sorting distinct cargo to the different CCVs. Indeed, Ohno et al found that the adaptor complexes bind to short targetting sequences present in cargo molecules for the CCVs (Ohno et al., 1995). Subsequently, other adaptor protein complexes were identified (AP-3, (Dell'Angelica et al., 1997); and AP-4, (Dell'Angelica et al., 1999)). However, direct interaction of these adaptor complexes with clathrin has not been demonstrated to date.
Other, monomeric adaptor proteins were discovered later: Golgi-localizing, γ-adaptin ear homology domain, Arf binding proteins (GGAs, (Dell'Angelica et al., 2000)), AP180/CALM and the epsins. Like the tetrameric adaptor proteins, the monomeric adaptor proteins are able to cross-link the outer scaffolding clathrin layer to the innermost transmembrane components.

Like in the other vesiculation systems, recruitment of the adaptor proteins to the membrane is governed by a small GTPase. Arf1 has been described in both AP-1 (Austin et al., 2000), AP-3 (Ooi et al., 1998), AP-4 (Boehm et al., 2001) and the GGAs (Dell'Angelica et al., 2000), and Arf6 was implied in mediating AP-2 recruitment (Paleotti et al., 2005)). However, in contrast to the other vesiculation systems, coat release seems to be independent of the nucleotide state of the small GTPase, but to be ATP (Holstein et al., 1996) and phosphorylation-dependent, as phosphorylation of AP-2 in its α and β2 subunits, and AP-1 in its β1-subunit, leads to dissociation of the clathrin coat (Jha et al., 2004; Wilde and Brodsky, 1996).

1.2.1.1. Structural studies on clathrin-coated vesicles

Clathrin has an unusual structure, termed "Triskelion": It is made up of three extended subunits, which radiate from a central hub (Ungewickell and Branton, 1981). A small protein was identified that was attached to these "legs", when isolating clathrin from CCVs. The two

proteins were termed clathrin "heavy chain" (190kD) and "light chain" (25kD; (Kirchhausen and Harrison, 1981)).

Each leg, i.e. each heavy chain, is about 475nm long (Kirchhausen et al., 1986), and the elongated structure is achieved by a heptad repeat of a central 71-residue motif, termed α-solenoid structure (clathrin heavy chain repeat). Each leg is comprised of the following subdomains: A proximal segment (adjacent to the central hub), a knee-like subdomain, a distal segment, and an ankle, a linker and a terminal domain, that is comprised of WD-40 repeats forming a β-propeller domain (Fotin et al., 2004a). The light chains are attached to a heavy chain via each proximal segment close to the central hub (Figure 2, taken from Fotin et al., 2004).

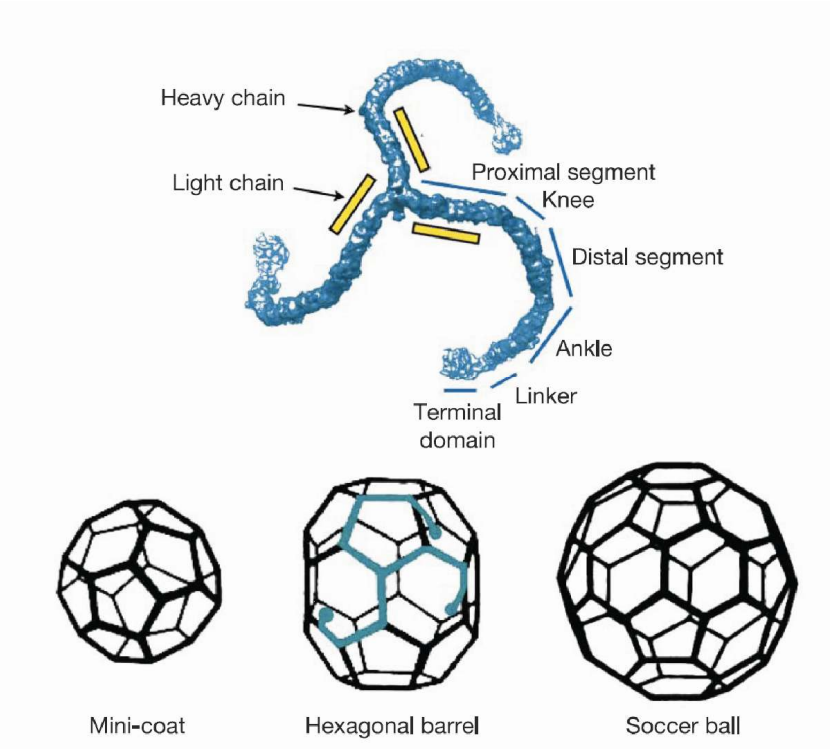

Figure 2: Scheme of the Clathrin triskelion and designs of Clathrin lattices (adapted from Fotin et al, 2004).

Upon coat assembly, clathrin assembles into a lattice of open hexagonal and pentagonal faces (Musacchio et al., 1999). The resulting coats show various designs, ranging from small assemblies with 28 ("mini-coats"), 36 ("hexagonal barrels") and 60 ("soccer balls") clathrins to even bigger aggregates (Crowther et al., 1976). In vitro reconstitution of clathrin-coated vesicles from the isolated components yield relatively homogeneous preparations, with a large proportion of hexagonal barrels (Vigers et al., 1986a; Vigers et al., 1986b). These vesicles have been studied extensively using negative stain (Crowther et al., 1976) and cryo EM (Fotin et al., 2004a; Fotin et al., 2004b; Fotin et al., 2006; Musacchio et al., 1999; Smith

et al., 1998; Vigers et al., 1986a; Vigers et al., 1986b). The clathrin triskelions assemble in a pattern where the clathrin legs make up the edges, and the triskelion hubs lie at the vertices (Smith et al., 1998). The legs radiate from the central hub, project slightly inward, and bend at both the knee and the ankle segments. Thus the interaction of different clathrin molecules to form a lattice is mediated by the α-solenoid structures interdigitating in the edges of the coat, and the interaction with the middle layer, i.e. the adaptor proteins, is mediated by the β-propeller in the terminal domain (Figure 2, taken from Fotin et al., 2004).

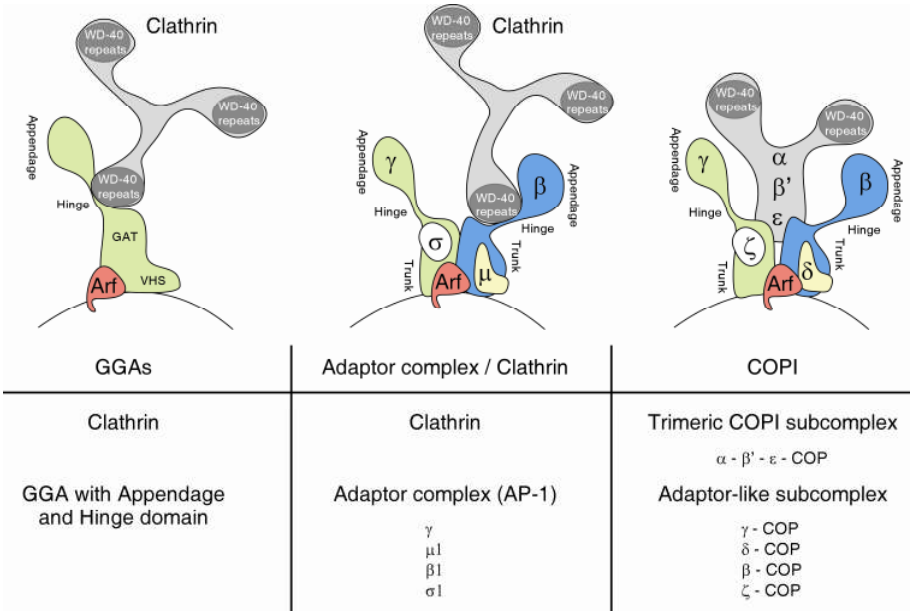

GGAs	Adaptor complex / Clathrin	COPI
Clathrin	Clathrin	Trimeric COPI subcomplex α - β' - ε - COP
GGA with Appendage and Hinge domain	Adaptor complex (AP-1) γ μ1 β1 σ1	Adaptor-like subcomplex γ - COP δ - COP β - COP ζ - COP

Figure 3: Structural similarities of coat proteins. In the table, protein subunits of the various coats are listed along with their functional homologies.

The structure of the adaptor proteins has also been extensively studied. The crystal structures of the core of both the adaptor protein AP-1 ((Heldwein et al., 2004)) and AP-2 (Collins et al., 2002) have been solved. Both tetrameric complexes exhibit a characteristic design, with two domains (the α and the β subunits) containing a trunk and an appendage domain linked by a flexible hinge, as illustrated in Figure 3 (modified from (Langer et al., 2007)), and interact with a wide range of binding partners. For example, AP-2 binds directly to phosphoinositides (Beck and Keen, 1991; Collins et al., 2002; Gaidarov and Keen, 1999; Rohde et al., 2002), cargo proteins (Ohno et al., 1995), cargo receptors (Claing et al., 2002) and coating machinery, like GTPases (Paleotti et al., 2005) and the scaffolding clathrin (Zaremba and Keen, 1983), reviewed by (Sorkin, 2004).

Monomeric adaptors, like the GGAs, show a similar design only by presence of the characteristic trunk-hinge-appendage subdomain structure (Figure 3), binding to cargo via their VHS (VPS-27, Hrs and STAM) domain (Puertollano et al., 2001a; Zhu et al., 2001), to the small GTPase Arf via its GAT (GGA and Tom1) domain (Boman, 2001; Boman et al., 2000), and to clathrin via clathrin boxes in the hinge region (Puertollano et al., 2001b).

The adaptor proteins as the linker between cargo proteins in the membrane layer and the outer scaffold clathrin have a special role during the coating process. Their affinity for cargo must be tightly controlled, allowing specific binding and recruitment to clathrin-coated pits that must be activated during the budding process only. This is achieved by conformational changes of the adaptor proteins, that are selectively triggered upon either phosphorylation or interaction with specific ligands. The following chapter focuses on these conformational changes in adaptor proteins.

1.2.1.2. Conformational changes in adaptor proteins

1.2.1.2.1. The adaptor protein 2 (AP-2) system

The AP-2 complex and its vital role in clathrin-mediated endocytosis is the most extensively studied vesicle coating system. It is also the first coating protein in which a conformational change was described (Matsui and Kirchhausen, 1990). Using limited proteolysis, Matsui *et al.* observed that the µ2-subunit of soluble AP-2 was more resistant to trypsin digestion than that of clathrin-coated vesicle-bound AP-2. Investigating this, Fingerhut *et al.* found that binding of AP-2 to cargo can be modulated by phosphorylation (Fingerhut et al., 2001). Phosphorylation induced a 30-fold increase in affinity of AP-2 to Yxxϕ-based cargo-sorting signals, and phosphorylated AP-2 exhibited an increased binding to membranes. It was later shown that phosphorylation of µ2 is also essential for endocytosis (Olusanya et al., 2001).

In 2002, the x-ray structure of the core of AP-2 (without the ear domains of α- and β2-adaptin) was solved by Owen and coworkers (Collins et al., 2002). In this crystal structure, the binding pocket for Yxxϕ motifs is inaccessible, as it is covered by β2-adaptin. It was concluded that the crystallized form corresponds to the inactive, cytosolic form of AP-2, and that a conformational change would be required to open the binding site on µ2. It is likely that phosphorylation of Thr156 in the µ2-subunit, located in the linker connecting two µ2-domains, induces this conformational change, and that the increased affinity of phosphorylated AP-2 for cargo is due to the conformational change opening its binding pocket. Thus AP-2's affinity for cargo is directly modulated by a phosphorylation-induced conformational change.

Later, in 1999, Haucke *et al*. found a conformational change induced in AP-2 upon binding of Yxxϕ-based cargo signals. The authors investigated the interaction of AP-2 with synaptotagmin, a transmembrane protein that binds to AP-2 via its C2B domain and may act as an AP-2 recruitment site at the plasma membrane (Jorgensen et al., 1995; Zhang et al., 1994). In the presence of Yxxϕ-signal-bearing peptides, binding of synaptotagmin to AP-2 and recruitment of AP-2 to membranes was increased (Haucke and De Camilli, 1999). A conformational change of AP-2 upon binding of a Yxxϕ-signal-containing peptide was shown by altered susceptibility to limited proteolysis of AP-2's α-adaptin core domain. Later studies revealed that synaptotagmin binds AP-2 via µ2- and α-adaptin, and that the binding affinity of isolated µ2 (outside the context of the AP-2 complex) to a C2B-domain was not increased in the presence of a Yxxϕ-signal-containing peptide (Haucke et al., 2000). Therefore, it was proposed that the conformational change observed within AP-2 (Haucke and De Camilli, 1999) includes other subunits of the complex.

The conformational change induced by binding of a Yxxϕ-signal was interpreted as an activation of the AP-2 complex for cargo binding. This hypothesis was further supported by Boll *et al.* (Boll et al., 2002), who investigated binding of AP-2 to the low density lipoprotein (LDL) receptor via its signal sequence FDNPVY (consensus sequence: FxNPxY). They showed that LDL receptor signal-containing proteins bound the µ2 subunit on a site different from both synaptotagmin's C2B binding site and the Yxxϕ-signal binding site, and that the presence of Yxxϕ-peptides increased AP-2's binding to a FDNPVY protein. Like Haucke (Haucke and De Camilli, 1999), they detected a conformational change in AP-2 upon addition of a peptide containing a Yxxϕ-sequence. Again the susceptibility of β-adaptin to proteases changed in the presence of Yxxϕ-peptide. However, the binding site for FxNPxY-motifs remains unknown.

It is generally believed that the AP-2 complex undergoes a structural rearrangement during membrane recruitment that regulates its ability to bind to various cargo signals. It is of note that the conformational change observed by Haucke (Haucke and De Camilli, 1999) and Boll (Boll et al., 2002) is not induced by phosphorylation, as no kinases were present in their experiments. Thus, it may be speculated that two sequential conformational changes of the AP-2 complex take place during its recruitment to the donor membrane: the first one by phosphorylation to recruit the complex to the membrane and allow Yxxϕ-signal binding, and the second one, induced by ligand binding to the now-accessible Yxxϕ-binding site, to allow for subsequent binding of additional proteins.

The role of Yxxϕ-signal-containing proteins in clathrin-mediated endocytosis was further analyzed by Haucke (Haucke and Krauss, 2002). Using a liposome-based system, peptides bearing these signals were shown to induce AP-2 clathrin cage formation. Cargo proteins have been proposed to be crucial parts of the vesicle formation machinery, based on *in vivo* data showing that, of the large number of clathrin-coated pits formed spontaneously on the plasma membrane, only a small fraction proceed to form clathrin-coated vesicles (Ehrlich et al., 2004). The authors proposed that the presence of cargo proteins, e.g. Yxxϕ-signal containing proteins, stabilizes coated pits and allows them to proceed to form vesicles.

1.2.1.2.2. The adaptor protein 1 (AP-1) system

The AP-1 complex is thought to mediate transport from the TGN to endosomes/lysosomes (Traub and Kornfeld, 1997), although recent studies have proposed a role for AP-1 in recycling from endosomes to the TGN (Meyer et al., 2001; Meyer et al., 2000). The minimal machinery for AP-1 recruitment has been characterized (Crottet et al., 2002; Meyer et al., 2005; Wang et al., 2003). It is composed of the small GTPase Arf1 in its active, GTP-bound form, phosphatidylinositol phosphates as lipid components, and Tyr-based cargo signals present on the donor membrane. Like AP-2, AP-1 was shown to bind to certain cargo motifs (e.g. the cytoplasmic tails of cation-dependent and cation-independent mannose-6-phosphate receptors (MPR; (Glickman et al., 1989; Mathews et al., 1992; Meresse and Hoflack, 1993))), and to interact with the coating machinery GTPase Arf1 (Nie et al., 2003) and with clathrin (Zaremba and Keen, 1983).

Cargo binding to AP-1 is, at least in part, also regulated by phosphorylation (Ghosh and Kornfeld, 2003a). Like in the AP-2 system, AP-1's affinity to cargo peptides decreased dramatically upon dephosphorylation of AP-1 (Ghosh and Kornfeld, 2003a). Limited proteolysis of phosphorylated and dephosphorylated AP-1 revealed a conformational change, as the μ1-subunit exhibited higher susceptibility to trypsin in the phosphorylated form. The observed increases in susceptibility to limited proteolysis and cargo binding upon phosphorylation is analogous to the behaviour of AP-2 described by Fingerhut *et al.* (Fingerhut et al., 2001) and Ricotta *et al.* (Ricotta et al., 2002), indicating that, in both systems, a phosphorylation-induced conformational change is employed to activate cargo-binding of the adaptor protein complex. A likely candidate to mediate phosphorylation of AP-1 *in vivo* is GAK (Umeda et al., 2000).

Upon interaction of AP-1 with cargo peptides, i.e. the CI-MPR internal dileucine-type cargo motifs, a conformational change occurs within the core complex (Lee et al., 2008). This

conformationally changed AP-1 showed an increased affinity for Tyr- based cargo motifs (Yxxϕ), and the functional cross-talk between the binding sites for the dileucine-type motif and the tyrosine-based motif was found to be bidirectional. In addition, the conformational change also greatly stimulated binding of AP-1 to the small GTPase Arf1 in its GTP-bound form. Thus, in the AP-1 clathrin system, transmembrane cargo proteins serve as a part of the machinery to stabilize the Adaptor complexes on the membrane (Lee et al., 2008).

1.2.1.2.3. Golgi-localizing, γ-adaptin ear homology domain, Arf-binding proteins

Similarly, binding of cargo to the monomeric adaptor proteins GGAs (Golgi-localizing, γ-adaptin ear homology domain, Arf-binding proteins) is modulated by phosphorylation (Ghosh and Kornfeld, 2003b).
In GGAs, phosphorylation induces an effect opposite to that in adaptor complexes. Binding of GGA1 to cargo proteins (MPR) increases upon dephosphorylation of GGA1, whereas the inactive, phosphorylated form is cytosolic (Ghosh and Kornfeld, 2003b). According to Doray *et al.* (Doray et al., 2002), an internal AC-LL motif in GGAs 1 and 3 binds to and blocks the VHS binding site upon phosphorylation of Ser355, and dephosphorylation relieves autoinhibition. In order to investigate the phosphorylation-dependent conformational dynamics of GGA1/3, phosphorylated and dephosphorylated GGA1 were submitted to gel filtration and sucrose gradient analysis. A striking 2nm change in the Stokes radius of GGA1 was found upon phosphorylation, indicating a conformational change. The authors attributed this change to the AC-LL motif-containing hinge domain moving out of the VHS domain-binding pocket (Doray et al., 2002; Ghosh and Kornfeld, 2003b).

1.2.2. COPII-coated vesicles

Like in the clathrin system, a COPII coated vesicle is made up from two major coat building units: The adaptor protein-like Sec23/24 dimer, and the clathrin-like Sec13/31 dimer, that are recruited sequentially to the donor membrane. The structure of Sec23/24 and Sec13/31 heterodimers purified from yeast cells was first characterized by Lederkremer et al (Lederkremer et al., 2001) using negative stain EM. They described both the characteristic bone-like shape of the Sec23/24 heterodimer, and the elongated shape of the Sec13/31 dimer. The Sec13/31 complex is comprised of 5 globular domains arranged like pearls on a string, and make up the 28-30nm sized building unit of the outer scaffold of the COPII cage. The pre-budding complex of Sec23/24 with bound Sar1p was co-crystalized in 2002 by Bi and Goldberg (Bi et al., 2002), showing an intrinsic curvature of the lipid binding face matching that of COPII vesicles.

In 2006, the structure of minimal COPII cages consisting of Sec13/31 heterodimers was described by Stagg et al (Stagg et al., 2006). Using cryo-EM and single-particle averaging, they reconstructed a 30Å resolution map of self-assembled Sec13/31 cages. These cages contain 24 heterodimers of Sec13/31, and exhibit octahedral symmetry. In a cuboctahedron, four edges intersect at each vertex, which is strikingly different from the clathrin system, where a vertex is defined by crossing of three edges (see also 1.2.1 Clathrin coated vesicles). In 2007, the structure of the Sec13/31 complex was solved by Fath and Goldberg (Fath et al., 2007), and fitted into the 30Å map previously described by Stagg et al (Stagg et al., 2006). Although the Sec13/31 dimer resembles clathrin (it features an α-solenoid, rod-like structure, with a terminal domain comprised of a β-propeller motif), the relative orientation of the domains of the coating protein in the assembled coat is strikingly different from CCVs. Whereas in CCVs clathrin's β-propeller domains are pointing inward and are interacting with the adaptor proteins, in COPII cages the β-propellers of the Sec13/31 dimers actually comprise the 12 vertices of the cuboctahedron, and the α-solenoid structures do not interdigitate (Fath et al., 2007; Stagg et al., 2006). Thus, although clathrin and COPII coats utilize similarly designed building units (α-solenoid and β-propeller motifs) they do not seem to share a common construction principle.

Like in the other vesiculation systems, the coating process is governed by a small GTPase - in the COPII system, Sar1p (Nakano and Muramatsu, 1989). The GTPases' localization is determined by the bound nucleotide: The GDP-form is a soluble protein, whereas the GTP-bound form is bound to the corresponding donor membrane by an anchor located in the N-terminal domain. In the case of Sar1p, an amphiphatic helix is exposed upon Sec12-mediated GDP-to-GTP-exchange, that inserts into the lipid bilayer and effectively locks Sar1p on the membrane. Sec12 localizes to the ER (Barlowe et al., 1993; Barlowe and Schekman, 1993), and Sec12-mediated GTP-exchange is thought to convey specificity of COPII budding to ER membranes. Sequentially, Sar1p recruits the coating protein complexes, first heterodimeric Sec23/24, and then Sec13/31 (Matsuoka et al., 1998). Sar1p is then released from the membrane by Sec23 (the corresponding GAP), whose activity is increased by Sec13/31 on the donor membrane (Antonny et al., 2001; Yoshihisa et al., 1993). Sar1p dissociation from the membrane also leads to coat disassembly.

1.2.3. COPI-coated vesicles

COPI-coated vesicles were discovered in a cell-free assay that was used to study transport between Golgi cisternae (Malhotra et al., 1989). Subsequently, the proteins comprising the coat of these vesicles were identified: A large protein complex termed "coatomer" (Waters et al., 1991), and the small GTPase Arf1 (Serafini et al., 1991).

Arf1 is a member of the Ras family of small GTPases, and is myristoylated on its N-terminal glycine residue, a modification that is prerequisite for membrane binding and activity (Kahn et al., 1991).

Coatomer is a heptameric complex with a molecular weight of ~600kD (Waters et al., 1991). It is comprised of a trimeric and a tetrameric subcomplex (Figure 3, table 1, and reviewed in (McMahon and Mills, 2004)), and the whole complex seems to remain fully assembled during its life time in the cell (Lowe and Kreis, 1996).

Subunit	Size	motifs	Interaction partners
α-COP	140	α-solenoid, β-propeller (WD-40)	KKxx, KxKxx;
β-COP	107	trunk-hinge-appendage	Arf1
β'-COP	102	α-solenoid, β-propeller (WD-40)	KKxx, KxKxx; Arf1
γ1-COP	97	trunk-hinge-appendage	p24-family proteins, Arf1
γ2-COP	97	trunk-hinge-appendage	p24-family proteins, Arf1
δ-COP	57		δ-L motifs Arf1
ε-COP	35		Arf1
ζ1-COP	20		
ζ2-COP	23.5		

Table 1: Coatomer subunits: Size, motifs and interaction partners.

In the budding process, coatomer is recruited from the cytosol in a single step in an Arf-dependent manner (Hara-Kuge et al., 1994). This recrutiment en bloc is contrary to the clathrin and the COPII system, where two sequential steps are required to assemble first the adaptor proteins (or Sec23/24) and second the scaffolding proteins (clathrin or Sec13/31). This means that the proteins analogous to those forming the CCVs' inner shell and outer shell are recruited at the same time.

Structural similarities exist between the trimeric subcomplex comprised of the subunits α, β' and ε COP and the clathrin proteins, and between the tetrameric subcomplex consisting of β, γ, δ and ζ-COP and the 4 subunits of the adaptor complexes AP-1 to AP-4 of clathrin-coated vesicles (Eugster et al., 2000; Gurkan et al., 2006; McMahon and Mills, 2004; Schledzewski et al., 1999). Like in clathrin, the trimeric subcomplex contains α-solenoid structures and β-propeller domains (table 1, reviewed in (Devos et al., 2004)). The tetrameric adaptor protein-like subcomplex of coatomer also contains two subunits with the characteristic trunk-hinge-appendage-domain design also observed in the APs ((Eugster et al., 2000; Schledzewski et al., 1999; Watson et al., 2004), reviewed by (McMahon and Mills, 2004)). However, only limited structural data has been obtained on coatomer architecture. Only the structure of the appendage domain of γ-COP has been solved, showing a similiar overall fold as the α-appendage domain of AP-2 (Watson et al., 2004).

Thus, coatomer contains building units similar to those in the COPII / clathrin system. Their functions, though, seem to differ from those found in the other systems, as described below.

1.2.3.1. The COPI budding process

The COPI budding process can be divided up into 4 steps (Figure 4). In the following chapter, the most important aspects of each step will be discussed.

1. Arf1 recruitment (Figure 4, step 1).

In its inactive, GDP-bound form, the small GTPase Arf1 resides in the cytosol. Arf1 has been described to take part in the biogenesis of AP-1 (Austin et al., 2000), AP-3 (Ooi et al., 1998), AP-4 (Boehm et al., 2001) and COPI (Donaldson et al., 1992a; Palmer et al., 1993; Serafini et al., 1991) vesicles. Specificity for the respective donor membrane is presumably conveyed by two factors: transmembrane proteins that bear cytoplasmic receptor motifs and the corresponding nucleotide exchange factors (GEFs).

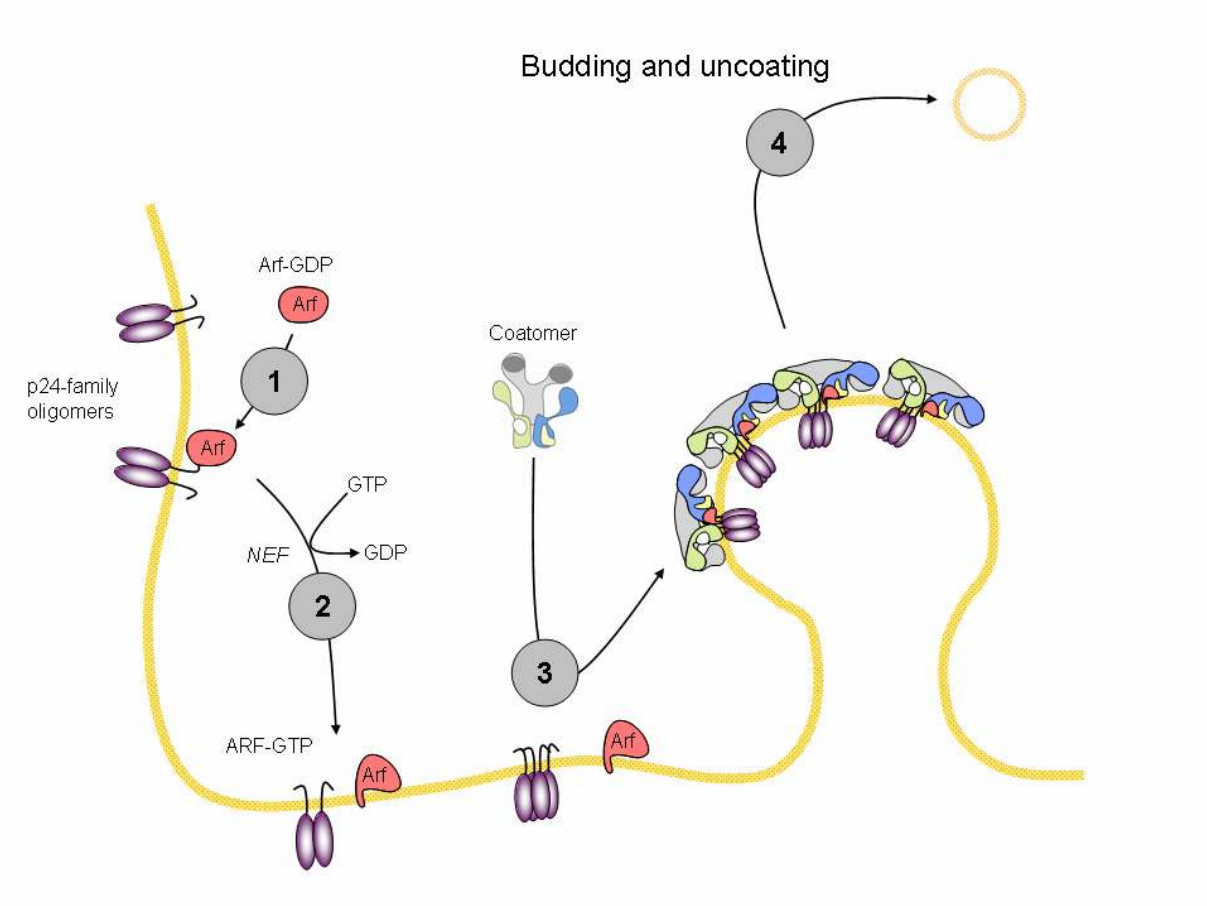

Figure 4: Scheme of the COPI budding process.

Two members of the p24-family of class I transmembrane proteins, p23 and p24, have been characterised to recruit Arf1-GDP to the donor Golgi membrane (Contreras et al., 2004; Gommel et al., 2001; Majoul et al., 2001), proposing these cytoplasmic domains as primary Arf1-GDP receptors. In addition, the early Golgi SNARE protein membrin has been put forward to act as an Arf1-GDP receptor (Honda et al., 2005).

The nucleotide exchange factors (GEFs) catalyze the exchange of GDP to GTP on Arf1, and share a characteristic Sec7 domain (Chardin et al., 1996). Sec7-binding to Arf1 is modulated by interactions with the lipid bilayer (Itoh and De Camilli, 2004; Terui et al., 1994). The GEF involved in COPI biogenesis is presumably GBF1, a large Sec7 domain GEF localized to the *cis*-Golgi (Niu et al., 2005; Zhao et al., 2002). GBF1 also showed sensitivity to Brefeldin A (BFA, (Niu et al., 2005; Zhao et al., 2002)), a fungal metabolite that was previously shown to inhibit nucleotide exchange on Arf1 (Donaldson et al., 1992b).

Binding of GTP leads to a conformational change in Arf1, exposing the N-terminal myristoyl-anchor and an amphiphatic helix, effectively anchoring Arf1-GTP on the donor membrane (Antonny et al., 1997; Franco et al., 1996). This conformational change also ensures the

specificity of the GDP-GTP-exchange to the donor membrane, as the exposure of the myristoyl-anchor is energetically unfavored in the cytosol.

2. Coatomer recruitment (Figure 4, step 2).

Arf1, in the activated GTP form, dissociates from the transmembrane receptors, i.e. p24-family proteins. A "priming complex" is formed, consisting of membrane-bound Arf1-GTP and oligomers of p24-family members. This complex is competent to recruit coatomer to the donor memrbane.

Coatomer binds to Arf1 via multiple interactions: ε-COP (Eugster et al., 2000), β- and γ-COP (Zhao et al., 1997; Zhao et al., 1999), and β' and δ-COP, as recently described (Sun et al., 2007b). The interaction with δ-COP was found to be nucleotide-dependent only in the context of the whole coatomer complex, as isolated δ-COP bound both Arf1-GDP and Arf1-GTP. Thus the binding pocket for Arf1 in δ-COP may be opened upon GTP-dependent membrane recruitment of coatomer, and may be reminiscent of the induced activation of AP-2 by phosphorylation during membrane recruitment.

The coating complex coatomer is, as described above, recruited en bloc. On the membrane, coatomer binds to cytoplasmic domains of transmembrane proteins, that are described below.

3. Interaction of coatomer with transmembrane proteins: Cargo binding and conformational change (Figure 4, step 3).

On the donor membrane, coatomer interacts via multiple subunits with the cytoplasmic tails of transmembrane proteins (Bethune et al., 2006; Dominguez et al., 1998; Letourneur et al., 1994; Sohn et al., 1996). Two classes of interaction partners have been characterized to date:

1. The p24-family proteins: coat receptors.

The p24-family are class I transmembrane proteins, termed p23, p24, p25, p26 and p27. They are thought to cycle in the early Secretory Pathway (Blum et al., 1999; Fullekrug et al., 1999; Nickel et al., 1997; Rojo et al., 2000), with distinct localizations for the individual members (Dominguez et al., 1998; Fullekrug et al., 1999; Nickel et al., 1997; Rojo et al., 2000; Rojo et al., 1997; Sohn et al., 1996; Wada et al., 1991). Members of the p24-family all consist of N-terminal signal sequence, a pair of conserved cysteins and a sequence predicted to form a coiled-coil domain in the lumenal domain, a transmembrane segment, and a small cytosplasmic domain (Figure 5).

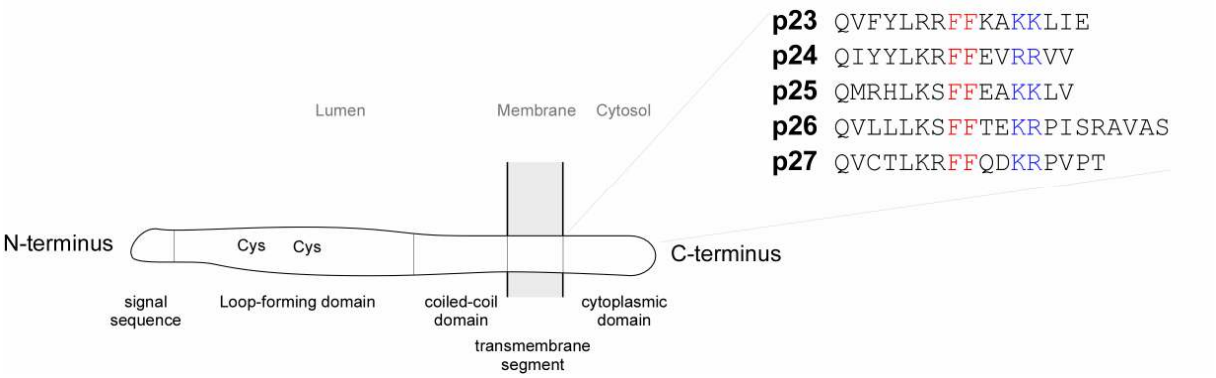

Figure 5: Scheme of p24-family members structure and sequences of cytoplasmic domains.

The coiled-coil domain is presumably responsible for the formation of homo- and hetero-oligomers of the p24-family members (Emery et al., 2000; Fullekrug et al., 1999), a prerequisite for the distinct interaction of their cytoplasmic tails with cytoplasmic proteins. The cytoplasmic domains of all p24-family members contain two distinct motifs: A diphenylalanine (FF, colored in red in Figure 5) motif and a dibasic motif (KKxx, KKx_n or KRx_n with n >3) at their C-termini (imaged in blue in Figure 5). Binding to coatomer is dependent on both motifs, as mutation of either the KKxx- or the FF-residues significantly reduces binding, and mutation of both motifs abolishes the interaction (Bethune et al., 2006; Cosson and Letourneur, 1994; Reinhard et al., 1999; Sohn et al., 1996).

p24-family members bind to caotomer not via α- and β'-COP, but via the subunit γ-COP (Bethune et al., 2006; Fiedler et al., 1996; Goldberg, 2000). The interaction of coatomer with the dimeric cytoplasmic domain of the transmembrane protein p23 was shown to induce a conformational change and aggregation of the complex in vitro (Reinhard et al., 1999). This aggregation likely represents coatomer polymerization during COPI vesicle formation, as COPI vesicle-bound coatomer and coatomer polymerized by the cytoplasmic domain of dimeric p23 *in vitro* showed identical patterns after limited proteolysis, indicating similar conformations (Reinhard et al., 1999). Recently, it was shown that all members of the p24-family proteins and some additional cycling membrane proteins bind as dimers to two independent sites in the appendage and the trunk domain of the coatomer subunit γ-COP, and that dimers of p23 induce a conformational change in the trunk domain of γ-COP (Bethune et al., 2006).

Although COPI vesicles can be generated from liposomes with a certain lipid composition using coatomer and Arf1 alone (Spang et al., 1998), the presence of lipopeptides representing cytoplasmic domains of p24-family members allows COPI vesicle budding independent of the lipid composition of the donor membranes (Bremser et al., 1999). They were also found to be a stoichiometric component of a population of COPI vesicles (Fiedler

et al., 1996; Sohn et al., 1996). However, recently a population of COPI vesicles devoid of p24-family members has been described (Malsam et al., 2005). Here, other, yet unidentified transmembrane proteins may take over the role of the p24-family members.

2. The KKxx / KxKxx motif: Cargo.

The dibasic ER retrieval signals are the best characterized cargo sorting motifs binding to coatomer (Cosson and Letourneur, 1994; Letourneur et al., 1994). KKxx motifs were shown to bind to the coatomer subunits α- and β'-COP (Letourneur et al., 1994), and recently the distinct but overlapping binding sites for both KKxx and KxKxx motifs were identified in the β-propeller / WD-40 repeats at the N-termini of α- and β'-COP (Eugster et al., 2004). Most KKxx / KxKxx-motif bearing proteins bind with an affinity in the low micromolar range (Bethune et al., 2006). Thus, the β-propeller domains on α- and β'-COP serve a function distinct from or additional to the one observed in both the clathrin system (interaction with the adaptor proteins) and the COPII system (formation of vertices).

3. Other cargo binding motifs:

Proteins cycling between the ER and the early Golgi contain a specific signal sequence that allows them to exit the ER to travel to the Golgi, and then be captured and transported back. A KDEL-motif acting as an ER retrieval signal in the C-terminal of lumenal ER resident proteins was identified by Munro and Pelham (Munro and Pelham, 1987; Pelham et al., 1988). The corresponding receptor ("KDEL-receptor", (Lewis and Pelham, 1990; Semenza et al., 1990) was characterized as an integral membrane proteins with 7 transmembrane spans (Scheel and Pelham, 1998), and binds to coatomer via a dilysine-motif and a phosphorylated serine (Cabrera et al., 2003). Binding of ligand (i.e. KDEL proteins) is pH-dependent (Wilson et al., 1993), induces oligomerization of the receptor (Majoul et al., 1998) and leads to retrieval of the receptor-protein complex from the Golgi to the ER (Lewis and Pelham, 1992) by the COPI pathway (Majoul et al., 2001).

Two other binding motifs in cytoplasmic domains of transmembrane proteins have been identified to date: The δ-L-motif with the consensus sequence WxxW/Y/F, mediating binding to the coatomer subunit δ-COP, identified in yeast in the ER-localized Sec71p protein (Cosson et al., 1998); and the RxR motif, first described in the cytoplasmic loops and C-terminal tails of the ATP-sensitive K^+ channel (Yuan et al., 2003; Zerangue et al., 1999). The binding site for RxR-motifs on coatomer has recently been identified on β- and δ-COP (Michelsen et al., 2007), and was found to show a striking resemblance to the Yxxϕ-binding site of the adaptor complexes in the clathrin system.

4. Uncoating and fusion with the target membrane (Figure 4, step 4).

COPI coat hydrolysis is mediated by nucleotide exchange on Arf1, i.e. GTP- to GDP-exchange on Arf1 leads to coat dissassembly (Tanigawa et al., 1993). After complete budding, GTP hydrolysis is induced by interaction with an ArfGAP (Cukierman 1995), a process that could be reconstituted in vitro by addition of the purified catalytic domain of ArfGAP1 to COPI vesicles generated from purified Golgi membranes (Reinhard et al., 2003). Two other ArfGAPs have been shown to interact with coatomer: ArfGAP2 (Randazzo, 1997) and ArfGAP3 (Liu et al., 2001). Thus, for preparation of stable, coated COPI vesicles in vitro using GTP, no ArfGAP proteins must be present.

Fusion of a COPI vesicle with its target membrane is governed by two classes of proteins: SNAREs (soluble NSF attachment protein receptors, (Sollner et al., 1993)) and tethering proteins. Initial binding of the vesicles to their respective target membranes is mediated by tethering proteins. There are two classes of tethering proteins: Elongated coiled-coil proteins (Barr and Short, 2003) and large multiprotein complexes (Whyte and Munro, 2002). While multiprotein complexes have mostly been described in exocytosis (Whyte and Munro, 2002), coiled-coil proteins are involved in Golgi and endosomal fusion steps: The coiled-coil proteins Giantin and Golgin 84 are taken up into COPI vesicles, and mediate together with p115, GM130 and GRASP65/CASP docking of the vesicle to the target membrane.

The specificity of vesicle-membrane fusion is ensured by complementary pairing of SNARE proteins (McNew et al., 2000): The target membranes contain three-helical target(t)-SNAREs, that form a tetrahelical bundle with the vesicle(v)-SNARE present in the COPI vesicle (Parlati et al., 2000; Weber et al., 1998).

1.2.3.2. Summary: Comparison of COPI with the other vesiculation systems

The different coating proteins share some striking structural and functional homologies. However, in each system, similar motifs are put to different use, and the budding process differs on the molecular, functional level.

All vesiculation systems exhibit a three-layered structure: The inner layer is comprised of the lipid bilayer, and contains the transmembrane cargo and transmembrane coat recruitment machinery. The middle layer containing the adaptor- and adaptor-like proteins mediates the interaction between the outer, scaffolding coating protein layer and the transmembrane layer.

There are two conserved building motifs found in the coating proteins of all three vesiculation systems: α-solenoid structures and β-propeller domains. The α-solenoid structures are curved, elongated domains comprised of alpha helices arranged in a manner similar to a Jelly fold. While functions of the α-solenoid structures in the COPI system have not been

elucidated to date, these domains have distinct functions found in the COPII and the clathrin system: In clathrin, these domain form the legs of the clathrin molecule, and interdigitate to form the clathrin lattice (see 1.2.1.1 Structural studies on clathrin-coated vesicles). In the COPII system, in the Sec13/31 dimer, the α-solenoid structures do not interdigitate. Here, they serve as the linkers, forming the edges of the Sec13/31 lattice (see 1.2.2 COPII-coated vesicles).
The second building unit, the β-propeller domains, also have distinct functions in the three vesiculation systems: In the clathrin system, the terminal β-propellers serve as an interaction hub to mediate binding to the adaptor proteins and accessory proteins (see 1.2.1.1 Structural studies on clathrin-coated vesicles). In the COPII system, these domains form the vertices of the Sec13/31 cage (see 1.2.2. COPII-coated vesicles), and in the COPI system, they contain the binding sites of the coatomer complex to dibasic ER retrival signals (see 1.2.3.1 The COPI budding process).

The COPI system shows additional structural homology to the adaptor proteins. Two subunits of the adaptor-like subcomplex of coatomer, γ-COP and β-COP, display a subunit design similar to the one found in the adaptor proteins and the GGAs: The subunits contain a trunk and an appendage domain that are connected by a flexible linker, a hinge region.
However, the COPI coat exhibits a striking difference to the other two vesiculation systems: In both the COPII and the clathrin system, coat recruitment is mediated in two sequential steps. The COPI coating protein, coatomer, though, is recruited to the membrane en bloc.
In each system, recruitment of these coating proteins is governed by a small GTPase: In the COPII system Sar1p, in the clathrin system Arf1 and Arf6, and in the COPI system Arf1.
The minimal machinery to obtain generate vesicles in vitro has been defined in each system:

In the COPII system, minimal, empty cages comprised of Sec13/31 dimers were obtained in the absence of Sar1p and Sec23/24 (Stagg et al., 2006). Clathrin coated vesicles could be obtained from liposomes, in both the AP-1 and the AP-2 system using certain lipid components (only for AP-1), tyrosine-based sorting signals as transmembrane component, adaptor proteins and clathrin. The minimal machinery required for COPI vesicle budding is comprised of p24-family members as transmembrane components, the small GTPase Arf1, and the coating protein coatomer (Bremser et al., 1999).

In the various forms of the clathrin adaptor proteins, conformational changes are employed to activate the protein coat for cargo binding and to trigger coat lattice formation. A distinct conformational change in the coating protein coatomer has been also described in the COPI system: Upon interaction with the dimeric form of the p24-family member p23, the subunit γ-

COP changes its conformation (Reinhard et al., 1999). This conformational change may represent a crucial step in COPI coat lattice formation, as the conformation of coatomer polymerized by dimeric peptides of p23 corresponds to the one found on COPI vesicles generated in vitro.

γ-COPs homologue in the AP-2 complex, the μ2-subunit, also undergoes a conformational change during the budding process. Here, phosphorylation induces a conformational change that opens a binding pocket for Yxxϕ-based motifs (Matsui and Kirchhausen, 1990). Interaction with these Yxxϕ-motifs then induces a second conformational change in AP-2 that modulates binding of AP-2 to other cargo proteins (Haucke and De Camilli, 1999). This event was found to involve other subunits of the AP-2 complex, indicating that the conformational change in the AP-2 system is not a local event in the μ2-subunit (Boll et al., 2002), but that the whole adaptor protein complex changes into a membrane-bound form that is activated for cargo binding.

The structural details of the conformational change in the μ2-subunit are relatively well understood, and the crystal structure of the core of AP-2 has been solved. Only limited information exists on the structural and functional details in the COPI system, as only a fragment of one subunit of the coating protein, the trunk of γ-COP, has been crystallized to date (Watson et al., 2004). And although the key steps in the COPI vesicle budding process have been characterized, only little is known about the structural details and functional dynamics of the coating protein coatomer in the formation of a COPI vesicle.

1.3. Aims of present work

In the present work, the structural dynamics of coatomer were addressed by:

1. Characterisation of the conformational change in coatomer using single-pair, single-molecule FRET:
The conformational change in coatomer described by Reinhard (Reinhard et al., 1999) and Bethune (Bethune et al., 2006) represents a key step in the formation of a COPI vesicle. The polymerized, membrane bound form of coatomer undergoes a conformational change in gamma-COP upon recruitment to the membrane, that is triggered by binding of members of the p24-family, the transmembrane machinery found in COPI vesicles (Sohn et al., 1996).
In other coating systems, conformational changes are used specifically to activate the complexes for cargo capture, or formation of the coat lattice (reviewed by (Langer et al., 2007)). Here we ask if the conformational change induced in gamma-COP can be triggered by all p24-family members, and if it is a local event or affects the conformation of other subunits, i.e. the whole complex. To this end, we employed a combination of biochemical methods and a new biophysical method that allows direct observation of one subunit of individual coatomer complexes: Single-molecule, single-pair fluorescence resonance energy transfer (FRET).

2. Cryo-electron microscopic studies on COPI vesicles:
The structures of a clathrin vesicles and COPII vesicles have been solved, and recently cryo-EM studies have provided new insights into structural details and the architecture of these vesicles. Compared to the other vesiculation systems, relatively little is known about the architecture and structure of COPI vesicles, with only limited information obtained recently (Donohoe et al., 2007). In the present work, we generated COPI vesicles in vitro from purified Golgi membranes, coatomer and Arf1, and submitted these preparations to cryo-electron tomography.

2. Results

2.1. Conformational dynamics of coatomer

2.1.1. A conformational change in γ-COP: Screening p24-family members

Previous studies revealed that the coatomer complex has multiple binding sites for its different interaction partners (Bethune et al., 2006; Eugster et al., 2004; Sun et al., 2007a), and that a conformational change is triggered in the γ-subunit upon interaction with dimeric p23, a p24-family member (Reinhard et al., 1999). This conformational change causes coatomer to shift into an unsoluble, membrane-associated conformation, that is also found on COPI vesicles generated in vitro (Reinhard et al., 1999).

All members of the p24-family in their dimeric form bind to coatomer via two independent binding sites in the trunk and the appendage domain of γ-COP (Bethune et al., 2006), in contrast to the di-basic motif-containing cargo proteins that bind to α- and β'-COP (Eugster et al., 2004). We therefore investigated if binding to coatomer of all the p24-family proteins in either their monomeric or dimeric form would induce the conformational change observed with p23, and if cargo proteins can also trigger the conformational change. The sequences of the peptides used in this study are depicted in table 2.

p23	QVFYLRRFFKAKKLIE	p24 family members
p24	QIYYLKRFFEVRRVV	
p25	QMRHLKSFFEAKKLV	
p26	QVLLLKSFFTEKRPISRAVHS	
p27	QVFLIKSFFSDKRTTTTRVGS	
OST48	HMKEKEKSD	model cargo peptide

Table 2: Sequences of peptides used in this study. They represent the cytoplasmic tails of the p24-family members and of a model cargo protein, a subunit of the oligosaccharyl transferase 48 (OST48). The specific signal sequences are highlighted: The di-aromatic motif (FF, blue) and the dibasic-like motifs (red) in the p24-family members, and the KxKxx-ER-retrieval signal in OST48. The corresponding dimeric peptides were generated by introduction of an additional cystein at the C-terminus of the peptide, and mild oxidation.

To this end, we made use of the previous finding that the conformational change in γ-COP leads to precipitation of the complex, and that preciptated coatomer can be separated by centrifugation from the conformationally unchanged complex (Reinhard et al., 1999).

Coatomer was incubated at increasing concentrations of the various monomeric and dimeric peptides for 1h at room temperature, and centrifuged. The supernatants were discarded, and the pellets analyzed by SDS-PAGE and Coomassie staining, as shown in Figure 6.
Only small amounts of coatomer are precipitated in the absence of peptides (lane 2), or in the presence of monomeric p23 (lane 3) and monomeric p24 (lane 7). Dimeric p23 induced polymerization of coatomer in a dose-dependent manner, as expected (lane 4-6, (Reinhard et al., 1999)). Similarly, dimeric p24 caused precipitation dependent on its concentration (lanes 8-10). In contrast, only marginal polymerization of coatomer is caused even by highest concentrations of dimeric p25, p26 and p27 (lanes 11-13).
OST48, known not to bind to γ-COP but to α- and β'-COPs, did not cause significant polymerization (lane 14).

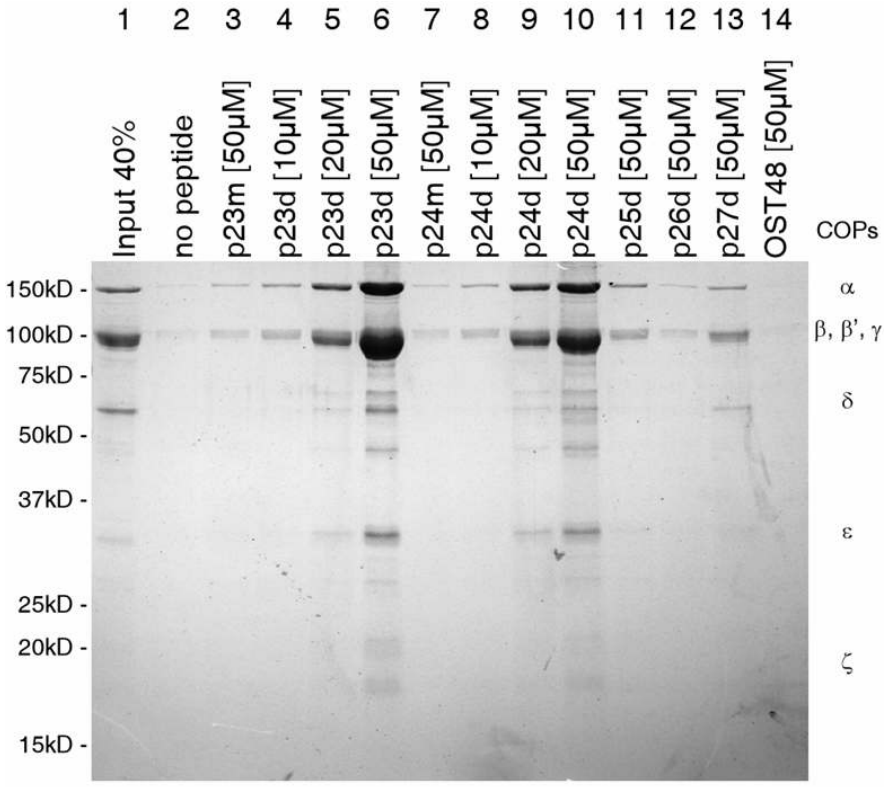

Figure 6: Precipitation of coatomer by p24-family proteins. Rabbit liver coatomer was incubated with peptides corresponding to the cytoplasmic tails of the proteins investigated, at the concentrations indicated. After incubation at room temperature for 30min, the samples were centrifuged and the pellets submitted to SDS-PAGE and stained by Coomassie.

As a result, of the dimeric cytoplasmic domains of p24-family proteins that all bind to γ-COP with similar affinity (Bethune et al., 2006), only p23 and p24 induce a conformational change in coatomer, and none of the peptides cause a conformational change when added in their monomeric form.
We now proceeded to ask whether this conformational change is a local event in γ-COP, or if the whole complex changes its conformation upon recruitment to the donor membrane and vesicle formation.

2.1.2. Limited proteolysis and screening of other coatomer subunits

The conformational change in γ-COP induced by dimeric p23 was first analyzed using limited proteolysis of the precipitated complex, showing an increased susceptability of a fragment of γ-COP in the polymerized form, that was also found on COPI vesicles (Reinhard et al., 1999). These findings imply that the conformational change in γ-COP, induced by dimeric cytoplasmic domains of p23, is an event that takes place during vesicle formation.
Here we used a similar approach, digesting coatomer with the protease Thermolysine, and screening the cleavage patterns of different subunits of coatomer. This allows screening of cargo proteins and all p24-family members in their monomeric and dimeric forms in a single set of experiments.

To this end, coatomer was incubated with both monomeric and dimeric peptides representing the cytoplasmic tails of p23 and p24, and dimeric peptides of the respecitve tails of p25, p26 and p27, and monomeric OST48. After allowing for ligand binding, the samples were treated with low concentrations (0.008µM) of thermolysine, and were incubated at room temperature for the times indicated. The reaction was then stopped by addition of EDTA (40mM), and the samples were submitted to SDS-PAGE and analyzed by Western blotting with an antibody directed against α-COP (Figure 7).
Strikingly, the susceptability of α-COP to proteolysis by Thermolysine was only decreased in the presence of both dimeric p23 and p24 (lanes 7,8 (p23d) and 11,12 (p24d)), as a double-band at 150kDa is still present even after 2h of protease treatment (lanes 8 and 12). The monomeric peptides of p23 and p24 were unable to alter the susceptibility of α-COP to Thermolysine (lanes 5,6 (p23m) and 9,10 (p24m)). In addition, neither monomeric OST48 nor the other members of the p24-family members in their dimeric form were able to modify the susceptability of α-COP for the protease (lanes 13-20).

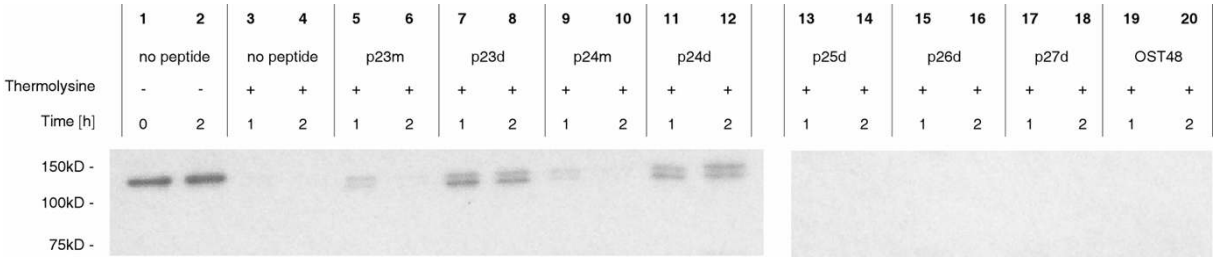

Figure 7: Limited proteolysis of coatomer. The complex was incubated with the peptides indicated at a concentration of 25µM for dimeric peptides and 50µM for monomeric peptides, and submitted to limited proteolysis by Thermolysine. The samples were then submitted to SDS-PAGE and analysed by Western Blotting with an antibody directed against α-COP.

Thus, the susceptatibility of α-COP changes only in the presence of the two p24-family members that are also capable of precipitating the complex in vitro. Interestingly, p23 and p24 are the only two p24 proteins that are able to recruit Arf1-GDP to the membrane, forming the priming complex in the early stages of COPI vesicle budding (Contreras et al., 2004; Gommel et al., 2001).

To validate these findings, we used an independent method that allows direct observation of the subunit investigated: Fluorescence resonance energy transfer (FRET). By selectively monitoring the conformation of the labeled α-subunit, we can analyze if the observed differential susceptability of α-COP is induced by γ-COP changing its conformation and covering up or revealing domains of α-COP after the conformational change. To this end, coatomer has to be specifically labeled on a single subunit with two fluorophores forming a FRET-pair.

2.1.3. Labeling of coatomer with fluorescent dyes

Various labeling approaches were considered to achieve specific labeling of one subunit of coatomer:

Coatomer is a heptameric complex that cannot be recombinantly expressed in prokaryotic expression systems. The individual subunits are not soluble by themselves, and only oligomeric subcomplexes displayed limited solubility (α-β'-ε-COP), which were not suitable for specific labeling.

A well-established approach that has been successfully employed to study the conformational dynamics of proteins is directed mutagenesis of all cysteins in the target protein, and the subsequent, site-specific introduction of two cysteines in different positions,

followed by specific labeling of their sulfhydryl-groups by thiol-reactive derivatives of the dyes. For coatomer, however, this approach is not feasible, as coatomer contains too many cysteine-groups (human α-COP (P53621) contains 27 cysteine-residues).
We also tested an approach based on the reversible dissociation of the coatomer complex (Pavel et al., 1998). Coatomer can be dissociated using an amine-reactive reagent, di-methyl maleic acid anhydride (dmma). Dmma reacts with primary amines, forming an amide bond and a free carboxylic acid moiety, thus "inverting" the charge at the position of the amino acid with the primary amine. This leads to a step-wise dissociation of the complex, with level of dissociation dependent on the excess of dmma employed. In addition, the dissociation was found to be subunit-specific, i.e. subcomplexes split up in a characteristic pattern implying differential reactivity to amine-reactive reagents.
The dissociation of coatomer did not yield satisfying amounts of soluble, dissociated subunits. However, these findings lead us to examine amine-reactive derivatives of the fluorophores in order to introduce the dyes into the coatomer complex.

2.1.4. Labeling with amine-reactive dyes

To this end, we incubated the purified complex with N-Hydroxyl-succinimidyl-ester-derivatives (NHS-esters) of the dyes Cy3 and Cy5. To ensure deprotonation of reactive ε-amino-groups we increased the pH to 8.0, and conducted the reaction at 0°C (ice water). Labeled complex was separated from the free dye by a small gel filtration column (Sephadex G-50, see materials and methods), purified by immunoprecipitation with an antibody specific for native coatomer (CM1, (Palmer et al., 1993)) and submitted to SDS gel electrophoresis. The labeling of individual subunits was detected by scanning of the gel using a confocal setup with the corresponding lasers focused into the gel (see materials & methods). Figure 7 shows these fluorescence intensity traces of coatomer labeled with Cy3, purified by immunoprecipitaion and submitted to SDS gel electrophoresis (6% gels).

The specifity of the reaction was found to be dependent on the concentration of dye reagent used for the reaction. With a high concentration of labeling reagent, all large subunits of coatomer were found to be labeled (Figure 8 D). The bands showing significant fluoresence intensity correspond to α-, β-, β'- and γ-COP, with the relative degree of labeling dependent on the concentration of labeling reagent used (Figure 8B-D).

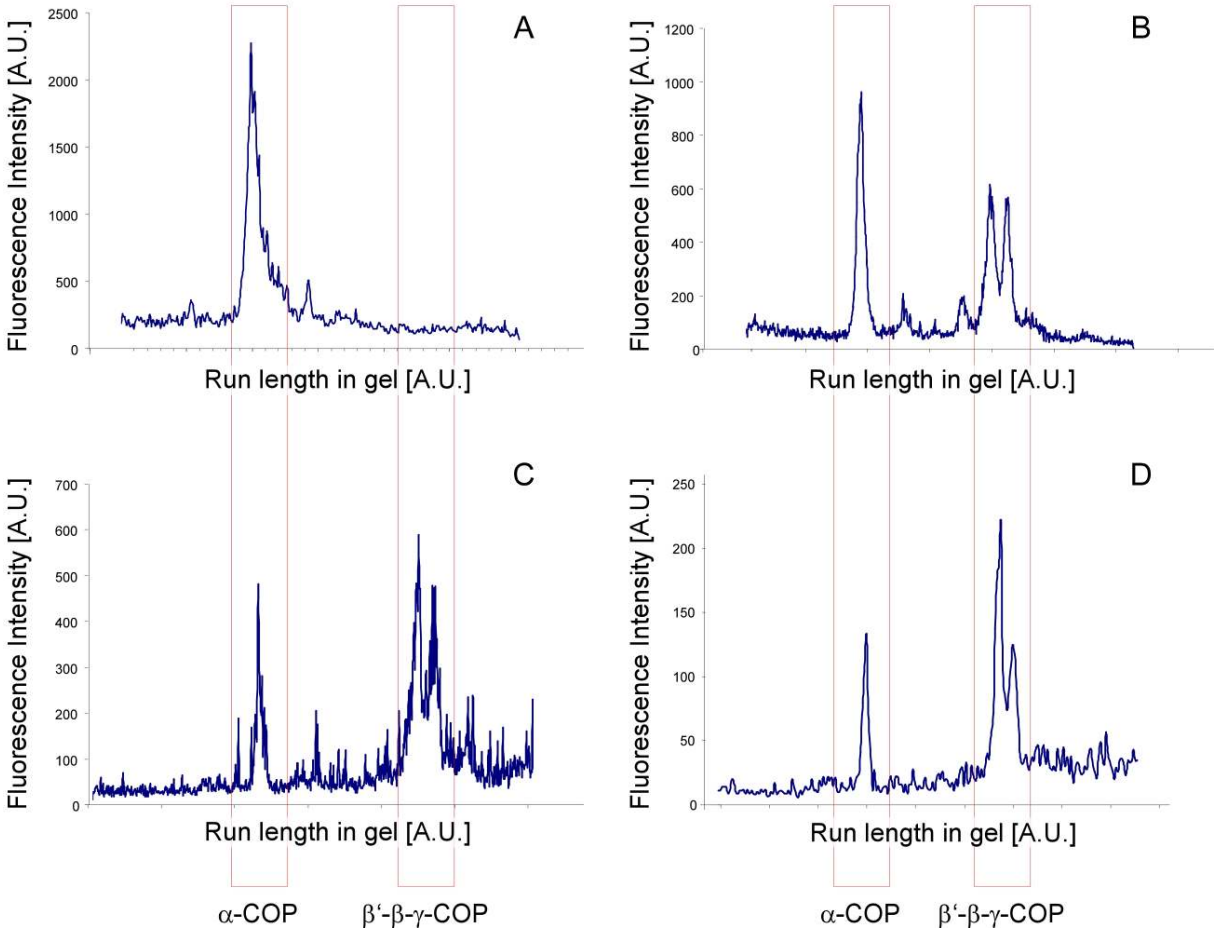

Figure 8: Analysis of coatomer after labeling with different concentrations of amine-reactive derivatives of the fluorescent dye Cy3. The samples were purified by immunoprecipitation, and submitted to SDS-PAGE (6%), and the fluorescence intensity traces were recorded upon excitation at 532nm. **A**: 600pmol Cy3-NHS-ester. The single fluorescence peak coincides with the position of α-COP. **B**: 1.5nmol Cy3-NHS-ester. Besides the prominent peak for α-COP, additional peaks in the fluorescence intensity trace are visible, running with the 100kDa family of coatomer subunits (β-, β' and γ-COP). **C**: 8nmol Cy3-NHS-ester. Almost equel relative labeling of α-COP and the 100kDa-family coatomer subunits. **D**: 1µmol Cy3-NHS-ester. The labeling of the 100kDa-family subunits exceeds α-COP.

Using the conditions that were used to label coatomer scanned in Figure 8A, specific labeling of α-COP was achieved. Figure 9 shows a coatomer sample after labeling with Cy3 and Cy5, purification by immunoprecipitation with CM1 (Palmer et al., 1993), subsequent separation of the subunits by SDS gel electrophoresis (6-15% gradient gel), and staining with Coomassie. Bands representing COPs are indicated with the corresponding greek letters. Additional bands are impurities, mainly introduced by the antibodies used for immunoprecipitation.

Fluorescence intensity traces of the lanes corresponding to the Cy3- and Cy5-emission channels, detected by scanning with a confocal setup (see Materials and Methods), are shown in Figure 9 C and D, respectively. The fluorescence intensity shows a prominent peak in both channels at a molecular mass corresponding to alpha-COP.

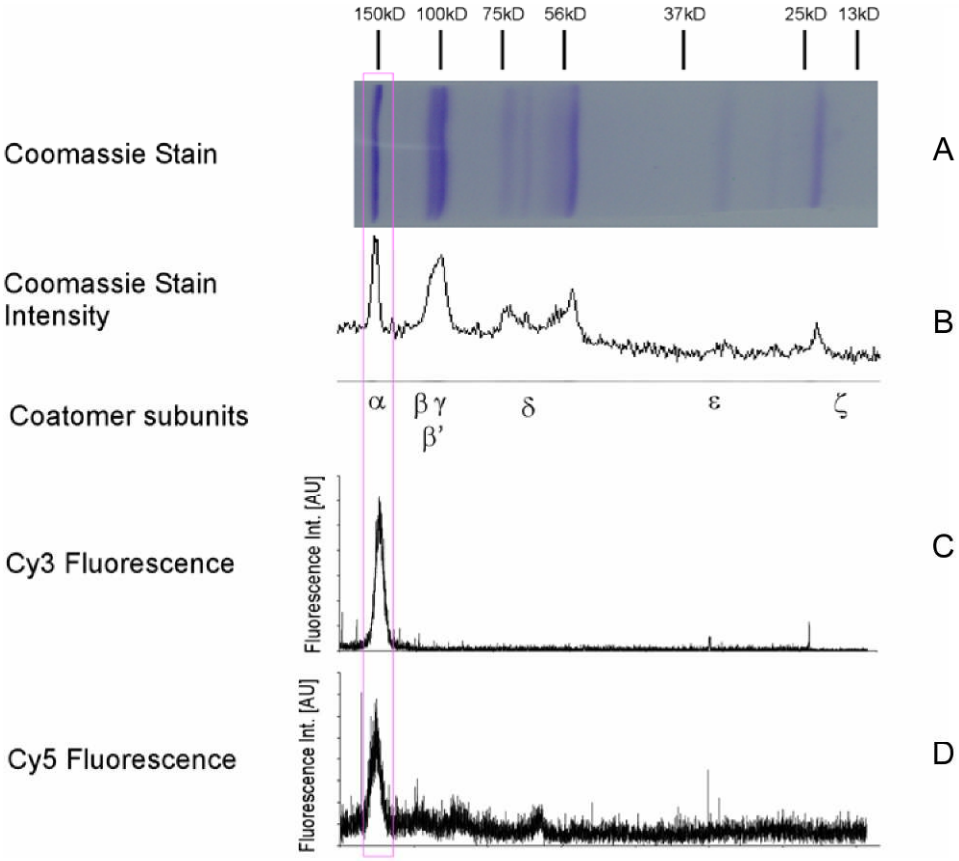

Figure 9: Analysis of coatomer after labeling with amine-reactive derivatives of the fluorescent dyes Cy3 and Cy5. **A**: Coomassie stained SDS-PAGE gel of Cy3-Cy5-labeled coatomer purified by immunoprecipitation with CM1. **B**: Coomassie intensity trace, individual subunits are inidcated. **C**: Cy3 fluorescence (excitation 532nm) and (**D**) Cy5-fluorescence (excitation at 635nm) intensity of labeled coatomer separated by SDS-PAGE and purified by immunoprecipitation with CM1. (The unlabeled bands at ~50kDa and ~25kDa represent IgG heavy and light chains, respectively).

Total fluorescence emission of the protein bands was calculated for the alpha-subunit and the beta, beta' and gamma-subunits. An average of 96% of the emission in the Cy3 channel and 90% of the emission in the Cy5 channel results from the protein band corresponding to the α-subunit. Thus, almost exclusive labeling of one subunit within coatomer, namely alpha-

COP, was achieved. The labeling efficiency was estimated as described in Materials and Methods, and found to be about one Cy3 and one Cy5 dye per coatomer.

2.1.5. Functionality of labeled coatomer

As described above, coatomer was specifically labeled on its α-subunit. Next, we investigated whether labeled coatomer retains its functionality, i.e. its capability to bind to ligands and membranes, and to form COPI vesicles in vitro.

First, binding of cytoplasmic tail domains of membrane proteins to the labeled complex was investigated in pull-down experiments. To investigate if both the γ-COP binding sites for p24-family members and the α- / β'-COP cargo binding sites retained their capability to bind to their binding partners after labeling, labeled and unlabeled coatomer was incubated with immobilized fusion proteins harbouring the cytoplasmic domains of OST48 or dimeric p23. Bound coatomer was recovered, submitted to SDS gel electrophoresis and analyzed by Western blotting with antibodies directed against α-COP and δ-COP. As shown in Figure 10, both labeled and unlabeled coatomer show similar binding to these domains (compare lanes 5 and 6, and lanes 7 and 8), and no unspecific binding of labeled or unlabeled coatomer was observed (lanes 3 and 4).

In order to analyze whether bound coatomer is in fact labeled, the blot was analyzed with antibodies directed against the dyes Cy3 and Cy5. Coatomer is labeled with the dyes exclusively on the alpha-subunit as shown in Figure 10, lanes 6 and 8. The remarkable specificity of the reaction is visualized by comparison of the input crude coatomer preparation after labeling (Figure 10, lane 2) with the bound samples (Figure 10, lanes 6 and 8), where a striking loss of non-coatomer protein is observed.

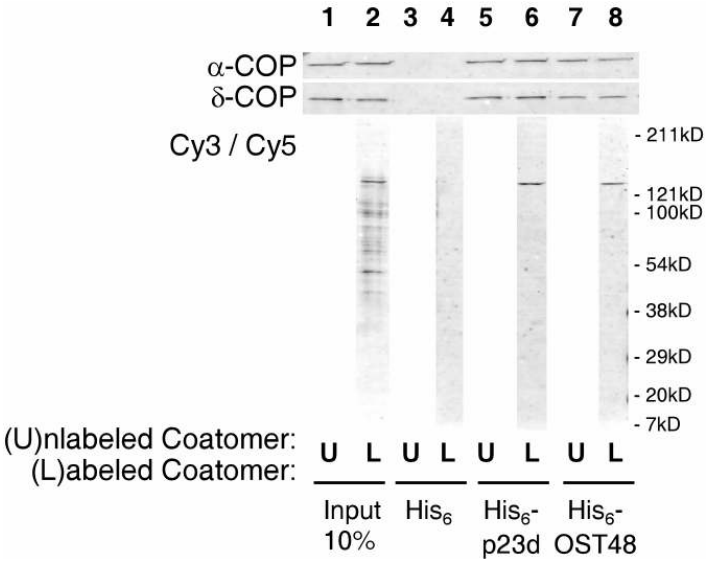

Figure 10: Functionality of labeled coatomer: Binding to the cytoplasmic domains of p23 and OST48. His_6-constructs of the cytoplasmic tails of p23d and OST48, or a His_6-construct as a control, were immobilized on Ni-Sepharose and incubated with identical amounts of labeled or unlabeled coatomer, and then washed. Subsequently, bound coatomer was eluted with SDS sample buffer, subjected to SDS-PAGE and detected by Western blotting (antibodies directed against α-COP, γ-COP and Cy3/Cy5).

Second, functionality of labeled coatomer was evaluated by analysing its ability to bind to Golgi membranes. This process depends on prior binding of the small GTP binding protein Arf1 in its active GTP-form to these membranes, and thus is GTP-specific. Partially purified, labeled or unlabeled complex was incubated with Golgi-enriched membranes and Arf1 in the presence or absence of GTPγS (a non-hydrolyzable analogue of GTP). Thereafter, the membranes were recovered by centrifugation, and the amount of coatomer bound was estimated using SDS-PAGE and Western blotting with antibodies directed against alpha-COP. The amount of membranes loaded was controlled by the presence of the membrane protein p24. Figure 11 shows that similar amounts of labeled and unlabeled coatomer are recruited to Golgi membranes (comparing alpha-COP in lanes 6 and 7), and that this recruitment is dependent on the presence of Arf1 in its active, GTP-bound form (compare lanes 4 and 5 with 6 and 7). No labeled or unlabeled coatomer was found in the pellet in the absence of Golgi membranes (Figure 11, lanes 8 and 9).

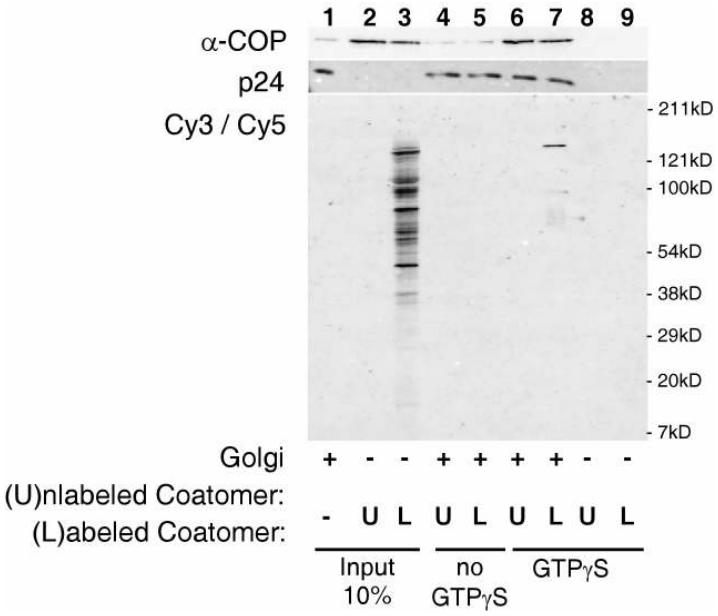

Figure 11: Functionality of labeled coatomer: Membrane binding assay. Identical amounts of labeled or unlabeled coatomer were incubated with purified Golgi membranes and Arf1 in the presence or absence of GTPγS. Subsequently, Golgi membranes were centrifuged and subjected to SDS-PAGE and immunoblotting (with antibodies directed against α-COP, p24 or the dyes Cy3/Cy5, as indicated).

The samples were redecorated with an antibody directed against the fluorescent dyes, to test whether coatomer bound to Golgi membranes (shown in Figure 11) is also labeled. Labeling was detected, and found to be exclusively on the α-subunit of coatomer, as shown in Figure 11, lane 7. The multiple bands visible in the crude input (Figure 11, lane 3;) are degradation products and other, contaminating proteins that are also labeled with Cy3 and Cy5.

Third, the capability of the labeled coatomer complex to support COPI vesicle formation was investigated. To this end, Cy3/Cy5-labeled coatomer was added to an in vitro COPI budding assay with purified Golgi membranes, Arf1 and GTPγS. A vesicle fraction was purified by differential centrifugation as described in Materials and Methods, and its protein content analyzed by SDS-PAGE and Western blotting. As shown in Figure 12, the coat protein pattern typical of COPI vesicles is obtained in the sample incubated with GTPγS, harvested from a 47% sucrose cushion. Decoration with anti-Cy3/Cy5 antibodies reveals a band that migrates with α-COP (lane 2). No detectable amounts of coatomer are found in a control fraction from a sample incubated in the absence of GTPγS.

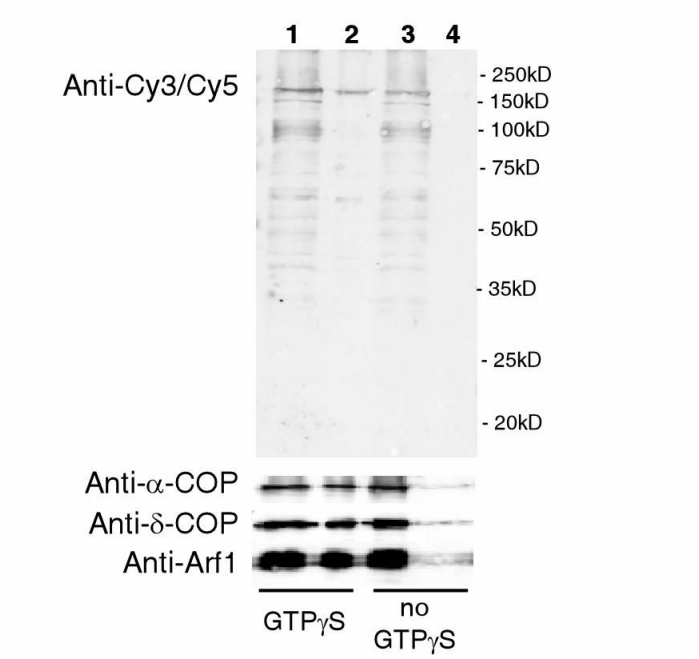

Figure 12: Functionality of labeled coatomer: In vitro formation of COP vesicles. Golgi membranes were incubated with Arf1 and labeled coatomer in the presence and absence of GTPγS. After centrifugation, the fractions containing purified vesicles were submitted to SDS-PAGE and analyzed by Western blotting with antibodies directed against α-COP, δ-COP, Arf1 and Cy3/Cy5, as indicated.

From these analyses we conclude that the functionality of coatomer is not compromised by the labeling process, and that functional coatomer bears the dyes on its α-subunit.

2.1.6. Specific immobilization of labeled coatomer

Initial FRET experiments involving ensemble measurements showed that, in order to investigate the conformational dynamics of coatomer, we had to design a single-molecule-sensitive assay. This new assay was designed to overcome the following three issues:

1. Coatomer precipitates upon interaction with dimeric p23 p24. As shown previously, the conformational change induced in γ-COP by dimeric p23 and p24 leads to precipitation of coatomer. This effectively excludes measurements in solution, as the complex both aggregates and is removed from the measurable pool of soluble proteins.
2. The preparation of coatomer from rabbit liver contains 10-30% of other contaminating proteins, that may also be tagged with a dye as described in the labeling procedures. These contaminations have to be removed prior to measurements.

3. The labeling approach described above generates a heterogenous population of labeled coatomer, with populations of coatomer carrying a varying number of dyes. The new assay must be able to specifically select singly donor- and acceptor-labeled coatomer.

Thus, a surface-based, single-molecule-sensitive assay using a scanning confocal microscope was developed.

A surface-based assay also allows monitoring of the conformational dynamics of individual, tethered coatomer complexes, as immobilization of coatomer effectively prevents precipitation and aggregation of the complex.
The surface-based assay also allows screening of individual labeled complexes, and selection of singly-donor and –acceptor labeled complexes by evaluating the number of attached dyes by specifically illuminating individual spots and assessing their fluorescene intensity trace over time. Such a selection is stringently required since the statistical labeling process used here generates coatomer molecules labeled at a 1:1 stoichiometry for Cy3 and Cy5, without excluding complexes labeled multiple times, as mentioned before.
Subsequently, the efficiency of the FRET signal can be calculated for each, singly-donor and singly-acceptor labeled coatomer complex. After sorting into a histogram, this allows monitoring of individual sub-populations of conformationally changed and unchanged complexes. In ensemble measurements, the read-out is always the averaged value for all different populations present in the measured sample. In contrast, in the setup described here, we can identify individual coatomer populations that have or have not undergone a conformational change.

Thus, as a first step, specific recruitment of coatomer from solution to a glass surface had to be established.

To ensure efficiency and specificity of this immobilization, we chose an antibody that binds native coatomer, CM1 (Palmer et al., 1993). This antibody is a monoclonal antibody available from hybridoma cell line supernatant, thus being first choice in both specificity and availability.

As a bulk protein to quench unspecific adsorption of coatomer and other contaminating proteins to the surface, we chose bovine serum albumin (BSA). Previous studies in our lab showed that surfaces incubated with specific coatomer binding partners and passivated with

BSA can be used to specifically recruit coatomer in an ELISA-like assay (Bethune et al., 2006).

The following criteria have to be addressed for the single-molecule-sensitive FRET studies we aimed at:

- The individual, labeled coatomer complexes must be spaced sufficiently far apart, so that their emission spots (point spread functions, PSF) do not overlap, to allow selection of individual complexes for subsequent aquisition of their fluorescence intensity traces over time for FRET efficiency calculation.
- A sufficient number of labeled coatomer complexes must be aquired in a typical scanning area of 20µm x 20µm for efficient data aquisition.

In the present study, two approaches were investigated to accomplish efficient and specific recruitment of coatomer to a glass surface, and retain functionality of the immobilised complex.

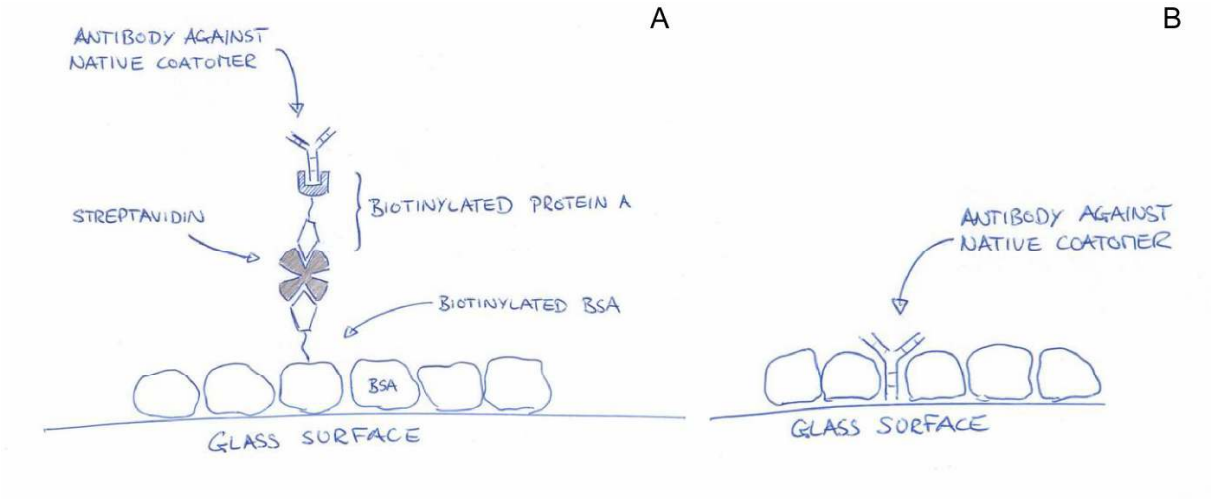

Figure 13: Immobilisation strategies to specifically tether labeled coatomer to a glass surface. BSA was chosen as a bulk protein to prevent unspecific adsorption to the surface. Both approaches are based on the monoclonal antibody CM1 that recognizes assembled coatomer only.

A. Biotinylated biotin-based immobilisation of coatomer using CM1

The first approach was based on a sandwich-concept (see figure 13A), with biotinylated BSA as an anchor function on the surface. The advantage of this method is that, with a mixture of biotinylated BSA and normal BSA forming a relatively homogenous layer on the glass surface, unspecific adsorption to the surface itself should be minimized.
To immobilize the CM1 antibody on this surface, recombinant streptavidin and biotinylated Protein A was applied to the surface, followed by a solution of CM1 antibody purified from the hybridoma cell line supernatant by Protein A affinity purification.
Subsequently, titration experiments were performed to find conditions to specifically recruit labeled coatomer. Here, however, increasing unspecific adsorption to the sandwich construction was detected upon additon of each, further component. After addition of relatively small concentrations of biotinylated Protein A, adsorption of labeled protein was detected even in the absence of CM1. Also, using different buffers (with higher salt concentrations to quench electrostatic interactions), detergents (up to 1% NP-40) and lowering of the density of the anchor functions did not quench unspecific adsorption.
Thus, the second approach was tested.

B. Direct, antibody-based immibilization using CM1

The second approach utilizes the same central anchor function to specifically immobilize coatomer, the antibody CM1. The antibody was purified by Protein A affinity purification and subsequently directly applied to the activated glass surface. To quench unspecific adsorption to the surface, the purified antibody was administered in a solution containing excess bulk protein, BSA.
To find conditions suitable for single-molecule-sensitive FRET experiments as described above, various concentrations of antibody and of coatomer administered to the surface were screened. As a starting value for the anchor functions, a concentration of antibody was chosen that had shown good results for biotinylated BSA (data not shown).
To control for unspecific adsorption to an antibody-BSA surface, an antibody directed against an unrelated protein, the Okt8 antibody directed against the CD8 receptor, was applied in a parallel set of experiments. To increase the stringency of the system, high-salt phosphate-based buffer and washing steps with buffers containing 0.5% NP-40 were used (see Materials and Methods). As previous studies showed that the ζ-subunit of coatomer partially dissociates from the coatomer complex if exposed to 1% of NP-40 for more than 30 minutes, only a short incubation (10min) with buffer containing 0.5% NP-40 was chosen.

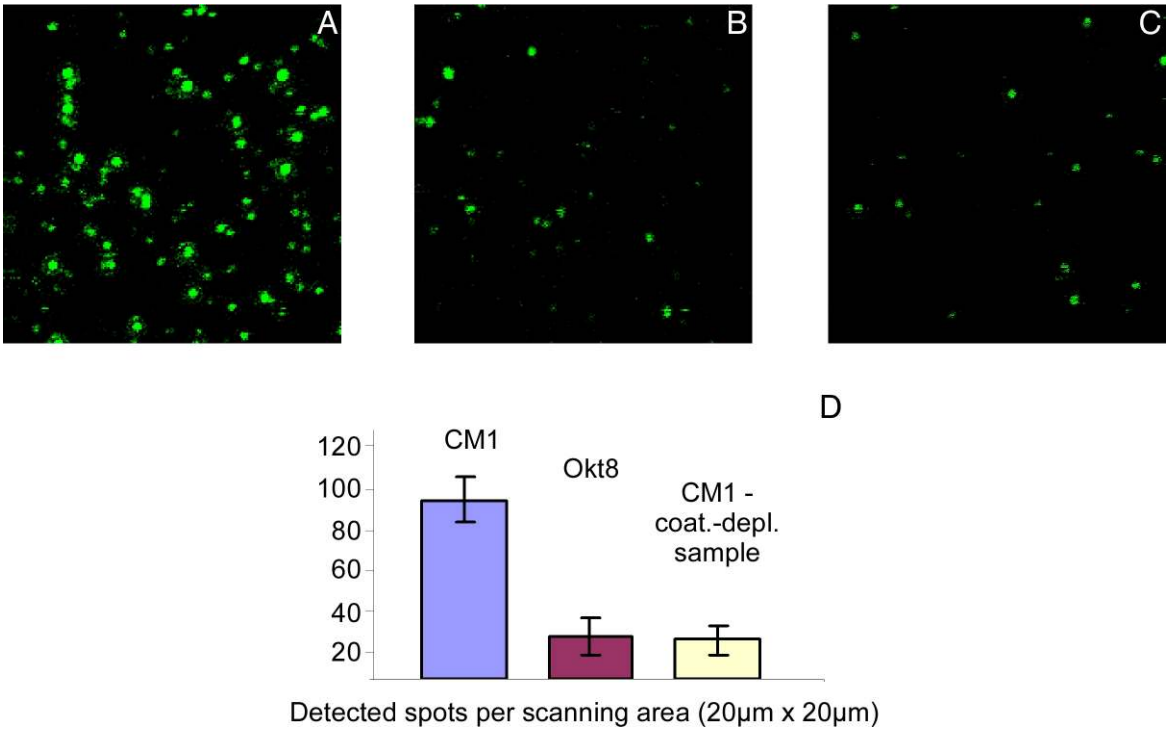

Figure 14: Low intensity surface scans (20µm x 20µm) of glass surfaces coated with a BSA-antibody solution. **A**: Scanned area of a BSA-CM1 surface incubated with 3ng of Cy3-labeled coatomer. **B**: BSA-Okt8 surface after administration of 3ng of Cy3-labeled coatomer. **C**: BSA-CM1 surface incubated with a sample depleted of coatomer. **D**: Quantification of surface densities for the described conditions (n=10).

Figure 14 shows a set of experiments with identical amounts of labeled coatomer applied to a BSA – CM1 surface. Unspecific adsorption was investigated by applying labeled coatomer to a BSA – Okt8 surface in identical conditions.

Labeled coatomer was detected by low intensity fluorescence scans of 20µmx20µm areas on the antibody-BSA surfaces as shown in Figure 14A-C. With the CM1 antibody, 86±13 (S_E, n=10) spots can be observed in one scanning area (Figure 14A).
Unspecific adsorption was quantified by adding an identical concentration of Cy3-labeled coatomer to a surface incubated with an unrelated antibody (Okt8, specific for the protein CD8; 21±8 spots (S_E, n=10), Figure 14B).

In order to test for unspecific adsorption of contaminating proteins in the coatomer preparations to the CM1-antibody surface, a sample of labeled coatomer was depleted of coatomer by three successive immunoprecipitations with an antibody directed against the α- and γ-subunits according to an established protocol (Wegmann et al., 2004). The coatomer-depleted supernatant, representing contaminating, labeled proteins in the coatomer

preparation, was administered to a CM1 surface in conditions identical to those used above. In a 20µmx20µm area, 19±8 (S_E, n=10) spots were detected (Figure 14C).

These results are quantified in Figure 14D, and show that coatomer can be specifically immobilized on a glass surface covered with an antibody-BSA mixture using the antibody CM1.
The conditions depicted in figure 14 were chosen for subsequent experiments, as both a sufficient number of spots was detected per scanning area, and the spots were separated far enough to allow selection of individual, labeled complexes.

2.1.7. Surfaces with Cy3-Cy5-labeled coatomer

Next, coatomer labeled with both Cy3 and Cy5 was immobilised on CM1-BSA surfaces prepared as described above. Figure 15 shows low-intensity surface scans of 20µmx20µm areas, excited with a 532nm laser (donor only).

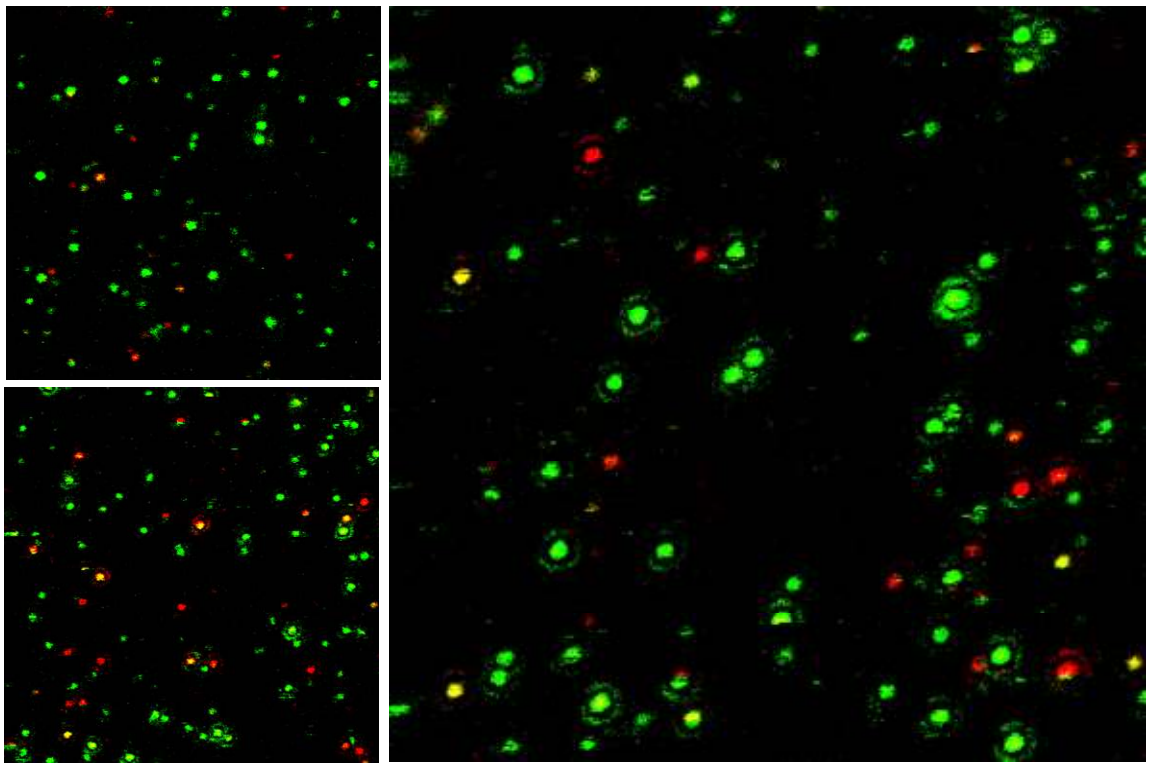

Figure 15: Low intensity surface scans (20µm x 20µm) of glass surfaces coated with a BSA-antibody solution and incubated with Cy3-Cy5-labeled coatomer. Samples were excited with a 532nm Nd:YAG laser, and FRET detected by acceptor emission (donor emission imaged in green, acceptor emission imaged in red).

About 30% of the spots show FRET, i.e. emission in the acceptor channel upon donor excitation, as depicted in Figure 15 (donor channel emission: green; acceptor channel emission: red). Different populations are clearly visible, with spots showing lower (yellow) and higher energy transfer efficiency (red).

2.1.8. Inter- or intramolecular FRET?

The detected FRET signal could derive from either intramolecular FRET or intermolecular FRET between two adjacent, labeled coatomer molecules. In order to discern intra- from intermolecular FRET, two separate labeling reactions were performed: One sample of coatomer was labeled with Cy3 only, and another sample was labeled with Cy5 only.
Subsequently, a BSA-CM1 surface was incubated with a 1:1 mixture of these labeled coatomer preparations, and examined by low-intensity surface scans. As shown in Figure 16A, no emission was observed in the acceptor channel upon donor excitation. The presence of Cy5-labeled coatomer on these surfaces was visualized by direct acceptor excitation (Figure 16B).
In addition, no intermolecular FRET by aggregation was detected after addition of dimeric p23 (Figure 16C, acceptor presence was confirmed by direct excitation, shown in Figure 16D).

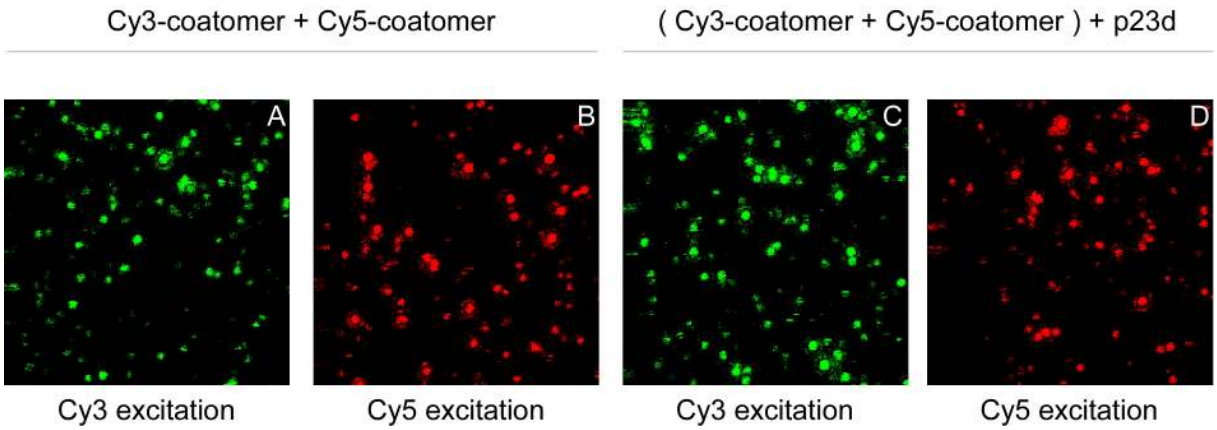

Figure 16: Low intensity surface scans (20µm x 20µm) of glass surfaces coated with a BSA-antibody solution and incubated with a 1:1 mixture of Cy3-labeled coatomer and Cy5-labeled coatomer. Samples were illuminated with 532nm for Cy3 excitation, and with 635nm for Cy5 excitation. No acceptor emission was detectable upon donor excitation both prior to and after addition of dimeric p23d (**A** and **C**), and the presence of Cy5-labeled coatomer was controlled by direct acceptor excitation (**B** and **D**).

From these data, we conclude that the acceptor emission observed for Cy3-Cy5-labeled coatomer is due to intramolecular energy transfer.

2.1.9. Assessing the number of attached dyes

To assess the number of attached dyes, the spots showing emission in the acceptor channel upon donor excitation were further analyzed by monitoring their fluorescence intensity traces over time. To this end, these spots were selected and photo-bleached by continuous illumination at 532nm, and their bleaching pattern, i.e. their fluorescence intensity trace over time, was recorded. For this analysis, only spots showing acceptor emission upon donor excitation were picked, as shown by the selected spots in Figure 17A and B (for details, see Materials and Methods).

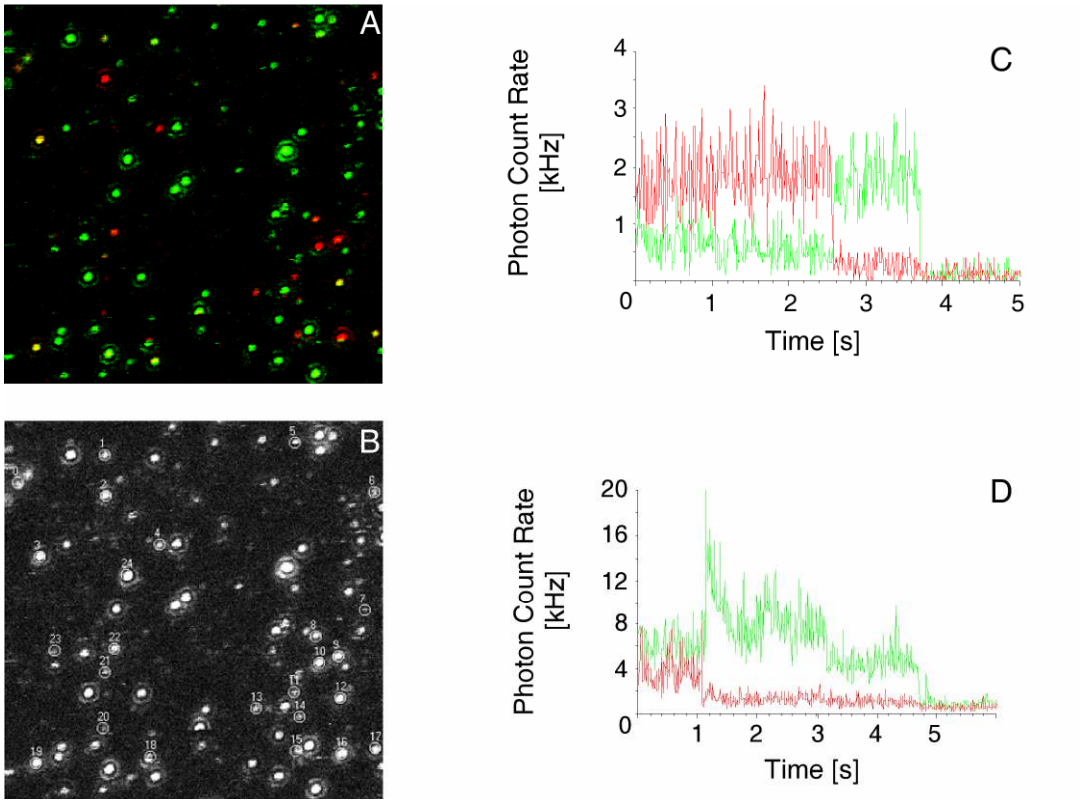

Figure 17: Single-pair FRET in coatomer. **A**: Low intensity surface scan (20µm x 20µm) of a glass surface coated with a BSA-antibody solution and incubated with Cy3-Cy5-labeled coatomer. **B**: Selection of spots (numbered circles) picked for subsequent recording of fluorescence intensity trace (see Materials and Methods for selection criteria). **C** and **D**: Representative fluorescence intensity traces of spots, as used for data acquisition and evaluation. Intensity traces showing a clear bleaching pattern, indicating singly donor- and acceptor-labeled molecules, with a simultaneous increase in donor emission upon acceptor bleaching, and single bleaching events in both the donor and the acceptor channel, as in B,

were further analyzed. The trace depicted in **D** shows multiple intensity changes after 1.5, 3, and 4.8 seconds indicating labeling with more than one Cy3 fluorophor.

Figure 17 shows typical fluorescence intensity traces recorded in these experiments. Traces were used for subsequent energy transfer efficiency calculation only if they fulfilled the following criteria:

1. A single bleaching event in both the donor and the acceptor channel, leading to a drop to background levels in single step.
2. An increase in donor emission upon acceptor photobleaching.

Figure 17C shows a single bleaching event in the acceptor channel, with a simultaneous increase in donor emission upon acceptor photobleaching. Subsequently, donor emission drops to background level in a single step, thus indicating single donor and acceptor labeling.

Figure 17D displays a fluorescence intensity trace with multiple bleaching steps after 1.5, 3 and 4.8 seconds, indicating multiple labeling of the complex. These traces were discarded. Thus, the fraction of coatomer labeled with multiple donor and acceptor dye molecules is minimized in our FRET statistics.

2.1.10. Approximating the FRET efficiency E_{app}.

The FRET efficiency was approximated by evaluating the relative emission intensities in the donor and acceptor channel, using a ratiometric approach:

$$E_{app} = E_A / E_A + E_D$$

(see Materials and Methods, and (Deniz et al., 2001; Ha, 2001)). To this end, the following data were extracted from the fluorescence intensity traces: The total emission in the donor channel, the total emission in the acceptor channel, and background emission. Only traces with more than 200 photons in both channels were kept for subsequent analysis.

After correction for crosstalk, the FRET efficiency was calculated for each fluorescence intensity trace as described in Materials and Methods. Each complex was subsequently sorted into a normalized histogram.
The calculated FRET efficiencies for CM1-immobilized, Cy3-Cy5-labeled coatomer are summarized in Figure 18 (n=216). A major population with an energy transfer efficiency of

E_{app} = 55-70% can be clearly discerned, with its center at 63%, as determined by fitting a Gaussian function to the data (see Materials and Methods).

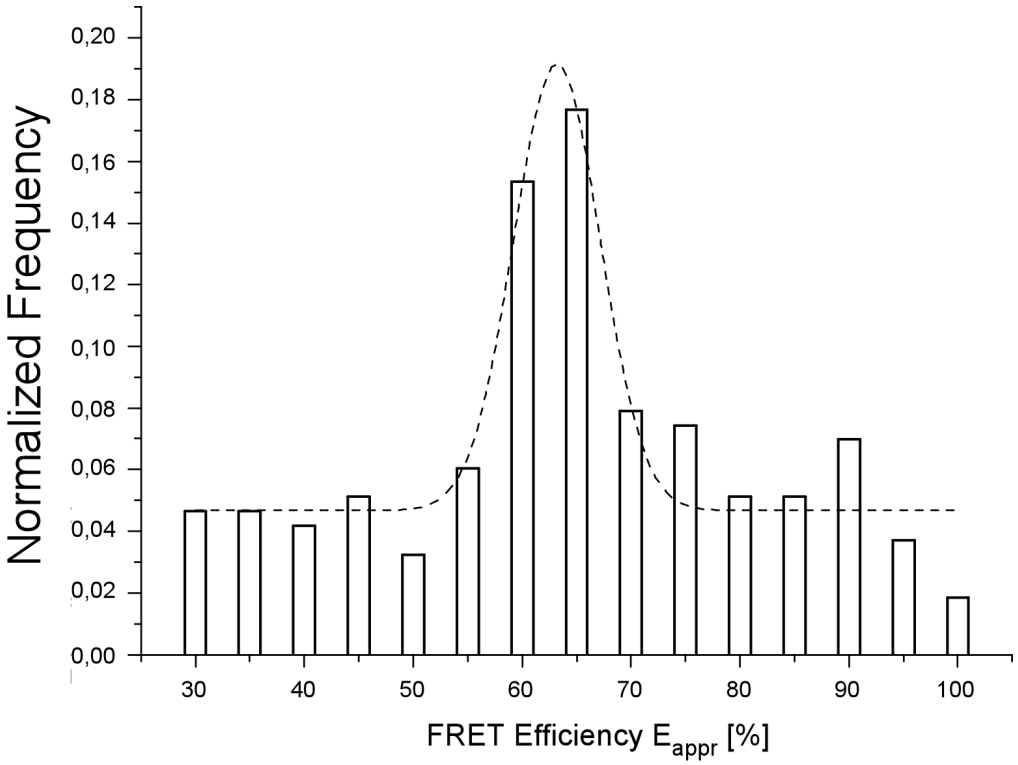

Figure 18: Normalized histogram for Cy3-Cy5-labeled coatomer, no peptide added (n= 214, class size: 5%). A major population can be identified, centered at a FRET efficiency of 63%.

2.1.11. Interaction of coatomer with cytoplasmic tail domains of ligand proteins

In order to investigate the interaction of coatomer with p23 and OST48, the FRET efficiencies of the labeled complex were analyzed after addition of synthetic peptides resembling the cytoplasmic tail domains of these proteins. Both ligands were used at a concentration of 20µM, i.e. well above the K_D and below saturation (Bethune et al., 2006).

First, the interaction of coatomer with OST48 was investigated. OST48 is a cargo protein that binds as a monomer to the predicted β-propeller domains on the α- and β'-subunits of coatomer (Eugster et al., 2004). The corresponding peptide was added and the FRET efficiencies of individual complexes were analyzed. As depicted in Figure 19, a major population is found that displays an energy transfer efficiency centred at 67%, with a broadened peak. Thus, after addition of OST48, the centre of the population has shifted

slightly from 63% to 67%, as seen in the overlay shown in Figure 19B. This shift is within the resolution limits of the method used.

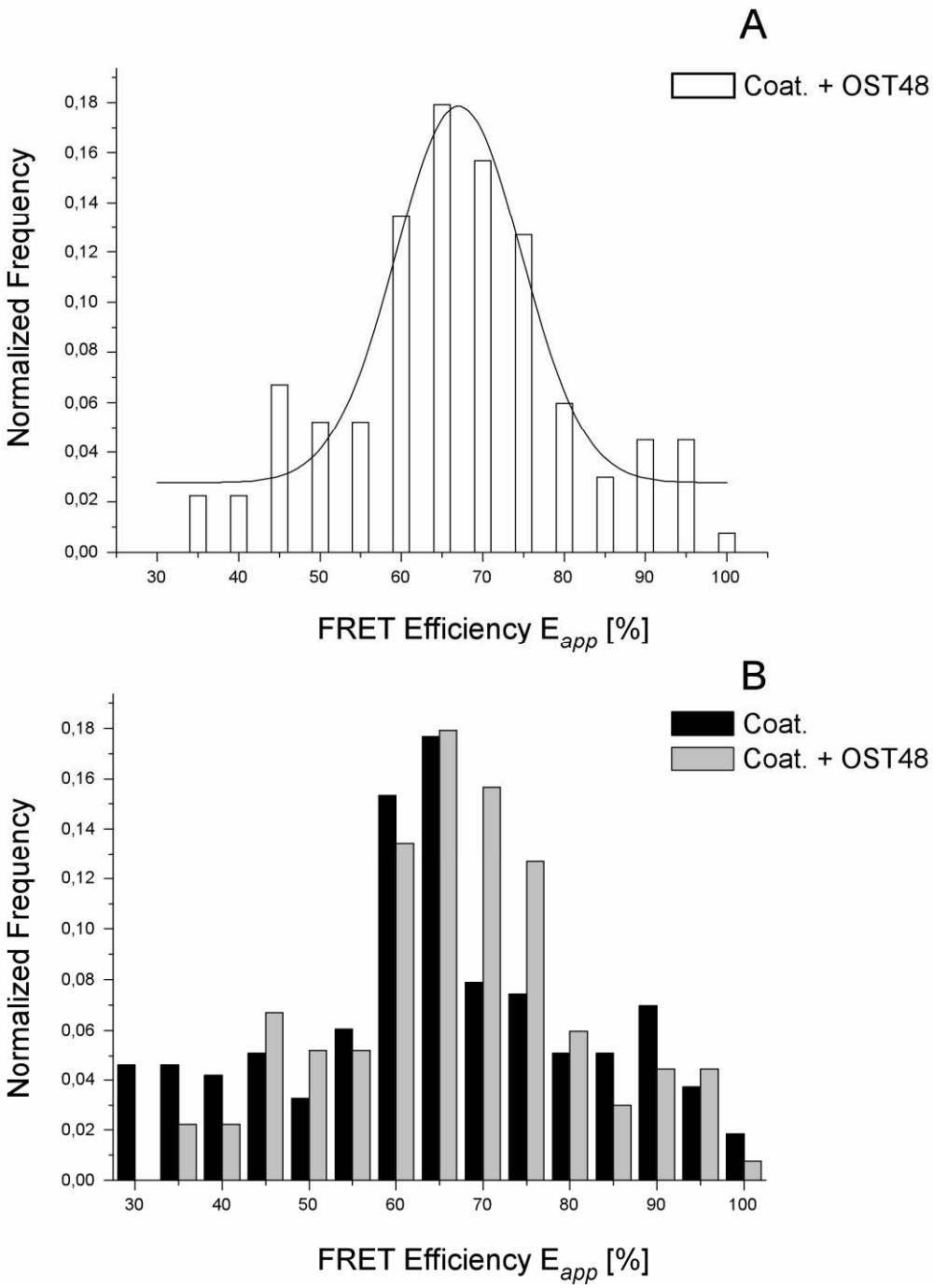

Figure 19, A: Normalized histogram for Cy3-Cy5-labeled coatomer, after addition of 20µM OST48 (n= 138, class size: 5%). The major population is centered at a FRET efficiency of 67%. **B**: Overlay of normalised histograms prior to and after addition of OST48.

Next, the interaction of coatomer with p23 was analyzed by adding a dimeric peptide representing the cytoplasmic tail of p23 to the surface.

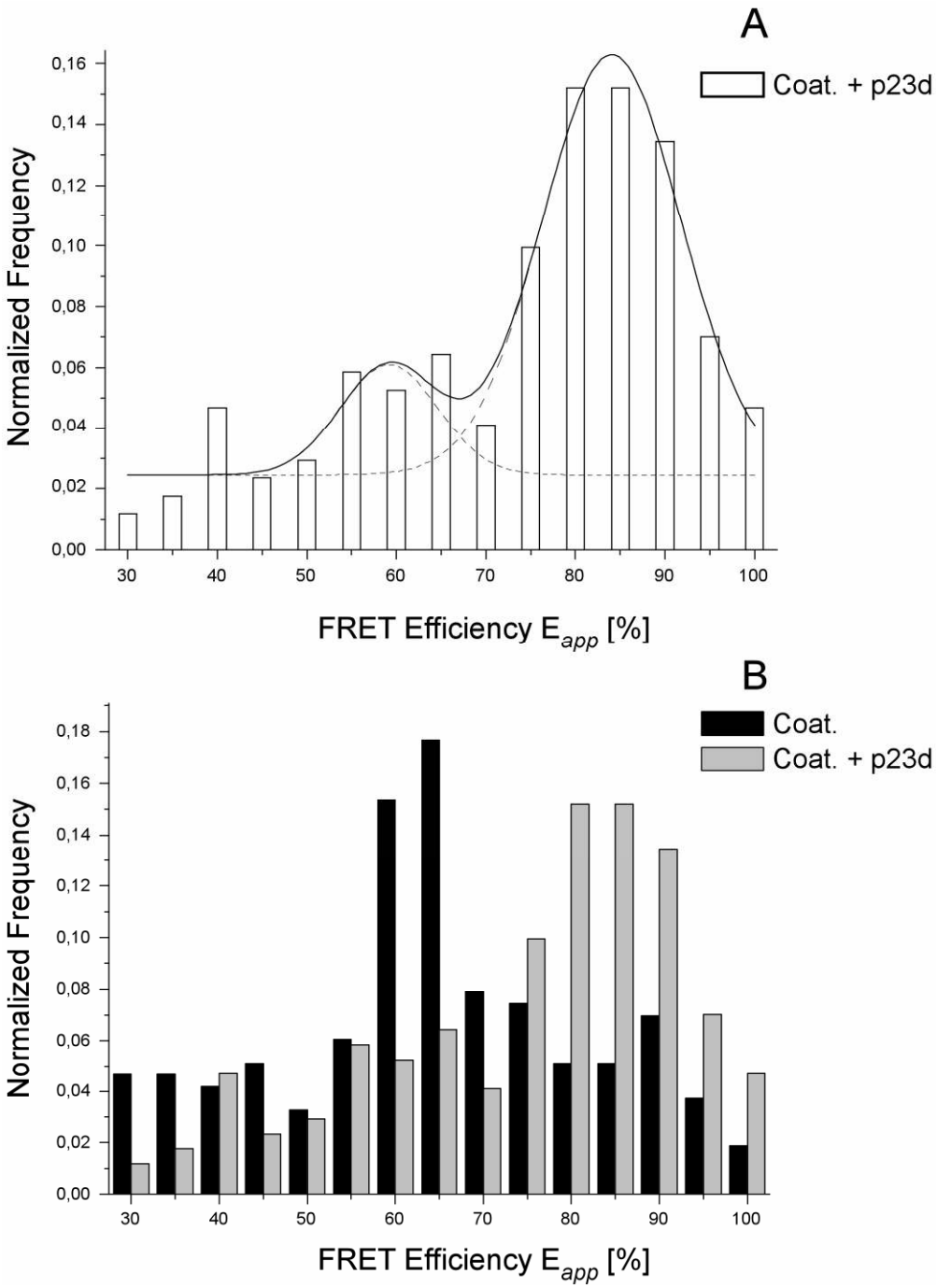

Figure 20, A: Normalized histogram for Cy3-Cy5-labeled coatomer, after addition of 20μM p23d (n= 176, class size: 5%). The major population is now centered at a FRET efficiency of 84%, a subpopulation centered at an efficiency of 59% was also detected. **B**: Overlay of normalised histograms prior to and after addition of dimeric p23.

A major population with a FRET efficiency peak at 84% was found, as depicted in Figure 20A. A subpopulation was also detected, with a peak centred at 59%, which may represent

coatomer with no p23 bound to the complex and an unchanged conformation (overlay in Figure 20B).

Hence, a striking shift of the FRET efficiency of the major population of single-pair FRET labeled coatomer molecules from 63% to 84% is observed upon binding of coatomer to dimeric p23, demonstrating that a conformational change induced in the trunk domain of γ-COP is transmitted to the α-subunit of the complex. This is of special interest, as no functional interaction between α-COP and γ-COP has been described to date.

The observed conformational change takes place in a subunit of coatomer that is competent to bind KKxx- and KxKxx-based ER retrieval signals. In the Clathrin system, cargo binding of the Adaptor complexes is tightly controlled by a series of conformational changes induced by phosphorylation and cargo binding (reviewed by (Langer et al., 2007)).

Thus, we investigated if binding of coatomer to proteins bearing the ER retrieval signal sequences is modulated by the conformational change induced by dimeric p23. To this end, we made use of an ELISA-like binding assay, to determine if both the K_D of coatomer for its protein binding partners and/or the number of binding sites changes during the conformational change (Bethune et al., 2006).

2.1.12. ELISA-like binding assay

In this assay, coatomer is immobilised on Protein A ocated 96-well plates using an antibody (CM1), and incubated with different concentrations of S-tagged fusion proteins of its binding partner. The amount of protein bound to coatomer is determined using an S-tag-specific detection system.
The construct used as a representative cargo protein here is comprised of the cytoplasmic domain of OST48 containing a KxKxx ER retrieval signal (see also table 2), of a His_6-tag for purification, and of an S-tag for detection.

First, we determined the K_D of coatomer for this protein by a series of independent experiments (K_D=0.35μM, SD=0.1μM). This is in excellent agreement with published data (0.9μM, (Bethune et al., 2006)).

Next, we perfomed a series of independent experiments to determine the K_D of this fusion protein in the absence and presence of dimeric p23. The binding curves are shown in Figure 21.

The K_Ds were calculated to be 0.34 µM and 1.2 µM. So, surprisingly, a slight increase in the K_D was observed upon addition of dimeric p23. Also, the total number of binding sites did not change significantly.

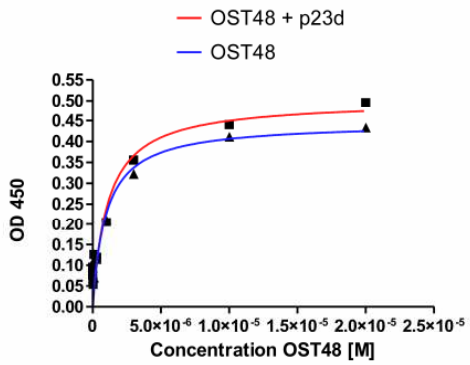

	OST48		OST48 + p23d	
	B_{Max}	K_D	B_{Max}	K_D
independent experiments	0,504	$3,04\ 10^{-7}$	0,541	$1,17\ 10^{-6}$
	0,524	$4,94\ 10^{-7}$	0,603	$1,72\ 10^{-6}$
	0,544	$2,20\ 10^{-7}$	0,495	$1,09\ 10^{-6}$
	0,495	$3,70\ 10^{-7}$	0,433	$9,59\ 10^{-6}$
Mean values	0,516	$3,47\ 10^{-7}$	0,518	$1,23\ 10^{-6}$
S_D	0,019	$1,00\ 10^{-7}$	0,062	$2,90\ 10^{-7}$

Figure 21: ELISA binding curves to monitor the K_D and the total number of available binding sites of coatomer for cargo proteins in the presence and absence of dimeric p23. The tables contain data of two sets (+/- p23d) of 4 independent experiments.

2.1.13. Rare events

Some fluorescence intensity traces showed striking dynamics in their intensity profile. In rare events, a fluctuation between two discrete emission states was observed. Figure 22 shows examples of these fluorescence intensity traces. The two states displayed in Figure 22 correspond to FRET effiencies of 84% and 55%, thus representing the efficiencies found for conformationally changed and unchanged coatomer.

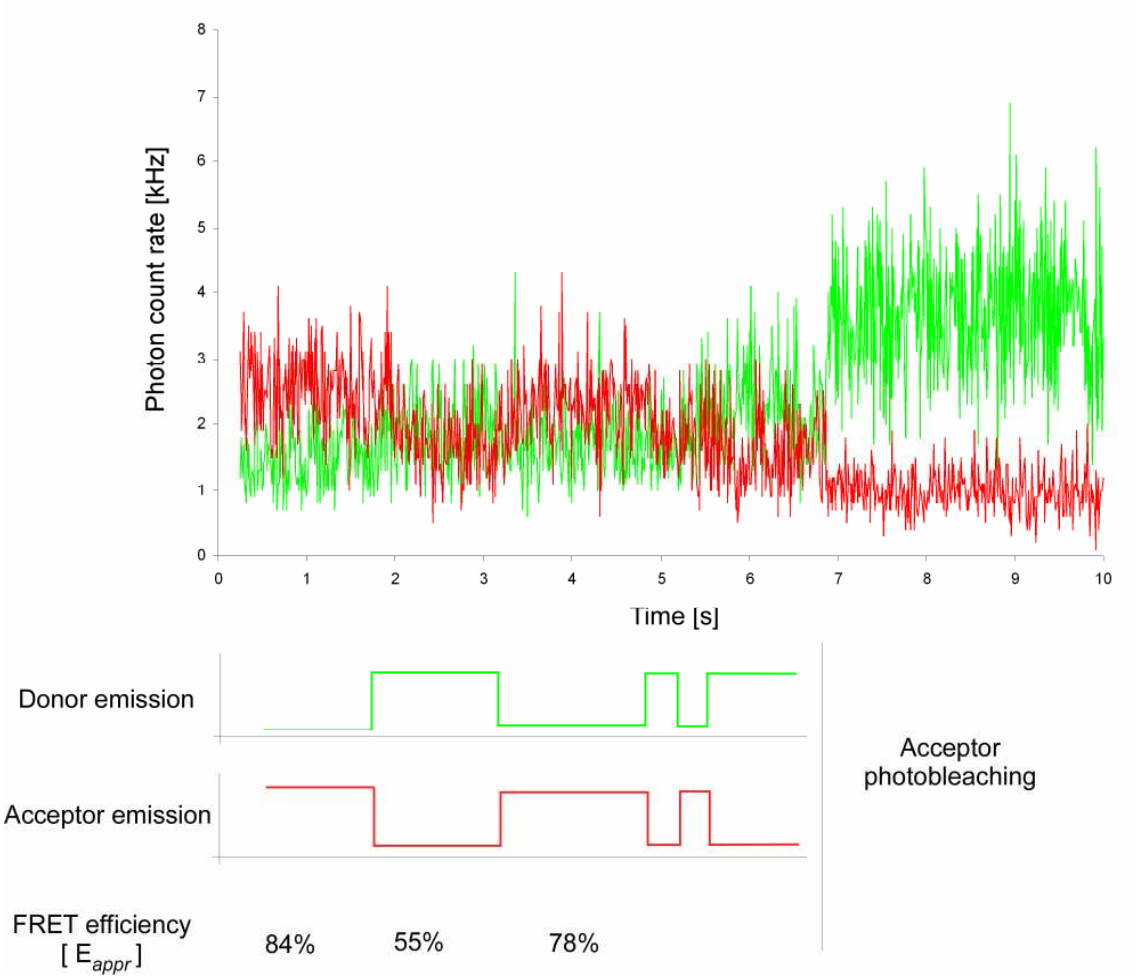

Figure 22: Fluorescence intensity trace of a Cy3-Cy5-labeled coatomer that oscillates between two FRET states. The calculated FRET efficiencies are listed in the bottom.

This fluctuation may indicate that during aquisition of the fluorescence intensity trace, the complex underwent the conformational change (until 2.1s), reverted back to the unchanged conformation (2.1s – 3.2s), and changed again (3.2s – 5.0s).

However, this live monitoring of the conformational dynamics was only rarely observed (1/100 spots).

2.2. Electron Microscopic investigation of COPI vesicles

The remarkable functional dynamics of coatomer observed in the experiments described raised the question as to the structure(s) of the heptameric complex after polymerization. Therefore, in a second project, we investigated the structure of COPI vesicles prepared in vitro using cryo-electron tomography. In contrast to the other vesiculation systems, where the cage structures have been characterised at the molecular level (Cheng et al., 2007; Collins et al., 2002; Fath et al., 2007; Stagg et al., 2006), only limited data is availbale on the structure of the COPI coat. Here we tested different experimental procedures that allow generation and purification of large amounts of COPI vesicles in vitro, and submitted them to cryo-electron tomography experiments.

2.2.1. Preparation of COPI vesicles in vitro

For initial screening experiments, the yield and purity of different COPI vesicle preperation assays were investigated. Three different methods to prepare COPI vesicles in vitro were tested:

The first assay follows the protocol described by Pavel et al. (Pavel et al., 1998). Using the non-hydrolysable GTP-analog GTPγS, purified Golgi membranes were incubated with cytosol as a source for coatomer and Arf1. After release of the vesicles using a high-salt buffer, the samples were applied on top of a sucrose gradient ranging from 50% to 20%. After centrifugation to equilibrium for 17h at 100000g, the fractions containing the COPI vesicles were harvested. Typically, this fraction displayed a buoyant density of 38-42% sucrose.

Figure 23 shows electron microscopic images of samples harvested from these gradients, and submitted to negative staining using 1% uranyl acetate (images taken on a FEI CM120 electron microscope, 120kV, defocus 2µm). The vesicles display a diameter between 60nm and 80nm, which is in excellent agreement with data published previously (Orci et al., 1998).

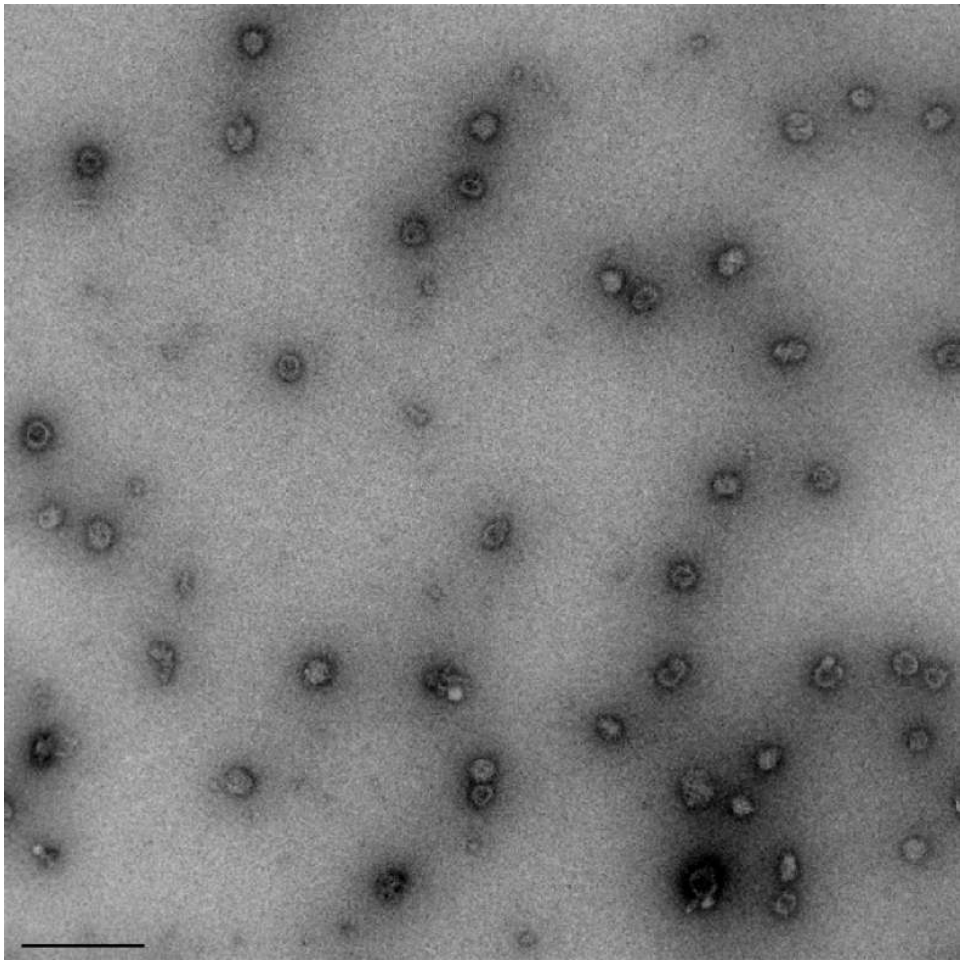

Figure 23: Images of GTPγS-COPI vesicles, purified by sucrose gradient and submitted to negative stain. Magnification: 16kx, scalebar: 500nm.

To increase both the stability of the coat and the amount of coated vesicles that can be purified, different chemical crosslinkers were tested. Addition of both formaldehyde and glutaraldehyde didnt increase the yield of vesicles from a COPI budding assay, as found in both negative stain electron microscopy and Western Blotting (data not shown).

In parallel, a second experimental approach was tested. Here, the individual components required for COPI vesicle budding were added separately, and as recombinant or purified proteins. This approach offers the advantages that less contaminating proteins (as opposed to using cytosol as a source) are present, and that stable GTP-coated vesicles can be isolated, because no ArfGAP proteins are present (see introduction; soluble ArfGAP proteins present in the cytosol mediate uncoating of COPI vesicles). In addition, the final purification was achieved using a short centrifugation of 1h onto a sucrose cushion with a concentration of 47% sucrose, with an upper cushion of 37%, significantly lowering the preparation time (see Materials and Methods, and (Beck et al., 2008)).

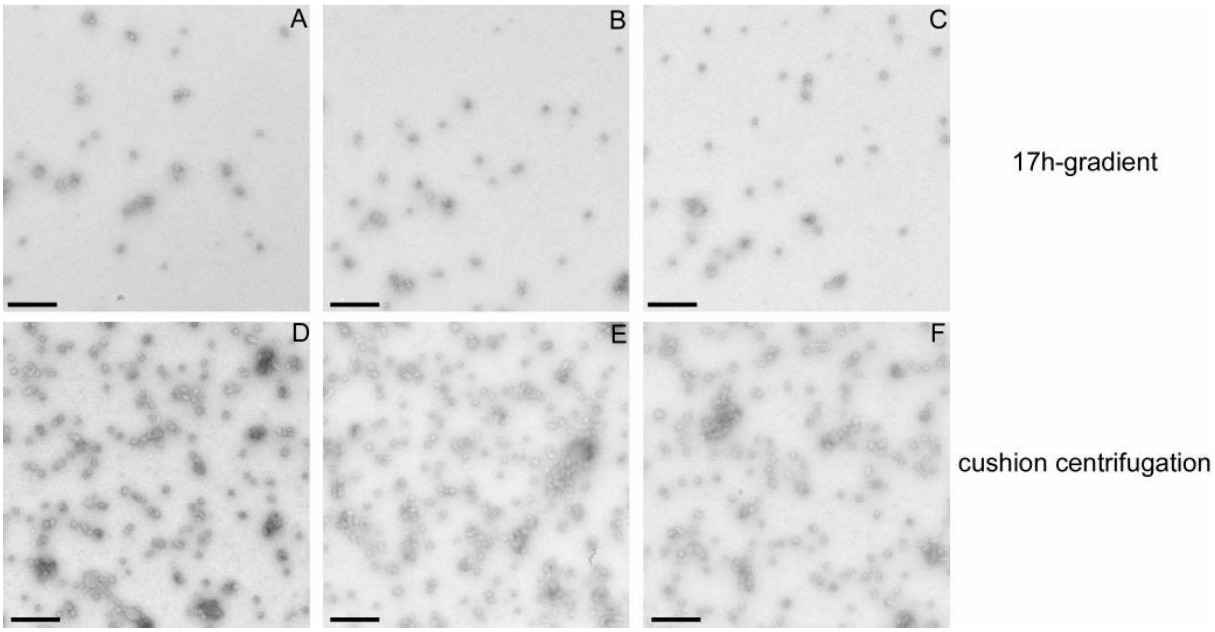

Figure 24: Images of GTPγS-COPI vesicles purified either via a 17h-gradient (A-C) or centrifugation on a sucrose cushion (D-F). Magnification 16kx, scalebar 500nm.

In initial screening experiments, to screen if the purity and yield of vesicles from this assay was comparable to the Pavel method using a 17h centrifugation, GTPγS was employed. Figure 24 shows images of vesicles prepared in both methods (figure 24A-C: 17h gradient centrifugaiton, figure 24D-F: 1h cushion centrifugation). The vesicle preparation shown in figure 24D-F contains minor membrane fragments, but a homogenous pool of COPI vesicles can be clearly identified.

The samples in Figure 24 were prepared using 0.25mg Golgi. To increase the overall yield of vesicles, the amount of all components was increased by a factor of 10. The fractions obtained in these experiments were submitted to negative staining experiments. Figure 25 shows images taken of samples diluted 1:1 prior to application to the grid. Clearly, a homogenous population of vesicles with a diameter of 60-80nm can be discerned.

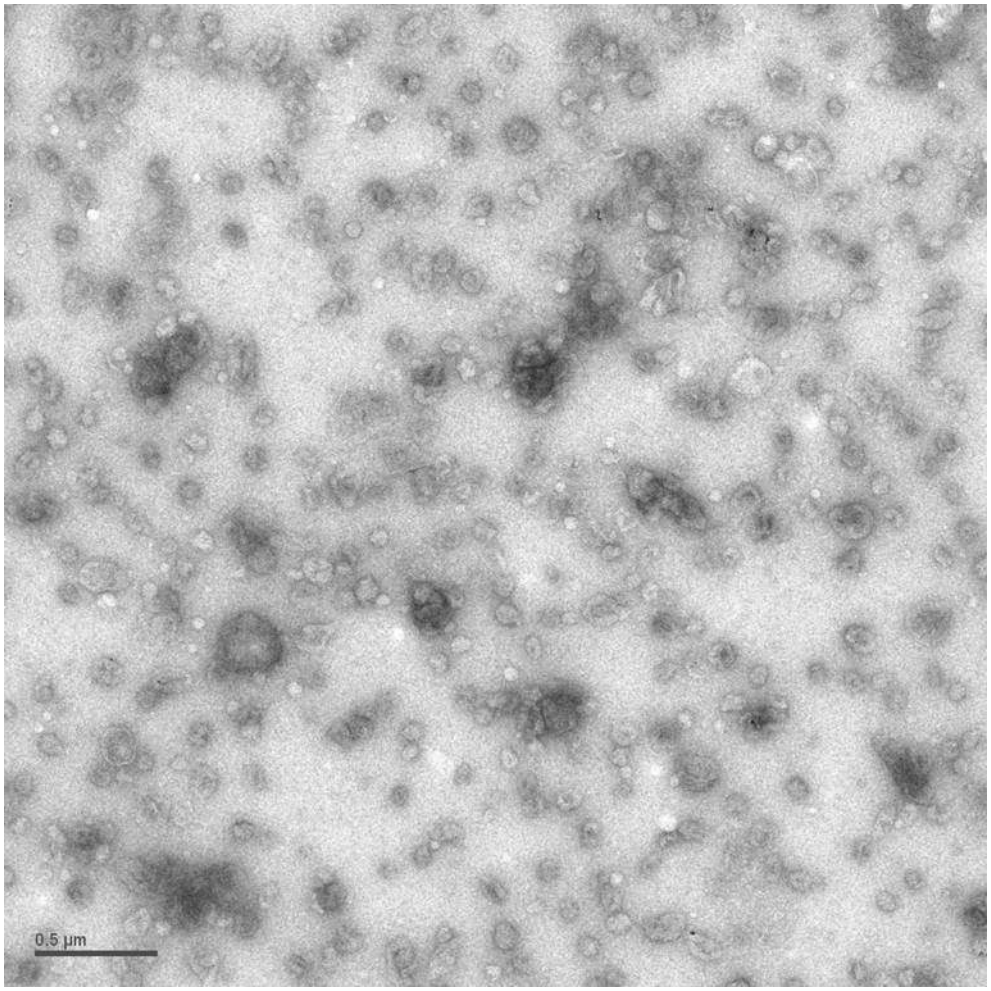

Figure 25: Images of COPI vesicles (upscaled sample, 2.5mg of Golgi) prepared with GTPγS, purified by centrifugation on a sucrose cushion, and submitted to negative stain. Magnification 19kx, scalebar 500nm.

Subsequently, COPI vesicles were prepared using GTP instead of GTPγS. Identical conditions as described above were used, and the fraction containing vesicles were applied to grids, submitted to negative stain and imaged. Again, COPI vesicles were detected, although the yield is lower by a factor of 5 as compared to GTPγS preparation. These fractions were taken for subsequent EPON embedding and for cryo electron microscopic experiments.

2.2.2. Embedding of chemically fixed vesicles into a matrix

Subsequently, we decided to screen and investigate the morphology of COPI vesicles prepared in vitro in a system that does not involve adsorption to a carbon backing. To this end, samples prepared as described above were subsequently embedded in a polymer matrix. The fraction containing vesicles was fixed with 1% glutaraldehyde and stained with

Ruthenium-Red. After sedimentation of the vesicles by a 100000g centrifugation, the pellet was stained with OsO4 and embedded in EPON.

Figure 26A and 26B show images of thin sections of these samples. Vesicles were found with diameters of 60nm to 80nm, which is in excellent agreement with the values estimated from the negative sain samples and data published previously (Orci et al., 1998). In these samples, donor membranes that sedimented in the centrifugation with the vesicles are also present (Figure 26). Clearly, the vesicles do not exhibit a round shape, but exhibit "edges" and "corners", i.e. the rim of the coat displays short spans with high curvature (marked with an asterisk in Figure 26B, and long spans with low or without curvature (marked by bars in Figure 26B).

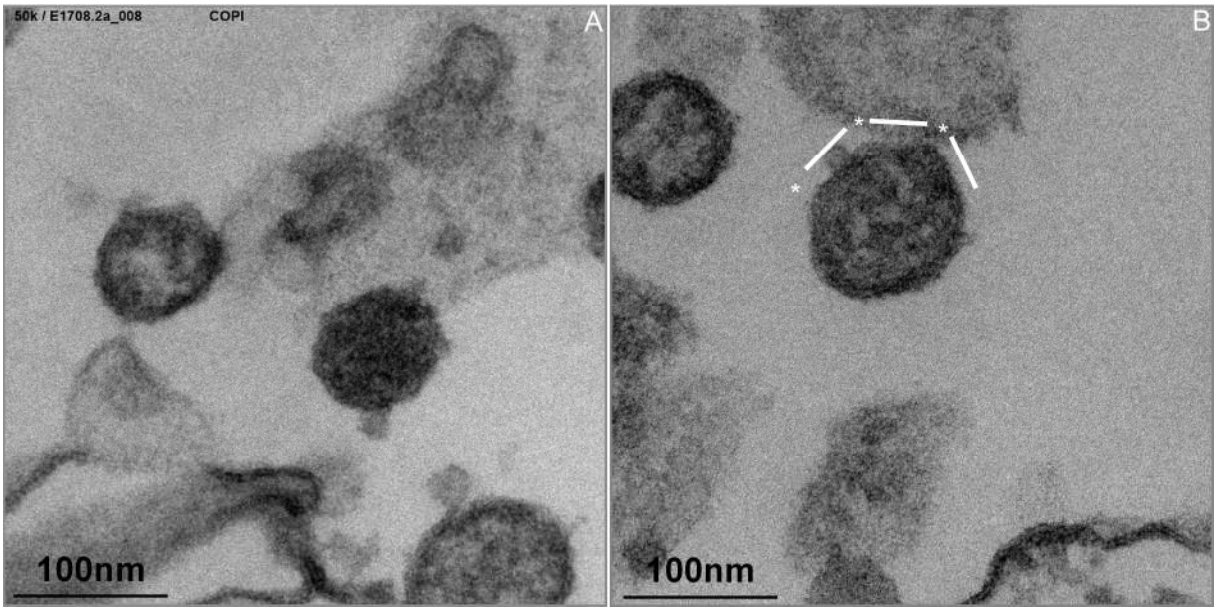

Figure 26: Images of COPI vesicles prepared with GTP in vitro, embedded in a polymer matrix and stained with Ruthenium Red and OsO_4. Magnification 50k, scalebars 100nm.

2.2.3. Cryo-electron microscopy of COPI vesicles generated in vitro

Samples of these fractions were mixed with gold particles as fiducials (10nm diameter), applied to Quantifoil grids, and snap-frozen in liquid ethane. Figure 27 shows images of these grids, taken at 300kV in a FEI Polara electron microscope with a Gatan stage. The samples exhibited extremely low contrast, as well as only a very limited number of particles in the vitreous ice. The low contrast does not allow clear identification of any vesicles, although particles with the right diameter may be present in solution (figure 27, marked with arrows). In addition, the vitreous ice displayed only a very limited stability in the beam.

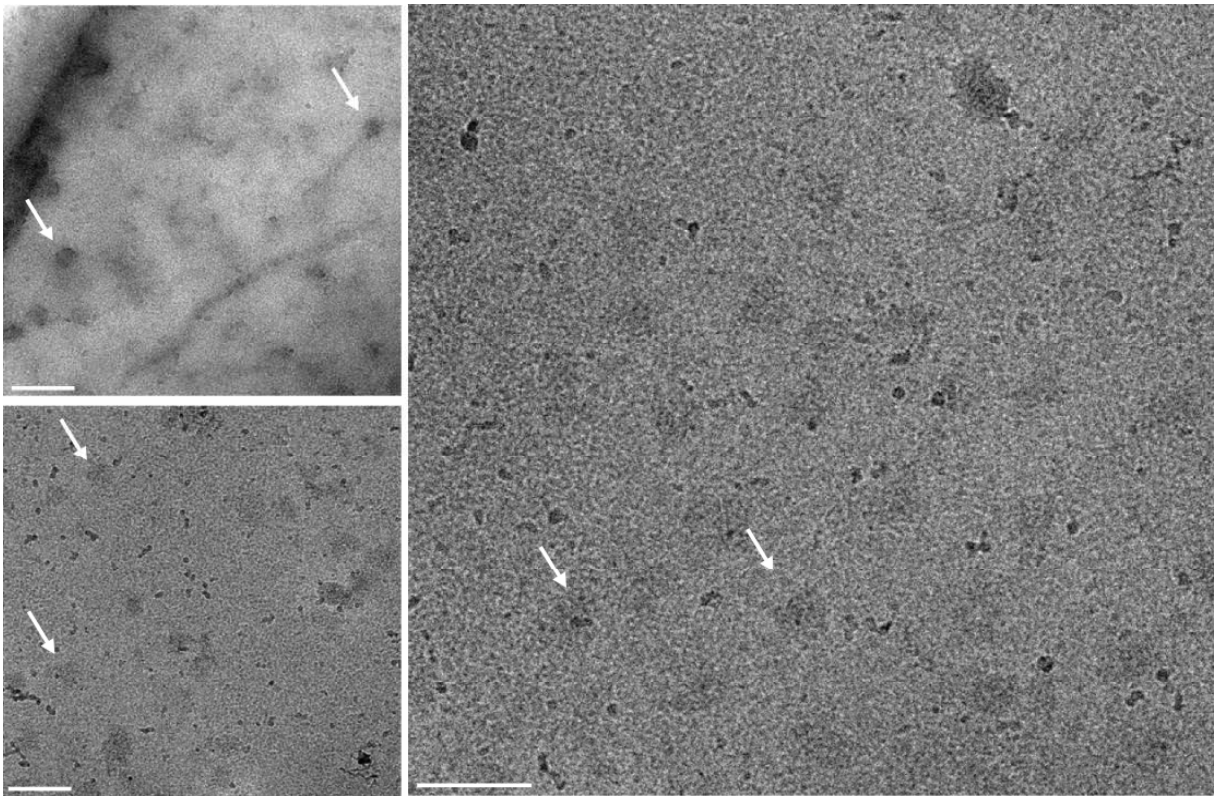

Figure 27: Images of COPI vesicles (upscaled sample, 2.5mg of Golgi) prepared with GTPγS, purified by centrifugation on a sucrose cushion, and submitted cryo electron microscopy. Magnification 16kx, scalebar 500nm.

Both issues may be primarily caused by the high sucrose concentration of the sample (ca. 42%). If the concentration of sucrose was lowered by dilution (1:8) to obtain a sucrose concentration of ca. 5%, no more particles were detected in the ice. However, the ice displayed better stability in the beam, and boiling occured only after application of a much higher electron dose.

Also, after dialysis of the sample against buffer without sucrose, no particles could be detected in the sample after application to a Quantifoil grid and cryo-EM imaging. To test the concentration of vesicles, the dialysed samples were applied to carbon-backed grids and submitted to negative staining. Here, particles could be detected, although the number of vesicles was decreased by a factor of ~10 (data not shown)

2.2.4. Using "backed"-Quantifoil

In the experiments described previously, the COPI vesicles showed significant adhesion to the carbon film in negative stain preparation. The density of vesicles found in these experiments indicated that a large quantity of vesicles is recruited to the carbon backing. Thus we investigated if we could make use of this behaviour for the cryo-EM experiments.

To this end, we applied thin films of two backing materials to standard quantifoil grids: First, we used thin carbon films (see Materials and Methods) with a thickness of ~40A. Second, we employed thin TiSi films (see Materials and Methods, and (Rhinow and Kuhlbrandt, 2008)). The advantage of these films is higher stability, and a lower refractive index as compared to standard carbon films. In the following experiments, however, we used carbon-backed Quantifoil, as this backing showed higher adsoprtion of COPI vesicles (data not shown).

In addition, using backed Quantioil, the sample can be repeatedly applied to the grid, leading to an increase in vesicle density on the backing. Furthermore, the grids were washed with buffer to reduce the sucrose concentration.

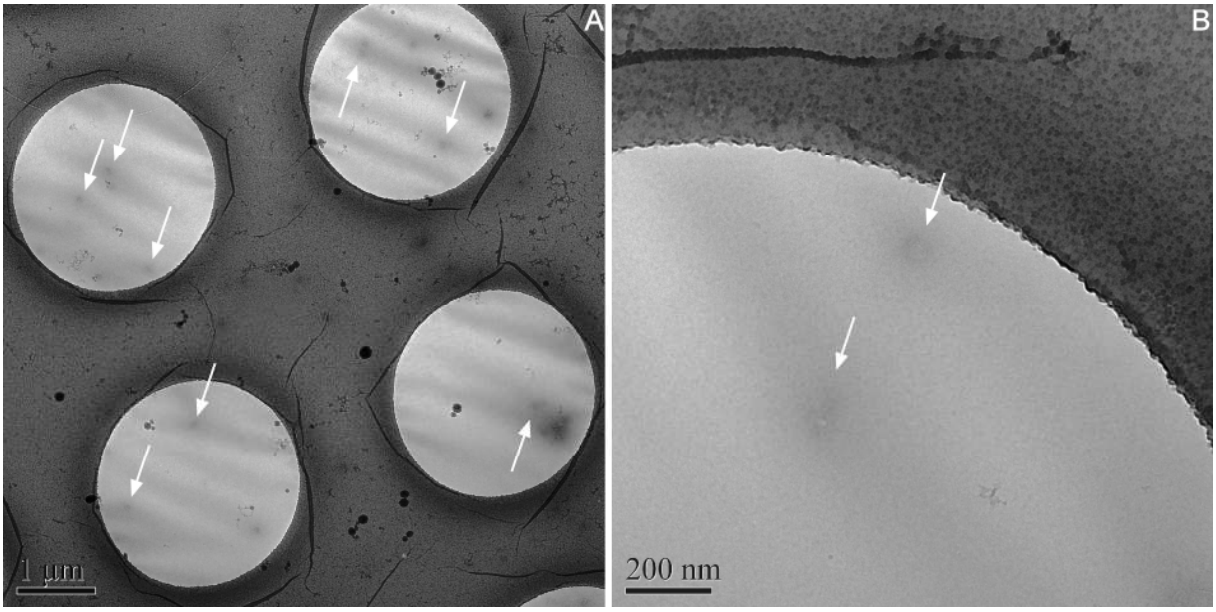

Figure 28: Low (**A**) and high (**B**) magnification Images of COPI vesicles, deposited on a carbon-backed Quantifoil grid, embedded in vitreous ice. Scalebars as indicated.

Figure 28 shows 2 images of carbon-backed Quantifoil, with identical samples applied three times and subsequent washing with buffer (2x). As seen in the low-magnification image, a number of particles with the dimensions of COPI vesicles can be identified in each Quantifoil-

hole (figure 28A, indicated with arrows). However, contrast was limited again, as shown in the high-magnification images (figure 28B).

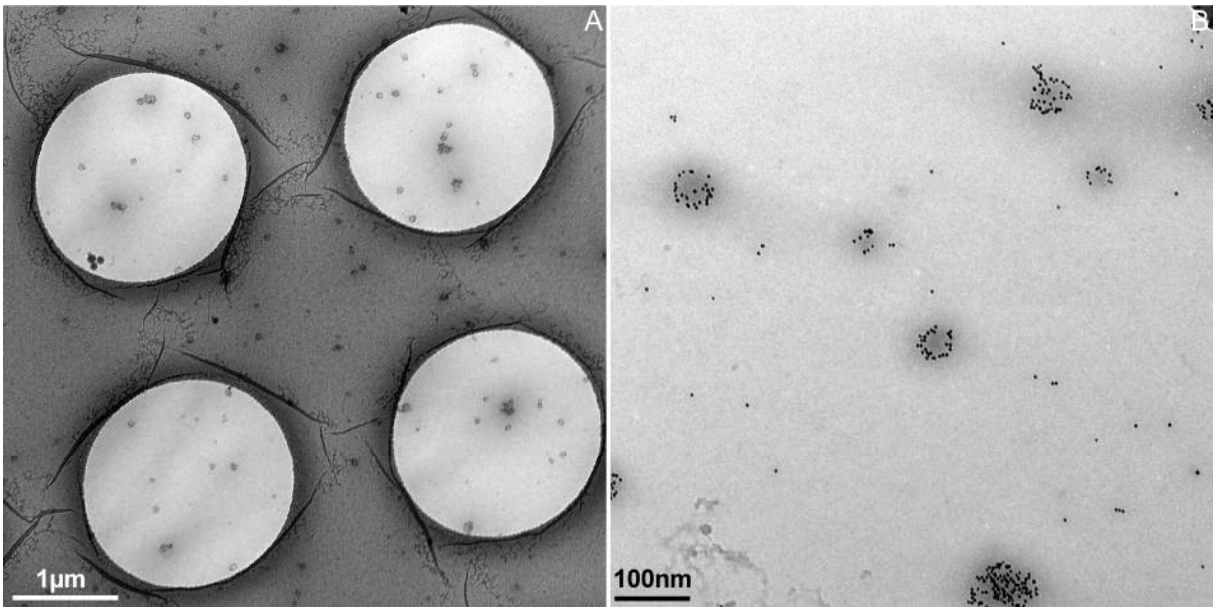

Figure 29: Low (**A**) and high magnification (**B**) Images of COPI vesicles with 6nm gold dots as ficucials deposited on a carbon-backed Quantifoil grid, and embedded in vitroues ice. Scalebars as indicated.

In Figure 29, gold particles with a diameter of 6nm were added to the sample prior to application to the grid as high contrast markers for alignment of images in a tilt series. In these conditions, the fiducials cluster around the vesicles (see Figure 29A and 29B). This greatly faciliated detection of the vesicles in the ice, but also blocked the protein coat from view.

To prevent fiducial clustering, the carbon-backed Quantifoil grids were pre-incubated with the fiducials, and the fiducials left to dry on the film. Subsequently, the samples were applied to the grid, and treated as described above.

Tomograms were recorded of the particles immobilised on these carbon films. Single-axis tilt series, ranging from angles of -60° to +60°, were recorded, and reconstructed using the IMOD software package (Kremer et al., 1996). Figure 30 shows a slice through a tomogram, with an enlarged view of a particle immobilised on the carbon film.

A particle with the right dimensions can be identified (Figure 30). The vesicle seems to be comprised of an inner and an outer layer. However, contrast is very limited, and no structural details can be discerned.

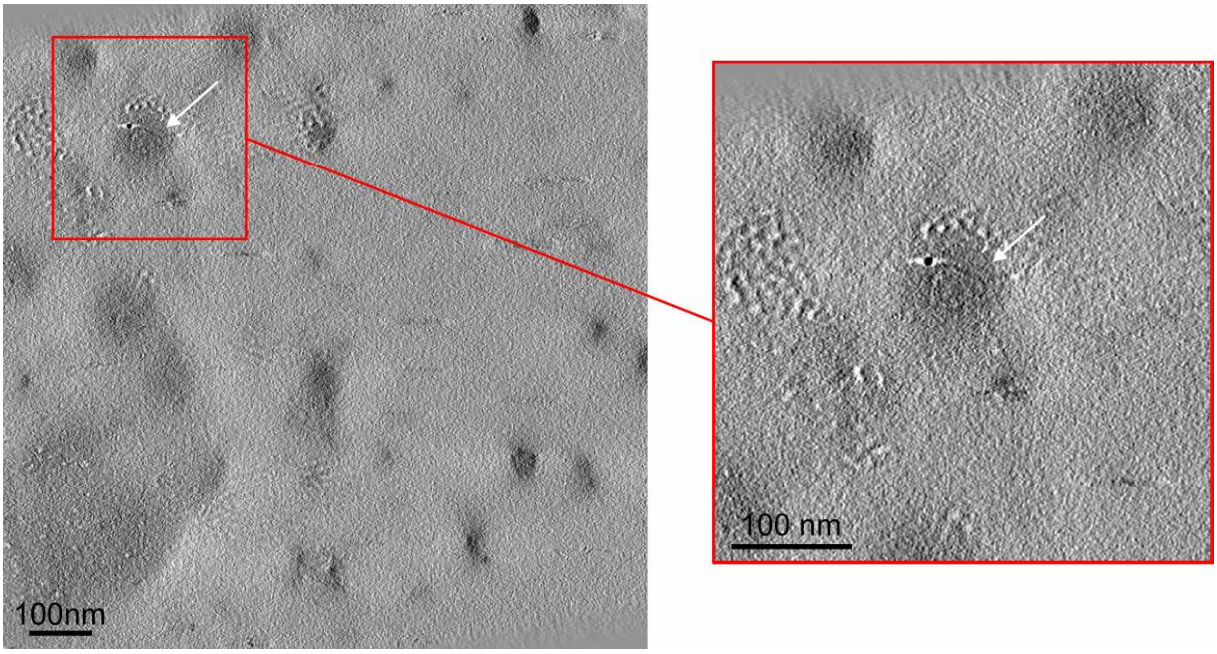

Figure 30: Section of a tomogram of a sample of purified GTPγS-COPI vesicles deposited on a thin carbon film, embedded in vitreous ice (scale bars: 100nm). A particle with a diameter of approximately 60nm can be discerned (marked with an arrow). The particle seems to be composed of an outer and an inner layer Magnification 26kx.

In addition, the particles did not exhibit a uniform, symmetrical form. This may be due to distortion caused by adhesion to the carbon film, or osmotic stress during the dilution and washing steps.

2.2.5. Direct preparation and imaging of COPI vesicles.

In the previous experiments, the detection and imaging of the COPI vesicles was severly impeded by the high sucrose concentration in the product fraction: The samples exhibited low contrast, and only limited stability in the electron beam. Thus, in a parallel approach, a protocol without a sucrose gradient-based purification was tested.

To this end, the components required for COPI vesicle biogenesis required in vitro (salt-washed Golgi membranes, Arf1, ARNO and coatomer) were incubated with GTP at 37°C. After 10 minutes, the samples were incubated with colloidal gold as fiducials (6nm), and directly applied to Quantifoil holey carbon grids.

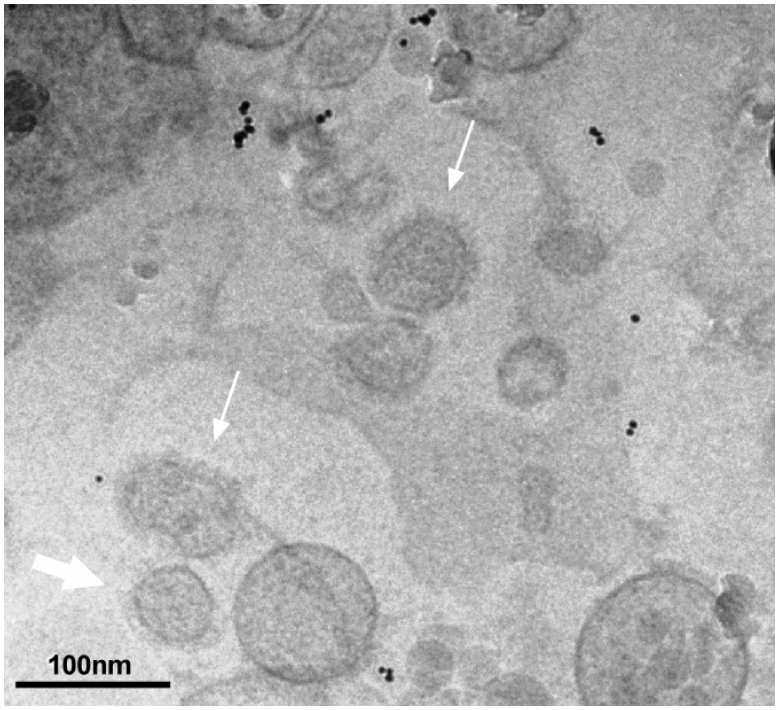

Figure 31: TEM image of GTP-COPI vesicles embedded in vitreous ice. As no sucrose gradient was used to purify the vesicles, the donor membranes are also present. Magnification: 26kx, scalebar: 100nm.

Figure 31 shows an EFTEM image of one of these samples recorded at 300kV on an FEI Polara. Clearly, a large excess of donor membranes is present. Some of these membranes seem to bear a proteinous coat (marked with thin arrows). In addition, a protein-coated vesicle with a diameter of 60-70nm can be identified (marked with thick arrow). In other areas, protein-coated buds were identified (see below).

These samples were subsequently used to record single-axis tilt series. Standard low-dose settings were strictly followed, with a magnification of 25000x at a defocus of -8 µm for initial experiments. The tomograms were reconstructed using the IMOD software package (Kremer et al., 1996).

Figure 32 shows slice through the tomogram of the area shown in Figure 31. A coated vesicle with a diameter of ca. 65nm (marked with thick arrow) can be identified, as well as coated membranes (indicated with thin arrows). A non-continous protein coat can be discerned.

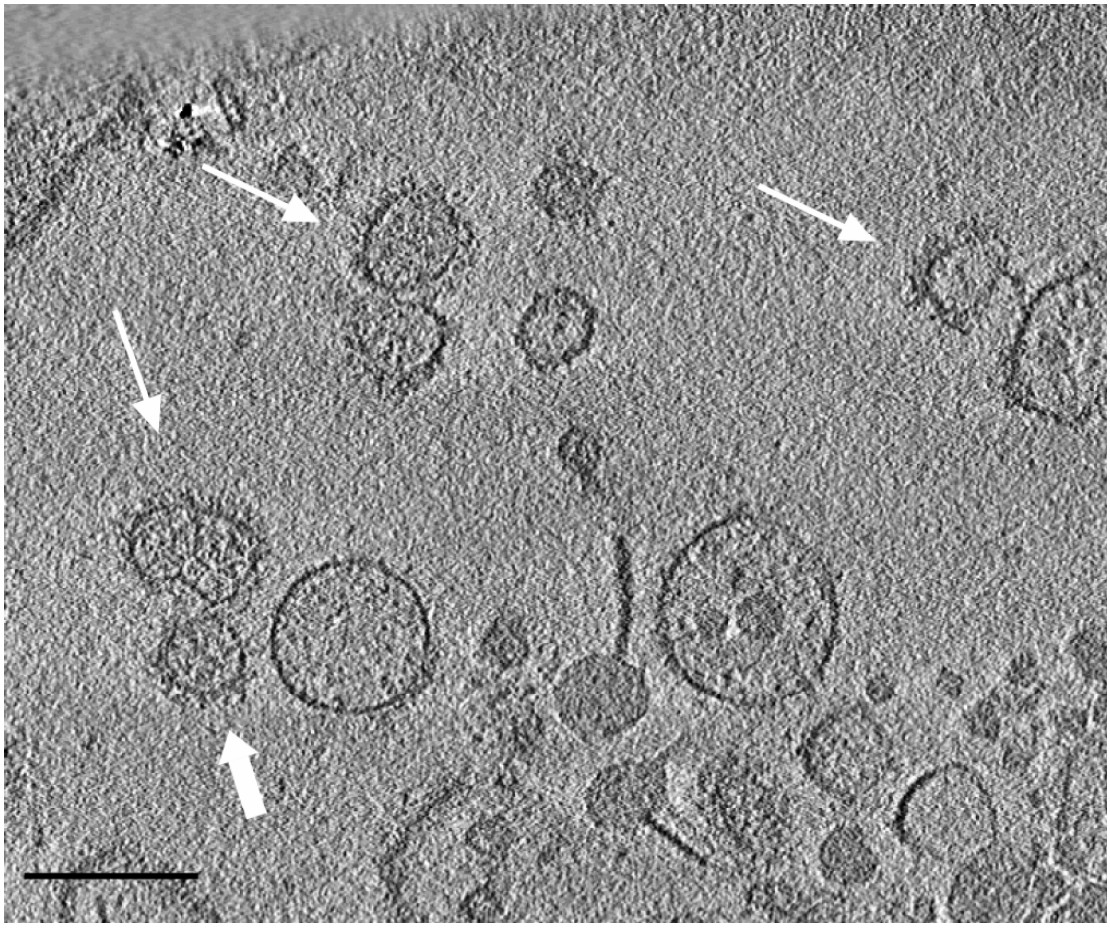

Figure 32: Section of a tomogram recorded of COPI samples containing COPI vesicles directly applied to a Quantifoil grid after preparation, without sucrose gradient or cushion purification. Slice thickness: 4.5nm. Scalebar: 100nm.

Figure 33 shows tomogram slices through a different area, of another sample containing GTP COPI vesicles directly applied to a Quantifoil grid. The boxed area is magnified in the series of z-slices depicted in the bottom, with each slice having a thickness of 2.9nm and a spacing of 5.8nm. Again, a non-continous proteinous coat can be clearly identified on the membrane.

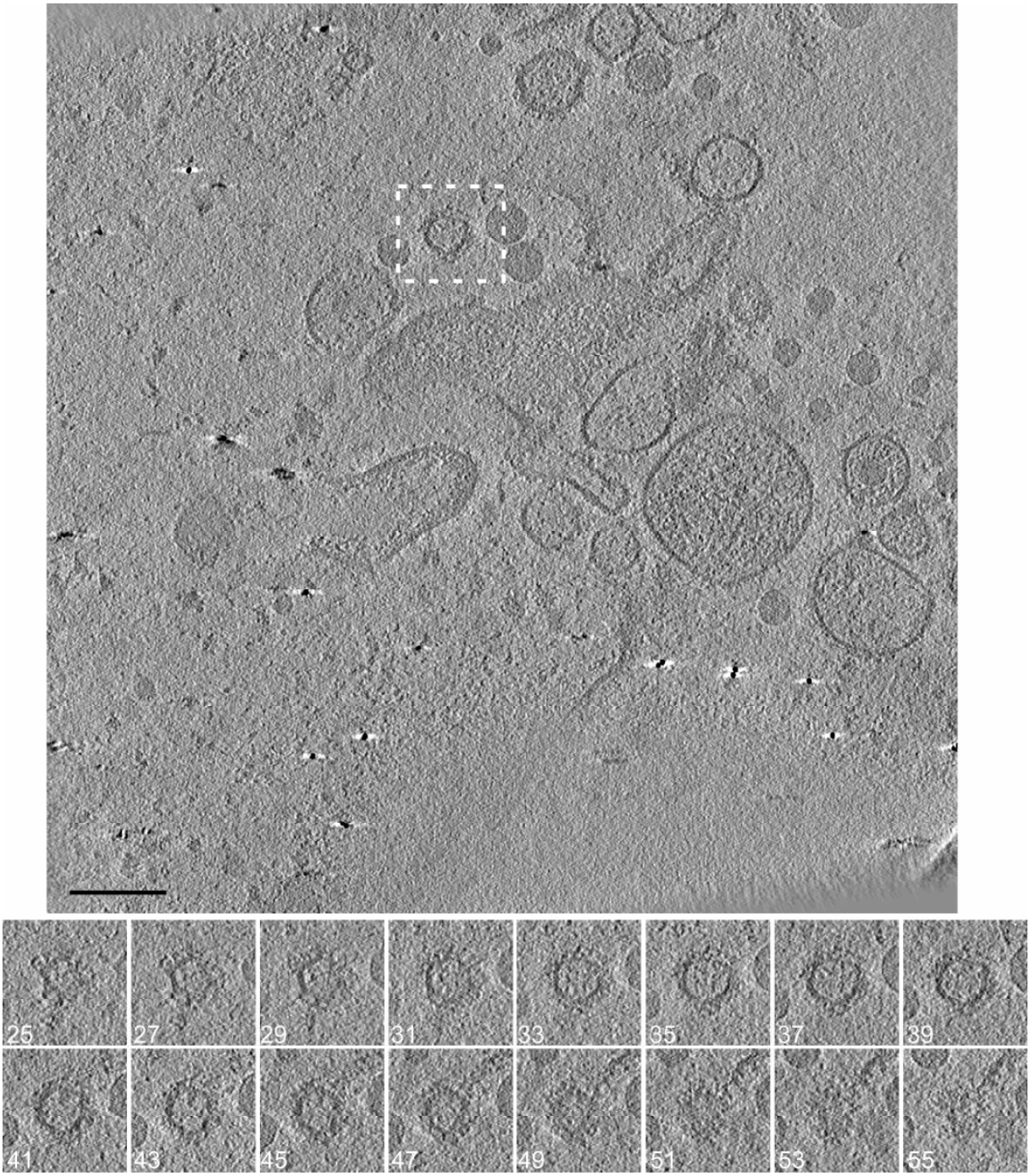

Figure 33: Sections of a tomogram recorded of COPI samples containing COPI vesicles directly applied to a Quantifoil grid after preparation, without sucrose gradient or cushion purification. Slice thickness: 2.8nm, slice spacing 5.9nm. Scalebar 100nm.

The area was extracted using the IMOD package again, and the membrane and the coat visualized using the software Amira 4.1.1 as described in Materials and Methods.

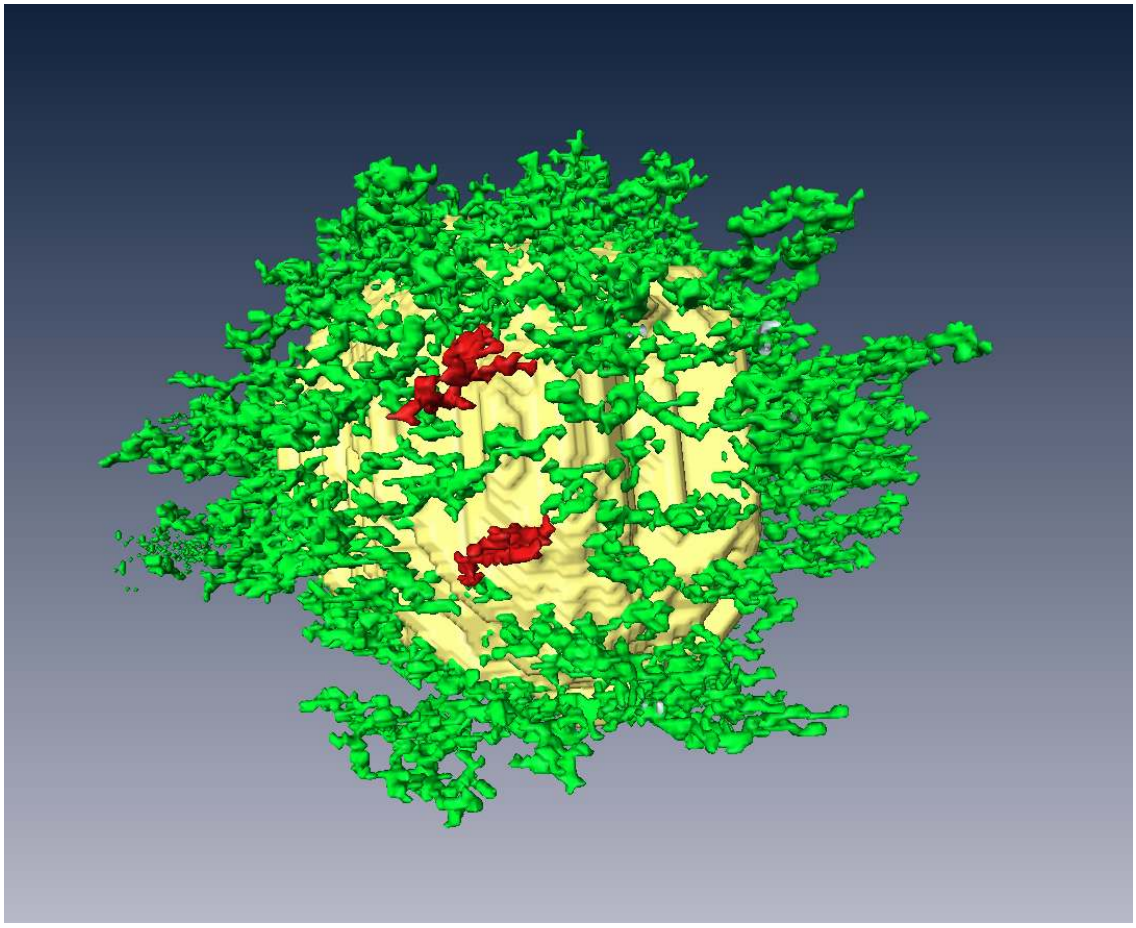

Figure 34: Rendering of coated vesicle boxed in Figure 33 using the Amira software package. Segmentation was done partly by hand and by thresholding. Membranes are imaged in yellow, and coating protein in green.

In this segmentation, the membrane was imaged in yellow, and the coating protein imaged in green. The coat seemed to be non-continuous and spiky (two of these "spikes" highlighted in red).

Figure 35 shows slices of tomograms of a different area. A protrusion can be identified on the donor membrane, forming a coated bud (boxed area). The diameter of the coated bud is approximately 60nm. A non-continous, proteinous coat can clearly be identified. Z-slices of the boxed area containing the coated bud are shown in the image sequence, with a slice thickness of 2.5nm and a spacing of 5nm. Slice numbers in the tomogram are indicated.

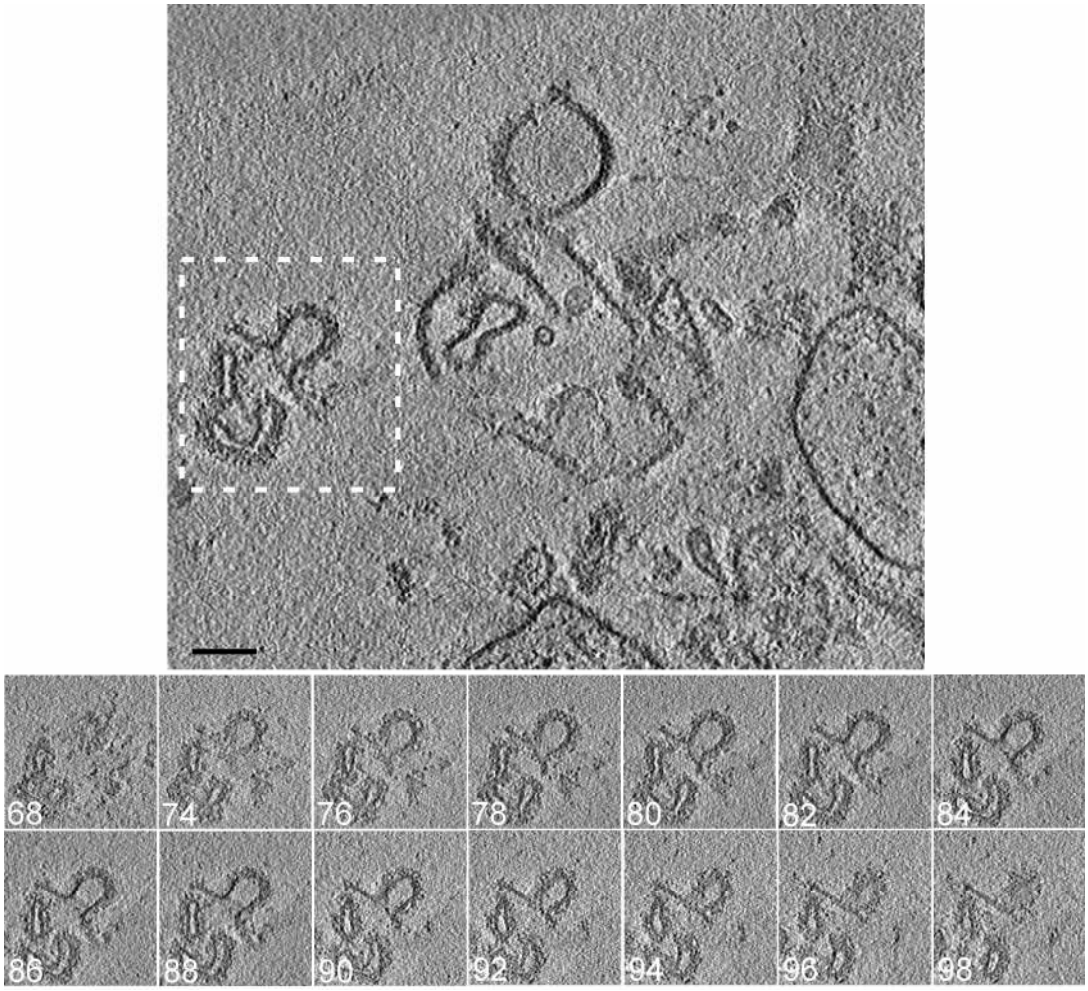

Figure 35: Sections of a tomogram of a sample directly applied to a Quantifoil grid after preparation, without sucrose gradient or cushion purification. In this area, a coated bud that is in the process of forming a COPI vesicle can be identified (boxed area). Scalebar 50nm. Slices of the boxed area are displayed on the right. Each slice has a thickness of 2.5nm, and the spacing between slices is 5nm (slice numbers indicated each).

The area was subsequently extracted using the trimvol command. Using the Amira 4.1.1 software, the membrane was marked manually, and the proteinous coat visualized by thresholding (see Materials and Methods). In Figure 36, the membrane is labeled in yellow, and the proteinous coat imaged in green. The coat seems to be non-continuous, but structural features or coat symmetry cannot be discerned at this resolution and contrast yet.

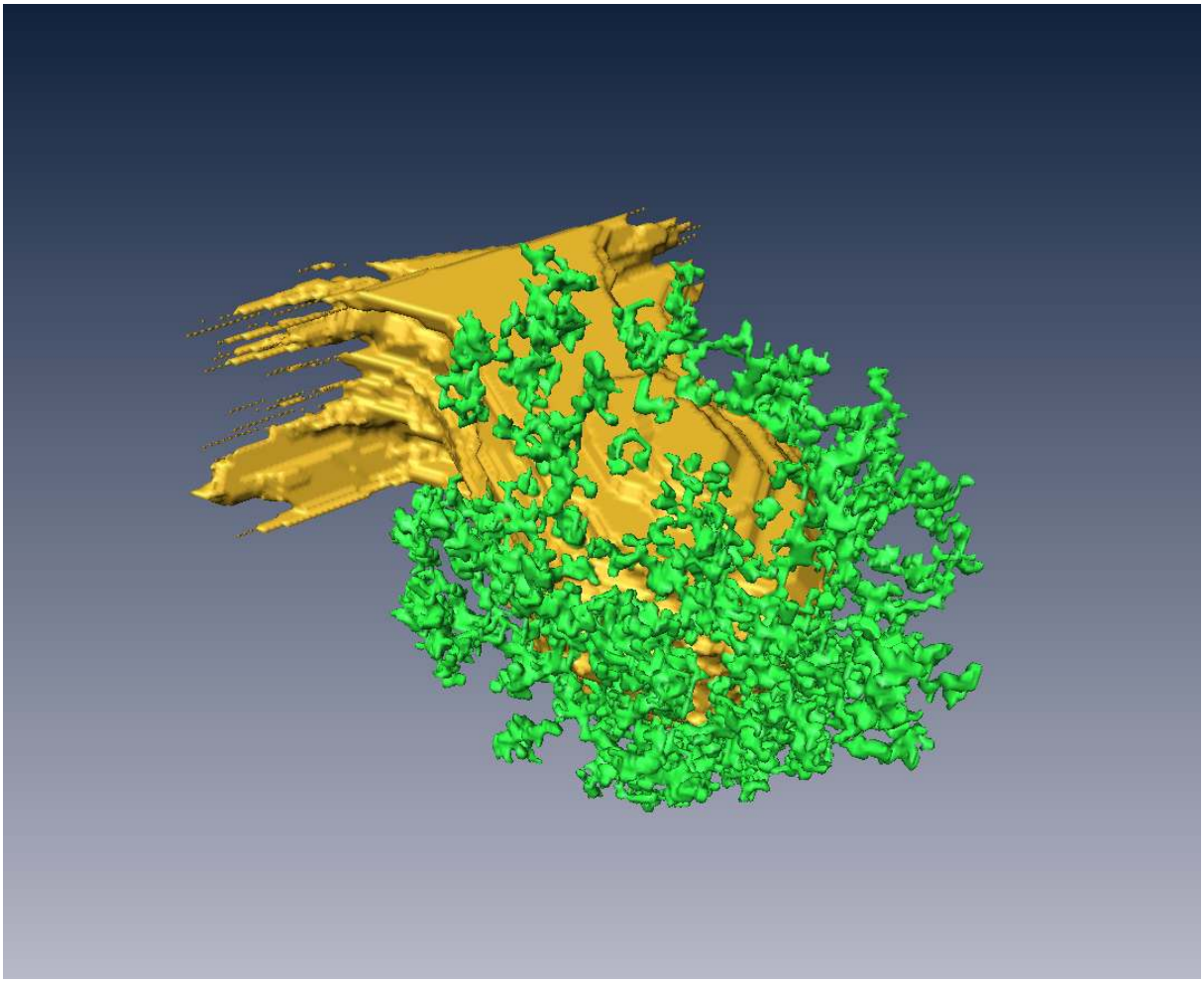

Figure 36: Rendering of the coated bud boxed in Figure 35 using the Amira software package. For this segmentation, selection of the membranes and the coat was done partly by thresholding. Membranes are imaged in yellow, and coating protein in green.

When this thesis was written, data acquisition on these samples was still in progress.

3. Discussion

Coated vesicles mediate intracellular transport of proteins and membranes. In the vesiculation process, specificity of coat recruitment and cargo capture must be tightly controlled. In both the AP-2-, AP-1- and GGA-based Clathrin system, the coating proteins undergo phosphorylation- and ligand-induced conformational changes that transform the soluble complex into a membrane-bound form and activate it for cargo binding.
Structural similarities exist between the different coating systems: All coating complexes contain both α-solenoid and β-propeller domains, and structural similiarities exist between the coatomer subunits α, β' and ε and the clathrin proteins, and between β, γ, δ and ζ-COPs and the 4 subunits of the adaptor complexes AP-1 to AP-4 of clathrin-coated vesicles (Eugster et al., 2000; Gurkan et al., 2006; McMahon and Mills, 2004; Schledzewski et al., 1999). However, in each system, the shared motifs are put to different uses, as described below.

3.1. Conformational dynamics of coatomer

3.1.1. Data presented in this work

Coatomer is a heptameric protein complex that, in its polymerized form, constitutes the coat of COPI vesicles. We have analyzed the conformational dynamics of individual coatomer molecules using single-pair, single-molecule FRET. A surface-based, single-molecule-sensitive setup allowed observation of conformational changes induced by ligand binding (Langer et al., 2008). These changes cannot be followed in solution when a conformational change induced in a complex causes aggregation and subsequent precipitation, as shown for coatomer (Reinhard et al., 1999). We are currently working on the automation of data acquisition that in the future will allow screening of multiple binding partners at varying concentrations.

Coatomer possesses different binding sites for different ligands. Cargo for retrieval to the ER binds to α- or β'-COP in its monomeric form via dibasic motif-containing signatures (Eugster et al., 2004). Dimeric cytoplasmic domains of cycling proteins bind to γ-COP at both its trunk and appendage domains (Bethune et al., 2006). Synthetic COPI vesicles can be generated from liposomes with a certain lipid composition using coatomer and Arf1 alone (Spang et al., 1998); however, when lipopeptides representing cytoplasmic domains of p24-family proteins were incorporated into liposomes, COPI vesicle budding was independent of the lipid

composition of the donor membranes (Bremser et al., 1999), characterizing these cytoplasmic domains as part of the minimal membrane machinery for COPI vesicles.
Upon binding of dimeric p23, the trunk domain undergoes a conformational change, leading to aggregation of coatomer (Bethune et al., 2006; Reinhard et al., 1999). Monomeric peptides of the cytoplasmic tails of p24 family proteins do not bind to coatomer (Bethune et al., 2006), and therefore were not investigated in this study.

As all p24-family members in their dimeric form bind to γ-COP, we investigated if all of them could also induce a conformational change to polymerize the complex. To this end, we utilised a centrifugation assay that allows separation of the conformationally changed, aggregated complex from the unchanged, soluble form. We found that, of all the p24-family members and cargo proteins tested, only p23 and p24 in their dimeric form are able to precipitate and polymerize coatomer.
To further test our findings, we performed a set of limited proteolysis experiments on coatomer incubated with either the monomeric or the dimeric forms of p23 and p24, and the other p24-family members and cargo proteins. As a result, again, only dimeric p23 and p24 were able to induce a conformational change in α-COP. Thus, of the p24-family members, only dimeric p23 and p24 serve as machinery to both recruit and conformationally change coatomer. This is of special interest, as these two proteins are the only members of the p24-family that are competent to recruit Arf1-GDP to the membrane, forming the initial priming complex on the donor membrane.
It will be of interest in the future to learn about the functions exerted by the other p24-family members binding to coatomer.

In order to monitor the conformational dynamics of an individual subunit, we took an independent, biophysical approach: single-molecule, single-pair fluorescence resonance energy transfer (FRET).
To this end, we have established labeling conditions that allow predominant labeling of the α-subunit of coatomer. Thus, changes in FRET efficiency indicate a conformational change of this subunit. The strong preference of the activated dyes to react with α-COP is not completely surprising, because α-COP is the largest subunit of coatomer and, with its analogy to the clathrin system, is expected to be exposed on the surface of the complex. In addition, differential reactivity of coatomer subunits with amino-reactive reagents has been observed previously (Pavel et al., 1998). Labeled coatomer may also be of significant use in future experiments that address live imaging of COPI biogenesis on supported bilayers using fluorescence spectroscopy (in a TIRF setup). This assay is currently established in a collaboration with the lab of Jim Rothman (Columbia University, New York, USA).

In our single-molecule sensitive assay, we found that labeling in these conditions afforded Cy3-Cy5-labeled coatomer that contained a major population with a FRET efficiency of 63%. This population could be monitored in subsequent binding experiments with its interaction partners.
After addition of OST48, a monomeric, cargo-type ligand binding to α-COP and β'-COP, a slight shift in FRET efficiency from 63% to 67% was observed. This shift is within the resolution limits of the method used.
Strikingly, binding of dimeric p23 to coatomer via γ-COP leads to a significant shift of the FRET efficiency of the major population from 63% to 84%. Thus, a conformational change induced in the trunk domain of γ-COP (Bethune et al., 2006) is transmitted to the α-subunit of the complex.

The observed transduction of the conformational change induced in γ-COP within coatomer to α-COP is of particular mechanistic interest, as no direct interaction between γ- and α-COP has been described so far. Therefore, at least one coatomer subunit is likely to serve as a "link" for transmitting the conformational information from γ-COP to α-COP. A candidate for this function is ε-COP, which has been reported to interact with both α- and γ-COP (Eugster et al., 2000).

3.1.2. Membrane protein capture and coat lattice formation

In light of the structural analogies of the tetrameric coatomer subcomplex β-γ-δ-ζ-COPs with the adaptor complexes, and similarity of α, β', and ε-COPs with the clathrin proteins ((Duden et al., 1991; Schledzewski et al., 1999); reviewed by (McMahon and Mills, 2004)), it is of interest to compare the functions of these complexes.
Adaptor complexes capture membrane proteins, and in a second step recruit clathrin, which forms the vesicular cage. In contrast, in the COPI system, coatomer is recruited to the membrane en bloc (Hara-Kuge et al., 1994), and thus the clathrin-related subcomplex (αβ'ε) is already present during the capture of membrane proteins, a process that is mediated by the adaptor-like subcomplex (βγδζ) by its γ-subunit. If the clathrin-related subcomplex has a function similar to clathrin's in forming a shell, then its capability to assemble a higher aggregate must come into effect. However, this must not occur before coatomer has captured membrane proteins, because otherwise coatomer could not exist as a soluble complex. In fact, when soluble coatomer binds to dimeric peptides that mimic the cytoplasmic tail of the membrane protein p23, the complex aggregates and precipitates (Reinhard et al., 1999). Therfore, our observation of the transmission of a conformational change through

coatomer from the trunk subcomplex to the clathrin-related outer subcomplex points to a link in the COPI system between membrane protein capture and cage formation. Accordingly, dimeric p23 or p24 protein captured by the trunk domain of γ-COP would represent membrane machinery for the formation of COPI vesicles, as opposed to cargo proteins that bind α/β'-COP and do not alter coatomer's conformation. Thus, the conformational change observed in α-COP could represent an initial step of coat lattice formation, rearranging α-COP to form a Clathrin-like shell or lattice on the donor membrane (Figure 37, A). This would be in good agreement with the findings that only p23 and p24 serve as primary Arf1 receptors on the donor membrane, and form the priming complex during initiation of the budding process.

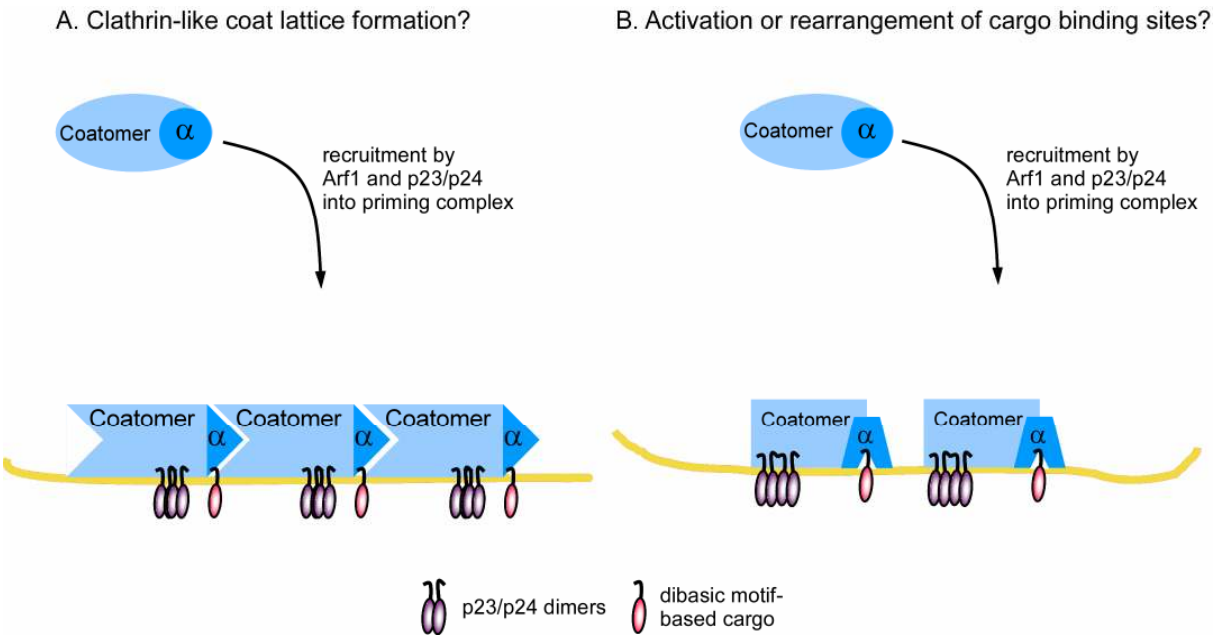

Figure 37: Model for putative role of the conformational change in α-COP during COPI vesicle formation.

In the light of additional mechanisms known from the clathrin system, it is tempting to speculate on further functions of the observed conformational change of coatomer.

As mentioned, clathrin-coated vesicles form upon sequential recruitment of adaptor protein complexes and clathrin to the respective donor membrane. During this process, the cargo binding affinity of the adaptor complexes is tightly regulated. Among other mechanisms, e.g. phosphoinositide binding (Rapoport et al., 1997) and phosphorylation (Collins et al., 2002; Fingerhut et al., 2001; Haucke and De Camilli, 1999; Ricotta et al., 2002), conformational changes induced by the binding of the cytoplasmic domains of transmembrane proteins

specifically activate binding of other cargo to the coating machinery (Boll et al., 2002; Haucke and De Camilli, 1999). In clathrin-coated vesicles, transmembrane proteins serve as cargo and membrane machinery of a vesicle at the same time, and it was proposed that endocytic coated pits may only proceed to form clathrin-coated vesicles if cargo is present (Ehrlich et al., 2004).

In the formation of COPI vesicles, the observed conformational change within α-COP might serve a similar purpose (Figure 37, B). As p24-family proteins are stoichiometric components of COPI vesicles (Malsam et al., 2005; Sohn et al., 1996), the conformational change induced by p23 upon binding to coatomer might represent a key step for recruitment of cargo during vesicle formation. The observed transduction of a conformational change from γ-COP to α-COP might modify the affinity of the cargo binding site in α-COP (Eugster et al., 2004) by rearranging this subunit upon recruitment of coatomer to the donor membrane via γ-COP. To investigate this, we made use of an ELISA-like binding assay previously established in out lab (Bethune et al., 2006). This assay allows determination of the K_D of coatomer for its ligands, and to monitor if the number of available binding pockets changes if the complex alters its conformation. Here, we immobilised coatomer on 96-well Protein A plates, and monitored the affinity of S-tagged binding partners by S-tag specific detection.
Presently, we did not see a significant change in both the K_D and the number of binding sites available for cargo proteins. Thus, the conformational change in α-COP does not open a binding pocket for cargo, as it does in the μ2-subunit of AP-2. However, the structural rearrangement may serve in a more indirect way: it may bring the β-propeller domains closer to the membrane during coatomer recruitment, thus faciliating interaction of coatomer's cargo binding sites with its target cargo transmembrane proteins. Then this rearrangement would not have any impact on the values obtained for both the K_D and the number of available binding sites, as the ELISA-like binding assay is not a membrane-based system.

Future efforts will focus on investigating such functional consequences of the conformational dynamics of coatomer.

3.2. Electron microscopy and tomography of COPI vesicles

As described above, the different coating proteins share certain structural homologies. In fact, all coating complexes contain both α-solenoid and β-propeller domains. However, these re-appearing motifs seem to be put to different uses in the different coating systems: In the Clathrin system, the β-propeller domains mediate interaction of Clathrin with the adaptor proteins and accessory proteins (Fotin et al., 2004b). In the COPII system, these domains (β-propeller) form the vertices of the assembled cages of Sec13/31 (Fath et al., 2007). In coatomer, the β-proeller domains have been characterised as the binding sites for KKxx- and KxKxx-based sorting signals (Eugster et al., 2004).

Whereas both the COPII (Fath et al., 2007; Stagg et al., 2006) and the Clathrin system have been described in detail at the molecular level (Cheng et al., 2007), little is known about the structure of coatomer and the COPI vesicle lattice yet. Recent electron microscopic studies showed "spiky" or "fluffy" coats on Golgi membranes and plant COPI vesicles (Bouchet-Marquis et al., 2008; Donohoe et al., 2007). Structural information is available on one subdomain of one subunit, the γ-COP appendage domain, only, with the overall fold and structure of this subdomain showing striking analogies to the fold of α-subunit of AP-2, (Watson et al., 2004).

In the present work, we tested various different preparation and purification protocolls to obtain samples of coated COPI vesicles generated in GTP-conditions. As samples containing sucrose showed only limited contrast and stability in the electron beam, a sucrose-free sample preparation was used. These samples contained a large number of both coated membranes and coated vesicles.

At the time when this thesis was written, data aquistion was still in progress. The first data sets shown in this work are promising in terms of both contrast and resolution, but the conditions for aquisition of high-resolution and high-contrast tomograms need to be improved, especially by imaging vesicles in thinner ice.

In the future, using the protocoll described in this work, we may be able to obtain tomograms of individual COPI-coated, Golgi-membrane-derived vesicles and resolve the structure of the coat lattice.

4. Materials and Methods

4.1. Materials

4.1.1. Reagents

Chemicals were bought from the companies BioRad (Munich, Germany), Roche (Mannheim, Germany), Sigma (Deishofen, Germany) and Merck (Karlsruhe, Germany) unless stated otherwise.

4.1.2. Peptides

Peptides were synthesized by the company Peptide Speciality Labs (PSL, Heidelberg, Germany) in a standard solid-phase-coupled procedure. Raw peptides were purified using RP-HPLC, and tested by MALDI-MS.

Dimeric peptides were generated by addition of a cysteine-residue at the C-terminus, as indicated in below.

Peptide	monomeric	dimeric
p23	QVFYLRRFFKAKKLIE	CQVFYLRRFFKAKKLIE | CQVFYLRRFFKAKKLIE
p24	QIYYLKRFFEVRRVV	CQIYYLKRFFEVRRVV | CQIYYLKRFFEVRRVV
p25	QMRHLKSFFEAKKLV	CQMRHLKSFFEAKKLV | CQMRHLKSFFEAKKLV
p26	QVLLLKSFFTEKRPISRAVHS	CQVLLLKSFFTEKRPISRAVHS | CQVLLLKSFFTEKRPISRAVHS
p27	QVFLIKSFFSDKRTTTTRVGS	CQVFLIKSFFSDKRTTTTRVGS | CQVFLIKSFFSDKRTTTTRVGS
OST48	HMKEKEKSD	
ERGIC53	QRSQQEAAAKKFF	CRSQQEAAAKKFF | CRSQQEAAAKKFF

4.1.3. Beads

For immunoprecipitation a 1:3 mixture of Protein A Sepharose and CL4B sepharose was used (both bought from BioRad, Munich, Germany) und stored at 4°C in an aqueous 20% EtOH solution

4.1.4. Molecular weight standards for SDS – PAGE

The following marker mixes were used:

- BMW-Marker (*broad molecular weight*) manufactured by BioRad (Munich, Germany) and a marker cocktail by PEQLab (Erlangen, Germany):

Myosine	200kD	β-Galactosidase	116kD
β-Galactosidase	116kD	Bovine serum albumine	66kD
Phosphorylase B	97kD	Ovalbumine	45kD
Bovine serum albumine	68kD	Laktat-Dehydrogenase	35kD
Ovalbumine	45kD	RE Bsp 98I	25kD
Carboanhydrase	30kD	β-Laktoglobuline	18.4kD
Trypsine-Inhibitor	20kD	Lysozyme	14.3kD
Lysozyme	14.3kD		
Aprotinine	6.5kD		

- A prestained Marker-Cocktail with recombinant protein standards bought from BioRad (Munich, Germany):

250kD

150kD

100kD

75kD

56kD

37kD

25kD

4.1.5. Protease – Inhibitors

To inhibit proteases in the Golgi and coatomer preparation, and upon purification of recombinant proteins, protease-inhibitor-cocktail tablets ("complete, EDTA-free") manufactured by Roche Diagnostics (Mannheim, Germany) were used.

4.1.6. Antibodies

4.1.6.1. Primary antibodies

Name	Epitope / directed against:	Dilution for WB / remarks
C1PL	β'-COP	1:3000 serum
CM1	native Coatomer	for immunoprec. and surfaces
883	α-COP	1:1000, cross-reactivity with N-terminus of γ-COP
ε-r	ε-COP	1:2000, rabbit
CY-96	Cy3 / Cy5	1:1000, monoclonal, mouse, bought from Sigma
1409B	α-COP	1:1000, rabbit
Elfriede	p24	1:5000, rabbit
δ-R	δ-COP	1:1000, rabbit
Okt8	CD8-receptor	for surface preps., bought from LGC Promochem, Wesel, Germany
Arf1	Arf1	Arf1-C1 (Reinhard et al., 2003)
γ-R	γ-COP	1:1000, rabbit

Table 3: Antibodies used in this study.

4.1.6.2. Secondary antibodies

Two systems were used for detection in Western blotting: Horseradish peroxidase-coupled goat-anti-rabbit and goat-anti-mouse IgGs manufactured by BioRad (dilution 1:5000) for detection using films, and fluorophore-conjugated secondary antibodies (goat-anti-rabbit, and goat-anti-mouse) for detection in the LI-COR Odyssey System (LI-COR BioSciences, Lincoln, USA).

4.1.7. Activated fluorophores

Activated fluorophores were bought from Amersham Biosciences (Freiburg, Germany). For primary amine-specific coupling to coatomer, the N-hydroxyl-succinimide ester derivatives of the dyes Cy3 and Cy5 were employed.

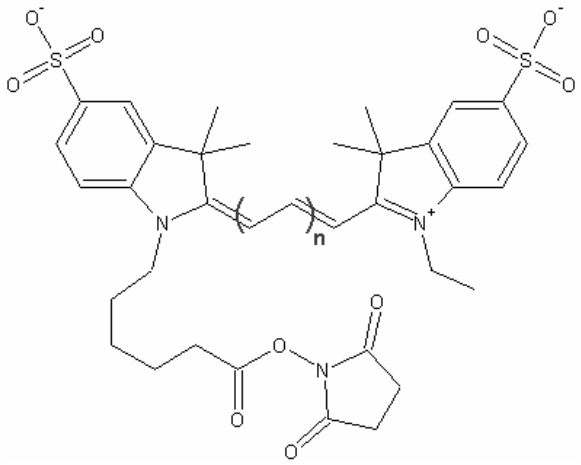

Figure 38: Structure of NHS-ester-derivative of the fluorophores Cy3 (n=1) und Cy5 (n=2).

4.2. Equipment

4.2.1. FPLC-Anlagen

In the preparation of coatomer from rabbit liver cytosol, we employed an FPLC-unit by the company BioRad (Munich, Germany) and an Ettan FPLC unit manufactured by Amersham Biosciences. The columns used are indicated in the corresponding protocols.

4.2.2. SMART

Purification of labeled coatomer was performed in a SMART system manufacted by Amersham BioSciences was used. Columns and conditions indicated in the protocols.

4.2.3. Spectrophotometer

The concentrations of labeled coatomer were measured in a UltroSpec 2000 UV/Vis Spectrophotometer by Amersham Pharmacia BioTech (Freiburg, Germany) in a 100µl-quartz glass cuvette.
The Bradfort assays were performed in a Rosys 2001 microplate photometer (Rosys, Wals, Austria).

4.2.4. Single molecule-sensitive confocal setup

For detection of coatomer labeling in the gels, and for the single-pair, single-molecule FRET experiments, a custom-built confocal microscope was employed. Figure 1 shows a scheme of the setup.

For excitation, two lasers were used: A cw-Nd:YAG laser (Lasergate, Kleinostheim, Germany) emitting at 532nm was employed for Cy3 excitation, and a red diode laser (PicoQuant, Berlin) pulsed by a PDL-808-Sepia control unit (80MHz, pulse width 100ps; PicoQuant, Berlin) and emitting at 635nm was used for Cy5 excitation.

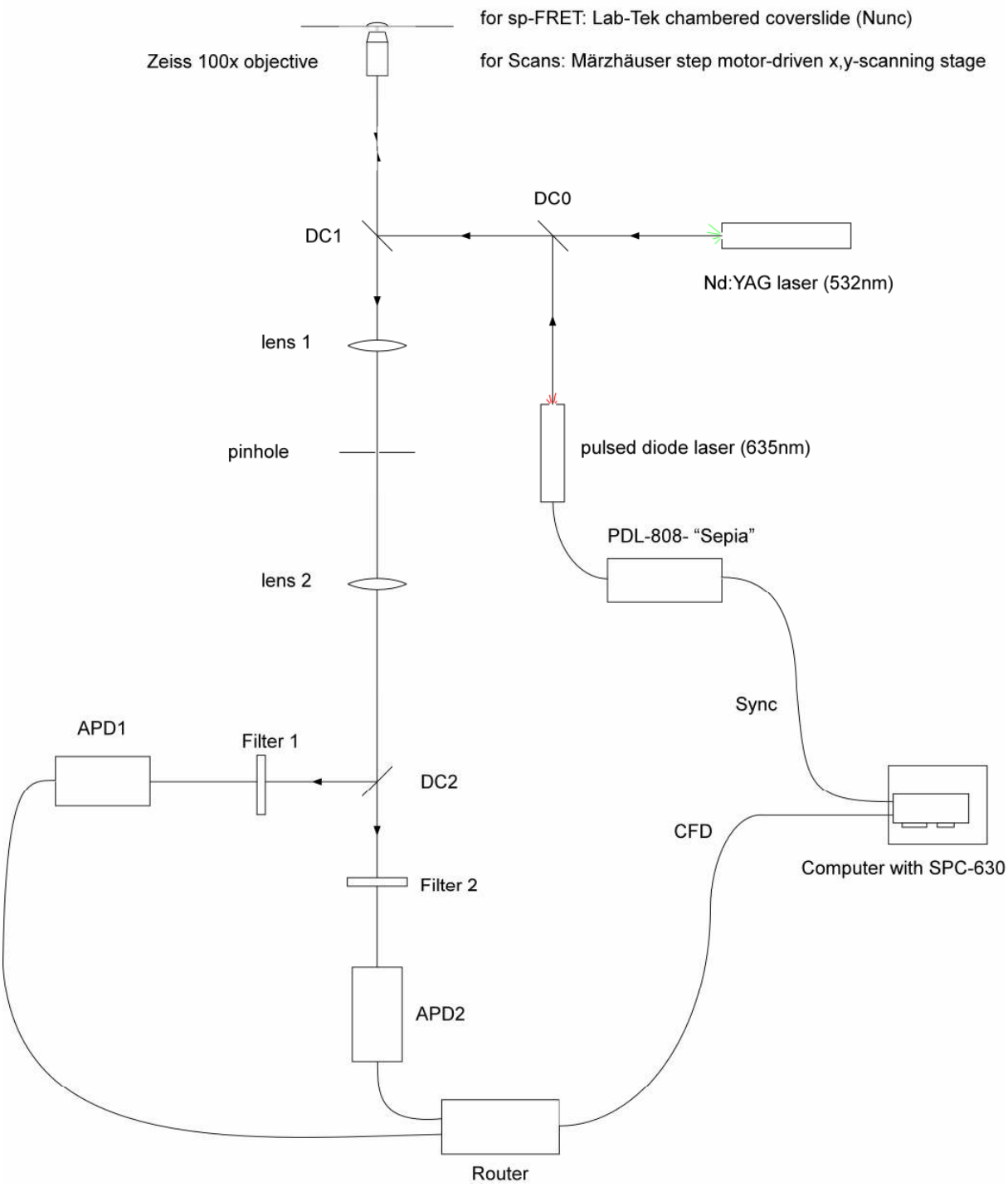

Figure 39: Scheme of the custom-built confocal setup used in this study. DC0, DC1, DC2: Dichroic mirrors; APD: Avalanche PhotoDiode. Filter 1: 575 DF 60, Filter 2: 675 DF 60.

Both laser beams were superimposed by a dichroic mirror (650DLRP; Chroma Technologies, Rockingham, USA; see figure 39) and directed in an inverted microscope (Axiovert 100TV; Zeiss, Jena, Germany). Another dichroic mirror in the microscope (DualBand Beamsplitter 532/633; Chroma Technologies, Rockingham, USA; see figure 39) directed the beam into a 100x oil immersion microscope lens with a numerical aperture of 1.4 (Zeiss, Jena, Germany),

and focused it on the glass surface of the chambered cover slide for single-molecule surface scanning, or in the gel for fluorescence scanning.

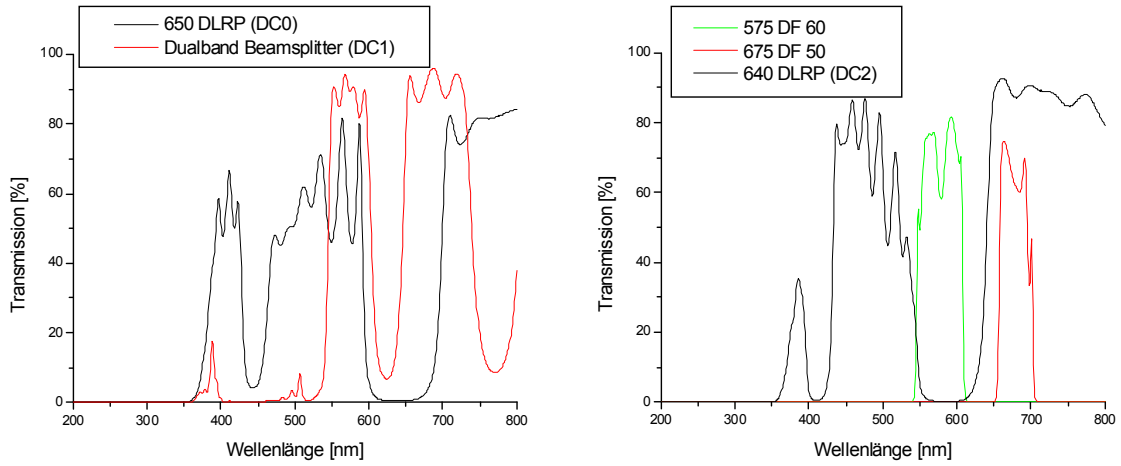

Figure 40: Properties of filters and dichroic mirrors employed in the single-molecule sensitive setup (DC0, DC1, DC2 and filters).

For surface scanning, a piezo stage (PI Analogue, Physik Instrumente) was used. For gel fluorescence scanning, a step-motor-driven *x,y*-scanning stage (Scan 100 x 100, MC2000, Märzhäuser, Wetzlar, Germany) was employed. Both setups were controlled by the same software (DAQLineScan, D.P. Herten and C.M. Roth, Heidelberg University). The average laser power was 25- 150μW for gel fluorescence scanning (dwell times: 1-5ms/pixel; spatial resolution: 10-100μm/pixel) and 3-5μW for single-molecule surface scanning (dwell time: 1ms/pixel, spatial resolution: 50nm/pixel, lower threshold: 10 photons, upper threshold: 30 photons).

Fluorescence emission was collected by the same microscope lens used for excitation, passed through the dichroic mirror, and focused on a pinhole (100μm). Prior to detection, the beam was spectrally separated by a nonpolarizing, dichroic mirror (DC2, 640DLRP; Chroma Techn.,Rockingham, USA; see figure 40). Reflected light was filtered by a 575DF60-Bandpass-Filter (Chroma Techn., Rockingham, USA), and recorded on the first avalanche-photo-diode (SPCM AQR-13; EG&G, Kanada; "donor channel"). Transmitted radiation passed through a 675DF50- Bandpass-Filter (Chroma Techn., Rockingham, USA), and was detected by a second avalanche-photo-diode (SPCM AQR-13; EG&G, Kanada; "acceptor channel"). The signals from both detectors were bundled by a router and collected by a PC-card (SPC-630, Becker&Hickl, Berlin,Germany).

4.2.5. Electron microscopes

The following electron microscopes were used at the Max-Planck-Institute of Biophysics, Frankfurt/Main, Germany:
A Philips CM120 transmission electron microscope, operated at 120kV (FEI Philips, Hillsboro, USA), a FEI Tecnai G2 Spirit transmission electron microscope, operated at 120kV (FEI, Hillsboro, USA) and a FEI Polara G2 Tecnai field emission transmission electron microscope (FEI, Hillsboro, USA).

4.3. Methods

4.3.1. SDS – PAGE

SDS-treated proteins were analysed using a modified, discontinous gel system (Laemmli, 1970). Both in the stacking and in the separation gel the voltage was kept constant (120V in the stacking gel, 180V in the separation gel).

4.3.1.1. Stock solutions for SDS - PAGE

Acrylamide-solution 1:	30%	Acrylamide (w/v)
	0.8%	N,N'-Methylenbisacrylamide (w/v)
Acrylamid-solution 2:	30%	Acrylamide (w/v)
	0.3%	N,N'-Methylenbisacrylamide (w/v)
4x separation gel buffer:	1.5M	Tris-HCl, pH 8.8
	0.4%	SDS (w/v)
4x stacking gel buffer:	0.5M	Tris-HCl, pH 6.8
	0.4%	SDS (w/v)
Elektrophoresis buffer	25mM	Tris
	192mM	Glycine
	0.4%	SDS (w/v)

4.3.1.2. Separation gels

If not stated otherwise, a custom-built gel system allowing a long separation gel (15cm) and simultaneous loading of 22 samples, or the Protean III gel system by BioRad were used. Homogenous separation gels contained 6%, 7.5%, 10% and 12% acrylamide and gradient separation gels contained a gradient of 7.5% - 16.5% acrylamide, as stated in the corresponding protocols. For the custom built gel system, the following composition was used

Gel:	**7.5%**	**10%**	**12%**	**7.5% - 16.5%**	
Acrylamide-solution 2	2.5ml	3.33 ml	4.0 ml	1.3ml	3.05ml
4x separation gel buffer	2.75ml	2.5 ml	2.5 ml	1.3ml	1.3ml
H_20	5.5ml	4.16 ml	3.5ml	2.9ml	1.15ml
TEMED	10µl	10µl	10µl	5.2µl	5.2µl
APS (10%)	40µl	40µl	40µl	20.8µl	20.8µl

The gel cartridge contain a separation gel volume of appr. 10ml (15x7x0.1cm). The gel solutions were added either directly or via a gradient mixer, and covered with isopropanol. The comb was already inserted during separation gel polymerization. For the Protean III system, the compositions listed in table 4 were used:

		Water	Tris 1.5 M pH 8.8	Tris 0.5 M pH 6.8	SDS 10 %	Acrylamide (30%)	APS 10 %	TEMED	total vol
		mL	mL	mL	uL	mL	uL	uL	mL
no of gels	separating gel %								
1	7,50	2,425	1,25		50	1,25	25	2,5	5,0025
1	10,00	2,025	1,25		50	1,65	25	2,5	5,0025
1	12,00	1,675	1,25		50	2	25	2,5	5,0025
1	15,00	1,175	1,25		50	2,5	25	2,5	5,0025
2	7,50	4,85	2,5		100	2,5	50	5	10,005
2	10,00	4,05	2,5		100	3,3	50	5	10,005
2	12,00	3,35	2,5		100	4	50	5	10,005
2	15,00	2,35	2,5		100	5	50	5	10,005
4	7,50	9,7	5		200	5	100	10	20,01
4	10,00	8,1	5		200	6,6	100	10	20,01
4	12,00	6,7	5		200	8	100	10	20,01
4	15,00	4,7	5		200	10	100	10	20,01
	stacking gel								
1	4,00	1,525		0,625	25	0,325	12,5	2,5	2,515
2	4,00	3,05		1,25	50	0,65	25	5	5,03
4	4,00	6,1		2,5	100	1,3	50	10	10,06

Table 4: Gel compositions used for the Protean III system.

4.3.1.3. Stacking gels

After one hour polymerization at room temperature, the isopropanol was removed and washed with H_2O. Residual H2O was removed using filter paper, and ca. 5ml of stacking gel solution with the composition described in Figure X were applied on top of the separation gel already in the cartridge. To from pockets, combs with 15 and 22 teeth were used. After 1h of polymerization at room temperature, the gels were packed in wet paper towels, sealed in plastic wrapping and stored at 4°C.

4.3.2. Sample preparations

4.3.2.1. Sample preparation for SDS – PAGE

The protein solution were diluted with 4x sample buffer in a ratio of 3:4, and heated either to 70° for 10 minutes, or to 95°C for 5 minutes, as stated in the protocol. After a short centrifugation, the samples were injected into the gel pockets.

4x SDS –sample buffer (reducing):	200mM	TRIS-HCl, pH 6
	12%	β-mercaptoethanol
	8%	SDS (w/v)
	20%	Glycerine (w/v)

Bromphenolblau was added to the sample buffer to obtain a blue-colored sample buffer, to faciliate loading of the samples.

4.3.2.2. Tri-Chloro-acetic acid (TCA) – precipitation

Desoxycholate (2% stock solution) were added to the protein sample to a final concentration of 0.2% and incubated at room temperature for 15 minutes. The sample was the adjusted to a final concentration of 10% TCA by addition of cold 50% TCA solution (stored in ice-water), and incubated on ice for 30 minutes. The sample containing the precipitated proteins was then centrifuged (Heraeus-Biofuge, 13000 g, 4°C, 15min), and the supernatant discarded. The precipitate was washed with cold aceton (stored at -20°C) and centrifuged again (see above). After removing the supernatant, the precipitate was dried at room temperature for 5 minutes, and the precipitates proteins resuspended in an appropriate volume of 1x SDS sample buffer.

4.3.2.3. Immunoprecipitation (IP)

Coatomer was purified or depleted using immunoprecipitation. The IP-γ buffer was used either with or without detergent, as stated in the corresponding protocol.

25	mM	TRIS-HCl, pH7.4
150	mM	KCl
1	mM	EDTA
0.5	%	NP-40

To bind ca. 30µg of coatomer, 200µl CM1 solution (hybridoma cell culture supernatant) and 120µl Protein A sepharose beads were used. For the incutation times stated below, the samples were agitated in an overhead shaker at room temperature, or overnight as stated in the protocol.

Step	**Buffer / Volume**	**Time**
Wash	IP-γ with Det. / 1ml	3x 10min
Addition / coupling of antibody	IP-γ with Det. / 500µl	1h
Wash	IP-γ with Det. / 1ml	3x 10min
Addition of coatomer .	IP-γ with Det. / 400µl	1h
Wash	IP-γ with Det.	3x 10min
Wash	IP-γ without Det.	10min
Elution with sample buffer	4x SDS sample buffer / 30µl	--

Subsequently, samples were submitted to SDS PAGE as described above.

4.3.3. Staining of proteins in SDS – gels

4.3.3.1. Coomassie-Staining

The gels were incubated in Coomassie staining solution for 1h at room temperature, which led to a complete staining of the gel. Using destaining solution, the gels were subsequently washed to give the appropriate staining levels.

Coomassie stock solution:	1g		Serva-Blue G
	4g		Serva-Blue R
	500ml		H_2O
Coomassie staining solution:	25%	(v/v)	Isopropanol
	10%	(v/v)	HOAc
	5%	(v/v)	Coomassie stock solution
Destaining solution:	10%	(v/v)	Isopropanol
	10%	(v/v)	HOAc

4.3.3.2. Silver stain

Gels were treated according to the following protocol. During all steps, samples were agitated at room temperature.

Step	**Solution**	**Time**
Fixation	50% MeOH, 10% HOAc	>1h
Wash	50% EtOH	2x 15min
Incubation with Natriumthiosulfate	10mg / 50ml $Na_2S_2O_3$ x $5H_2O$	1min
Wash	H_2O	2 x 20s
Incubation with $AgNO_3$-solution.	100mg / ml $AgNO_3$, 50µl Formalin	15min
Wash	H_2O	2 x 20s
Develop	(3g Na_2CO_3, $Na_2S_2O_3$ x $5H_20$) in 50ml H_2O; 50µl Formalin	<10min
Stop	12% HOAc	>5min

Upon reaching the desired staining levels, the reaction was stopped by addition of 12% HOAc.

4.3.4. Western blot analysis

4.3.4.1. Transfer of proteins separated by SDS-PAGE onto PVDF-membranes

Proteins were transferred from SDS-PAGE onto PVDF-membranes (Immobilon-P, Millipore, Eschborn) using a "semi-dry" procedure in Trans-Blot SD cells manufactured by BioRad (Munich, Germany). Per gel, 7 filter papers (Whatman 3mm) and a membrane were cut in

the size of the gel to be blotted. Two papers each were soaked in Anode buffers 1 and 2, and deposited on the anode board (anode 1 soaked paper on bottom). After application of the PVDF-membrane, the gel was deposited on top, and subsequently covered with the 3 remaining paper slips soaked in cathode buffer. After careful removal of air bubbles using a round object, the cathode plate was set on top. Proteins were then transferred onto the membrane at 24V (constant voltage) for 90 minutes.

Anode buffer 1:	300	mM		Tris
	20	%	(v/v)	Methanol
Anode-buffer 2:	25	mM		Tris
	20	%	(v/v)	Methanol
Cathoden buffer:	25	mM		Tris
	40	%	(v/v)	Methanol

4.3.4.2. Ponceau-Staining of proteins on PVDF-membranes

This method was used for staining of proteins separated by SDS-PAGE and transferred onto PVDF-membranes. The blots were inbutated for 5 minutes with Lyon-Ponceau-staining solution, and subsequently washed with dest. water until the desired destaining levels were reached.

Lyon-Ponceau-staining solution:	0.8	%	(w/v)	Ponceau
	4	%		TCA

4.3.4.3. Immunochemical detection of proteins on PVDF-membranes

Membranes with transferred proteins were either incubated 1h at room temperature or over night at 4°C in PBS-T containing 5% (w/v) milk powder. Subsequently, membranes were washed 2x10 Minuten in PBS-T. The blots were then incubated with the corresponding primary antibodies in PBS-T containing 1% BSA for 30 minutes at room temperature. The blots were washed 3x10 Minuten with PBS-T, and subsequently incubated with secondary antibody in PBS-T containing 3% milk powder for 30 minutes at room temperature. The blot was then developed using either one of the two following systems: 1. The ECL system by the company Amersham Pharmacia Biotech (Freiburg, Germany) for detection of peroxidase-coupled secondary antibodies. Here, the protocol of the manufacturer was used. For detection fo the chemoluminescence, CEA RP New films (Strangnas, Sweden) were used. 2.

The LI-COR Odissey system manufactured by LI-COR Biosciences (Lincoln, USA). For detection, the protocol of the manufacturer was followed.

4.3.5. Bradford assay

Protein concentrations were determined using staining solutions bought from BioRad (Munich, Germany). An appropriate volume of protein solution (about 10 – 20 µg) was diluted to a final volume of 800µl in mp water (triplicate measurements with different dilutions), with an 8-point calibration curve in a range of 2.5 – 20µg BSA (0, 2.5, 5, 10, 15, 20 and 25µg/ml final concentration, in 800µl final volume). Then, 200µl of Bradford reagent were added to all samples and incubated at room temperature for 10 minutes. 200µl of each sample were transferred into a microtiterplate and the optical density at 620nm measured in the microplate reader.

4.3.6. Isolation of coatomer from rabbit liver cytosol

To achieve a higher yield and purity of the coatomer complex, the original protocol by J. Pavel (Pavel et al., 1998) was slightly modified.

4.3.6.1. Isolation of rabbit liver cytosol

For one preparation, 3 livers (ca. 160g) from freshly killed rabbits (starved for 12h to reduce glycogen in the livers) were used. The livers were transferred into ice/water right after extraction, cut into thin slices (>1cm) and placed into homogenisation buffer (200ml). Homogenisation of the tissue was performed in a Warring blender with pulses of 2x 30s and a pause for cooling (2min) on ice. The homogenate was centrifuged at 15000xg at 4°C for 1h (Heraeus-Suprafuge 22, Rotor: HFA 12.500). The supernatant was filtered through 4 layers of mull and centrifuged at 100000 xg, 4°C (Ultracentrifuge, Rotor: TFT 50.38). The supernatant ("rabbit liver cytosol") was filtered through 4 layers of mull again.

4.3.6.2. Ammoniumsulfate precipitation of rabbit liver cytosol

Rabbit liver cytosol was diluted 1:2 with cold homogenisation buffer 2 and transferred into a glass beaker. Slowly, freshly pulverized Ammoniumsulfate was added to a final concentration of 35% under constant stirring on ice, and after completed addition stirred for another 45 minutes. The precipitate was centrifuged for 30 minutes at 10.000 xg, 4°C (Heraeus-Suprafuge 22, Rotor: HFA 12.500), and the supernatant was discarded. The precipitate was resuspended in 100ml of resuspension buffer, homogenized in a Douncer and dialysed 2x 1h and 1x overnight against 5l IEX-1 (Ion-EXchange chromatography buffer 1) each. Unsoluble

proteins were precipitated by a centrifugation at 100000 xg (Ultracentrifuge, Rotor: TFT 50.38) for 30 minutes at 4°C. This centrifugation was repeated until the supernatant was a clear solution. This fraction was then filtered through a membrane with a pore size of 0,45µm ("ammoniumsulfate precipitate, ASP").

4.3.6.3. DEAE anion exchange chromatography of ASP

A 300ml DEAD-FF column (Amersham Pharmacia Biotech, Freiburg, Germany) was equilibrated with 1l of IEX-1. Subsequently, the ammoniumsulfate precipitate was applied to the column at a flow rate of 10ml/min and washed with IEX-1 until baseline absorption was reached again. Bound protein was then eluted with mixture of 50% IEX-1 and 50% IEX-2 at a flow rate of 10ml/min. The whole protein peak was collected and the conductivity set to the value of IEX-1 ("DEAE-Pool").

4.3.6.4. SourceQ anionic exchange chromatography of the DEAE pool

A SourceQ column with a bed volume of 15ml (Amersham Pharmacia Biotech, Freiburg, Germany) was equilibrated with 50ml of IEX-1 (flow rate 2ml/min), and the DEAE-pool applied to the column over night (max. flow rate 1mg/ml). Subsequently, the column was washed with IEX-1 until baseline absorption was reached again. Bound protein was eluted in a linear gradient from IEX-1 to IEX-2 over 200ml. The eluate was collected in fractions of 3ml, and 5µl of each fraction submitted to SDS PAGE and Coomassie staining and Western blotting. The fractions containing coatomer were pooled and adjusted with conductivity buffer to the conductivity of IEX-1 ("SourceQ-Pool").

4.3.6.5. Concentration of the SourceQ-Pools

A SourceQ column with a bed volume of 1ml (Amersham Pharmacia Biotech, Freiburg, Germany) was equilibrated with 5ml IEX-1 (flow rate 250µl/min). The SourceQ pool was loaded onto the column with the same flow rate, and the column re-equilibrated to IEX-3. Coatomer was eluted in a linear gradient of IEX-3 to IEX-4 (0%-60% IEX-4) in a volume of 6.5ml. Coatomer was collected in fractions of 300µl and checked in Coomassie stained gels and by Western blotting against coatomer subunits. According to purity, different fractions were pooled. Protein concentration was adjusted to 5mg/ml, aliquoted into 10µl aliquots, snap-frozen in liquid nitrogen and stored at -80°C.

4.3.6.6. Buffers for coatomer preparation

Homogenisation buffer 1:	25	mM	Tris-HCl, pH 7.4
	500	mM	KCl
	250	mM	Saccharose
	2	mM	EDTA-KOH
	1	mM	DTT
	2 Tabl./100ml		Protease-Inhibitor, complete
Homogenisation buffer 2:	25	mM	Tris-HCl, pH 7.4
	2	mM	EGTA-KOH
	1	mM	DTT
Resuspension buffer:	25	mM	Tris-HCl, pH 7.4
	200	mM	KCl
	1	mM	DTT
	2 Tabl./100ml		Protease-Inhibitor, complete
IEX-1:	25	mM	Tris-HCl, pH 7.4
	200	mM	KCl
	1	mM	DTT
	10	%	Glycerine (w/v)
IEX-2:	25	mM	Tris-HCl, pH 7.4
	1	M	KCl
	1	mM	DTT
	10	%	Glycerine (w/v)
Conductivity buffer:	25	mM	Tris-HCl, pH 7.4
	1	mM	DTT
	10	%	Glycerine (w/v)
IEX-3:	25	mM	HEPES-KOH, pH 7.4
	100	mM	KCl
	10	%	Glycerine (w/v)

IEX-4:	25	mM	HEPES-KOH, pH 7.4
	1	M	KCl
	10	%	Glycerine (w/v)

Table 5: Buffers used for the preparation of coatomer from rabbit liver cytosol.

4.3.7. Labeling coatomer

A sample of purified coatomer (50μg protein) was incubated with dye solution (600pmol of Cy3-NHS-ester and Cy5-NHS-ester (in 2μl ddH2O each) for the single-molecule experiments) in a total volume of 20μl. The pH was set to 8.0 by addition of 1.5μl of previously adjusted pH-shift reagent (25mM HEPES KOH, 100mM KCl, pH 8.2). The sample was incubated for 3h on ice. Precipitated protein was removed by centrifugation at 100,000g for 15 min at 4°C. Unbound dye was removed by gel filtration on a Sephadex G-50 column with a bed volume of 1.5ml mounted in a SMART FPLC system (GE Healthcare; PBS buffer: see above). Labeled coatomer eluted in the void volume and these fractions were pooled and stabilized by addition of BSA to a final concentration of 1mg/ml.

Prior to addition of BSA, the labeling efficiency was estimated by relating the absorption at 280nm (protein; corrected for crosstalk by the dyes, 8% for Cy3 and 5% for Cy5) and at 552nm (Cy3, $\varepsilon(552)=150000$ and at 649nm (Cy5, $\varepsilon(649)=250000$). Using these conditions, we found about one donor (Cy3) and one acceptor (Cy5) dye per coatomer (0.943 ± 0.09 (S_D,n=6)).

4.3.8. Analysis of labeled coatomer subunits

Coatomer was purified by immuno precipitation with the antibodies CM1 (monoclonal, anti-β'-COP, mouse) and 883 (polyclonal, anti-α-COP, rabbit), as described previously (Wegmann et al., 2004), and its subunits were separated by SDS-PAGE under reducing conditions on 12% gels. Gels were prepared for fluorescence scanning by fixation in 30% (v/v) methanol. Thereafter, they were transferred into a chambered cover slide (Lab-Tek, Nunc GmbH, Wiesbaden) and scanned at excitation wavelengths of 532nm and 635nm in a confocal laser setup, as described above.

4.3.9. Isolation of rat liver Golgi

For one preparation, 11 male Wistar rats were killed and left to bleed out briefly. The livers were instantly upon excision transferred into precooled homogenisation buffer and cut into small pieces (<1cm). After weighing, 3 parts (v/w) of homogenisation buffer per liver mass were added.

The liver were then homogenized using an Ultrathorax for 30s at highest possible speed. The homogenate was transferred into 50ml Falcon tubes and centrifuged for 10min at 2200rpm at 4°C. The supernatant was filtered through 4 layers of mull to obtain Perinuclear supernatant (PNS). This supernatant was applied onto 20ml of a 1.25M Sucrose/Tris solution (ca. 16ml of PNS in SW-28 tube, appr. 10 tubes).

The samples were centrifuged for 1:30h at 25000rpm at 4°C. The interphase (IPH) was harvested with a plastic pipette (appr. 35ml). The sucrose concentration of this fraction was adjusted to 1.255M by adding 2M sucrose.

The IPH was then applied to a second gradient in SW-28 tubes, as described below (pour from bottom):

+ 10ml 0.5M Sucrose	top
+ 10ml 1.0M Sucrose	
+ 10ml 1.1M Sucrose	
+ 6ml IPH	bottom

The samples were then centrifuged for 2:30h at 25000rpm (4°C). The interphase between 0.5M and 1.0M sucrose was harvested, containing the Golgi (recognizable by white flakes on white layer). The purified Golgi membranes were then snap-frozen in liquid nitrogen and stored at -80°C.

4.3.10. Pull down experiments

The recombinant proteins used (Trx-His_6, Trx-His_6-p23d, Trx-His_6-OST48) were described previously (Bethune et al., 2006). Constructs (200pmol) with the cytoplasmic domains of OST48 or dimeric p23 and a Thioredoxin- (Trx) and His6-Tag were immobilized on Ni-Sepharose (Amersham Biosciences) in PBS buffer (see above) by incubation for 1h at RT. After three wash steps, the beads were blocked with 0.1% BSA (w/v). 2pmol of coatomer were added and incubated for 30 min at RT. After three wash steps with imidazole (30mM) and detergent (Triton X-100, 0.5%), bound coatomer was eluted from the Sepharose beads by incubation with SDS sample buffer at 95°C, separated by SDS-PAGE and visualized by immunoblotting.

4.3.11. Membrane binding assay

Rat liver Golgi membranes and Arf1 were prepared as previously described (Franco et al., 1995). 10μg of enriched rat liver Golgi membranes were incubated with Arf1 (1μg), GTPγS (100μM) and labeled or unlabeled coatomer (1μg) in a total volume of 50μl (25mM HEPES/KOH, 20mM KCl, 2.5mM $Mg(Ac)_2$, 0.2M saccharose, 1mM DTT, 1mg/ml ovalbumin, 40μM ATP, pH 7.2).
After incubation for 15 min at 37°C, the samples were loaded on top of a sucrose cushion (15% (w/v), 165μl per 50μl sample volume) and membranes and bound coatomer were precipitated by centrifugation at 20,800g for 30 min. The pellet was dissolved in SDS sample buffer, subjected to SDS-PAGE and analyzed by immunoblotting, as described above.

4.3.12. In vitro COPI vesicle budding assay

4.3.12.1. 17h gradient purification

For a typical COPI budding assay, the following components were mixed (in the order they are listed) for a "10ml-preparation":

AP Buffer:	25mM Hepes-KOH, pH 7.0, 2mM $Mg(OAc)_2$	1ml
DTT:	1M	2.5μl
Sucrose:	2M	516μl
KCl:	3M	45.9μl
Rat liver cytosol:	38.2mg/ml	1.254ml

The sample was incubated for 5 minutes at 37°C, and then 1.550ml of rat liver Golgi membranes (prepared as described above, typically 0.5mg/ml) and 10μl of a 100mM GTPγS solution were added.
The sample was incubated for 20 minutes at 37°C and then put on ice for 10 minutes. Subsequently, the sample was centrifuged for 20minutes at 10500rpm in an SS-34 rotor (in a Sorvall RC-6 centrifuge) at 4°C. The pellet was resuspended in 600μl of LSSB buffer, transferred into 1.5ml Eppendorff cups and incubated for 10minutes on ice. The samples were centrifuged again for 15minutes at 13000 rpm (Eppendorff centrifuge 5415 R) at 4°C.
The pellet was resuspended in 600μl HSSB and incubated for 10 minutes on ice, followed by a centrifugation at 13000rpm for 10 minutes at 4°C. The supernatant was again centrifuged for 15 minutes at 13000rpm at 4°C to remove large membrane fragments.

The sucrose concentration of this supernatant was adjusted to ~20%. Then the sample was applied on top of the following gradient comprised of the following layers in SW-55 tubes (poured from bottom):

sample containing COPI vesicles	top
+ 715µl 25% Sucrose	
+ 715µl 30% Sucrose	
+ 715µl 35% Sucrose	
+ 715µl 40% Sucrose	
+ 715µl 45% Sucrose	
+ 715µl 50% Sucrose	bottom

The gradients were centrifuged in a SW-55Ti rotor at 33000rpm for 18h at 4°C, and the gradient fractionated in 200µl fractions by incising the bottom of the tubes in a custom-built setup. The sucrose concentrations were determined and then aliquots of each fraction submitted to Electron microscopy or to SDS PAGE and Western blotting. Typically, the fractions with a sucrose concentration of 39%-42% contained a homogenous population of COPI vesicles.

4.3.12.2. 1h cushion centrifugation

Rat liver Golgi membranes were submitted to a high-salt wash (1M KCl final concentration, in AP buffer: 25mM Hepes-KOH, pH 7.0, 2mM $Mg(OAc)_2$), diluted to a sucrose concentration of <10% and incubated on ice for 10minutes.

After placing sucrose cushions (17%) at the bottom of the tubes, the membranes were pelleted by centrifugation at 12000rpm for 15min in a TLS-55 rotor. The supernatant was discarded, and the membranes resuspended in assay buffer containing 23% sucrose (125µl per 1mg of Golgi membranes). For a typical COPI vesicle budding experiment, 200µg of purified, salt-washed rat liver Golgi membranes were incubated with 40µg of labeled and unlabeled coatomer, 5µg purified Arf1, 10mM GTPγS, 1mM DTT, 85mM Sucrose, 90mM KCl, 50µM GTPγS in a total volume of 500µl assay buffer (25mM HEPES-KOH, pH 7.0; 2mM $Mg(OAc)_2$). The samples were incubated at 37°C for 10 minutes in order to obtain primed Golgi membranes. Then the samples were transferred on ice, and the vesicles released by incubation for 10 minutes on ice after addition of 20µl 3M KCl (final conc.: 200µM). The membranes were then precipitated by centrifugation at 16100 xg for 5 minutes at 4°C. The supernatant was transferred into SW-55Ti tubes with split adaptors, and underlayered with a cushion of 50µl 37% sucrose and 5µl 47% sucrose. After centrifugation at 32000rpm at 4°C, the pellets were harvested from the bottom in a volume of 17µl, mixed with SDS sample buffer, subjected to SDS PAGE and analyzed by immunoblotting.

4.3.12.3. Sucrose-free preparation of crude vesicles

For sucrose-free COPI vesicle preparation, rat liver Golgi membranes were submitted to a high-salt wash (1M KCl final concentration, in AP buffer (see above), diluted to a sucrose concentration <10% and incubated on ice for 10 minutes. The Golgi membranes were then spun down by centrifuging at 12000 xg for 5 minutes.
The components were added as described for the 1h cushion centrifugation, and incubated on ice for 5 minutes, and subsequently at 37°C for 10 minutes. The samples were then mixed in a 1:1 rationwith a solution of colloidal gold as high contrast markers for tomography, and directly applied to the Quantifoil grids.

4.3.13. Grid preparation for *negative staining*

Thin (~10nm) carbon-coated grids were generated by evaporating carbon by resistive heating onto mice and floating onto standard 400 mesh copper electron microscopy grids.
Before using these carbon-coated grids in negative staining, the grids were freshly glow discharged (30s). 3µl of sample were applied onto each grids, and allowed to adsorb to the carbon backing for 2 minutes. Using filter paper (Whatman Nr. 4, Whatman Corporation, Maidstone, UK), the sample was removed by blotting and 3µl of a solution of 1% uranyl acetate were added. The uranyl acetate was immediately blotted again with filter paper (see above), another drop of 3µl of 1% uranyl acetate added onto the grid and left to stain for 2 minutes. The grid was then blotted again with filter paper,and left to air dry (5 minutes) before inserting into the electron microscopy.

4.3.14. Grid preparation for cryo electron tomography

After glow discharging at 1000V for 30 seconds, the quantifoil grids (R2/2 on copper 300 mesh grids, Quantifoil Micro Tools GmbH, Jena, Germany) were examined in the light microscope for tears and holes in the carbon film.
Colloidal gold particles with diameters of 6,10 and 25nm (Aurion, Wageningen, The Netherlands) as fiducial markers were mixed with the sample to be frozen in a 1:1 ratio. The grids were secured in forceps, and a drop of 3µl of sample was applied to the carbon surface. The forceps were then fixed into a custom-built, gravity driven freezeplunging device (Deryck Mills, Max-Planck Institute for Biophysics, Frankfurt/Main, Germany). After blotting for 3 -10 seconds (depending on the viscosity of the sample), the grids were plunged into a reservoir of liquid ethane and transfered into a liquid nitrogen cooled aluminium sample

chamber, and kept in liquid nitrogen until the grids were transfered into the electron microscope (never warming above 130K).

4.3.15. Precipitation assay

Rabbit liver coatomer (0.1μM) was incubated with the indicated concentrations of peptides (10, 20 and 50μM for dimeric p23/24, and 50μM for the other peptides) in a total volume of 20μl of buffer (25mM HEPES-KOH, pH 7.4; 100mM KCl) for 30min at room temperature. The samples were then centrifuged for 15min at 40000g, and the supernatant discarded. The pellets containing precipitated protein were resuspended by addition of 5μl of 4% SDS buffer and 5μl of 4x SDS sample buffer. The samples were then submitted to SDS-PAGE and stained with Coomassie.

4.3.16. Limited proteolysis

Rabbit liver coatomer (0.1μM) was incubated in presence and absence of peptides in the corresponding concentrations (monomeric peptides: 50μM, dimeric peptides 25μM) for 1h at room temperature in 25mM Hepes-KOH pH7.4, 100mM KCl. Subsequently, Thermolysine (0.008μM) was added for the indicated periods of time, and proteolysis was stopped by addition of EDTA (final concentration: 40mM). After addition of SDS sample buffer, the samples were subjected to SDS-PAGE and analyzed by immunoblotting.

4.3.17. Antibody purification

50ml of CM1 or Okt8 hybridoma cell line supernatant were incubated with 500µl Protein A sepharose beads (Amersham Biosciences) at 4°C overnight after addition of an EDTA-free protease inhibitor tablet (Roche) and 5ml 10x PBS. Subsequently, beads were washed with 2x 15ml PBS and then resuspended in 1ml PBS and transferred to a disposable column (BioRad), The antibody was eluted with 3x 1ml of elution buffer (0.1M glycin, pH 2.8) into tubes already containing 175µl of neutralization buffer to immediately neutralize the solution (pretested on elution buffer not containing any sample).
The protein concentration was determined, aliquots (10µl) snap-frozen in liquid nitrogen and stored at -80°C.

4.3.18. Surface preparation

Antibodies were purified by Protein A affinity chromatography (as described above). 8-well chambered cover slides (Lab-Tek, Nunc, Wiesbaden, Germany) were cleaned and activated with oxygen plasma (30s, Tepla 100-E, Asslar, Germany) and incubated overnight at 4°C with PBS containing 10mg/ml BSA (Sigma-Aldrich, München, Germany) and 2μg/ml of purified antibody (CM1 or Okt8). All subsequent steps were carried out using PBS with 1mg/ml BSA. After 5 washing steps (800μl, 5min each), labeled coatomer (3ng) was added and incubated for 20 min at 4°C. After two wash steps with detergent (NP-40, 0.5%), the surfaces were washed five times without detergent (5min each). The surfaces were then directly scanned and the sp-FRET measured in the custom-built confocal setup described above.

4.3.19. Calculation of FRET efficiency E_{appr}

For FRET experiments, the surfaces were illuminated with the Nd:YAG laser with emission at 532nm. Only spots showing detectable intensity in the acceptor channel (>10 photons/pixel*ms) during low intensity surface scanning were selected for subsequent time-resolved fluorescence intensity recording, and each spot was irradiated until complete photobleaching occurred.
Only spots showing a single-step photo-bleaching event in the acceptor channel, a simultaneous increase in the donor channel, and a subsequent single-step photo-bleaching event in the donor channel were kept for subsequent evaluation (<5% of picked spots).
The time until acceptor photo-bleaching (T_{pb}), as well as the total number of photons in the donor ($I_{D,T}$) and acceptor channels ($I_{A,T}$) during this period, were extracted manually from the recorded data. In addition, the individual background of each spot was recorded after complete photo-bleaching for at least 30s ($I_{A,B}$ and $I_{D,B}$) as shown in figure 41.

With the parameters employed for imaging (dwell time: 1ms/pixel, spatial resolution: 50nm/pixel, lower threshold: 10 photons, upper threshold: 30 photons), the lowest detectable FRET efficiency is 25%. Thus coatomer complexes with a FRET efficiency below 25% are omitted from the histograms.

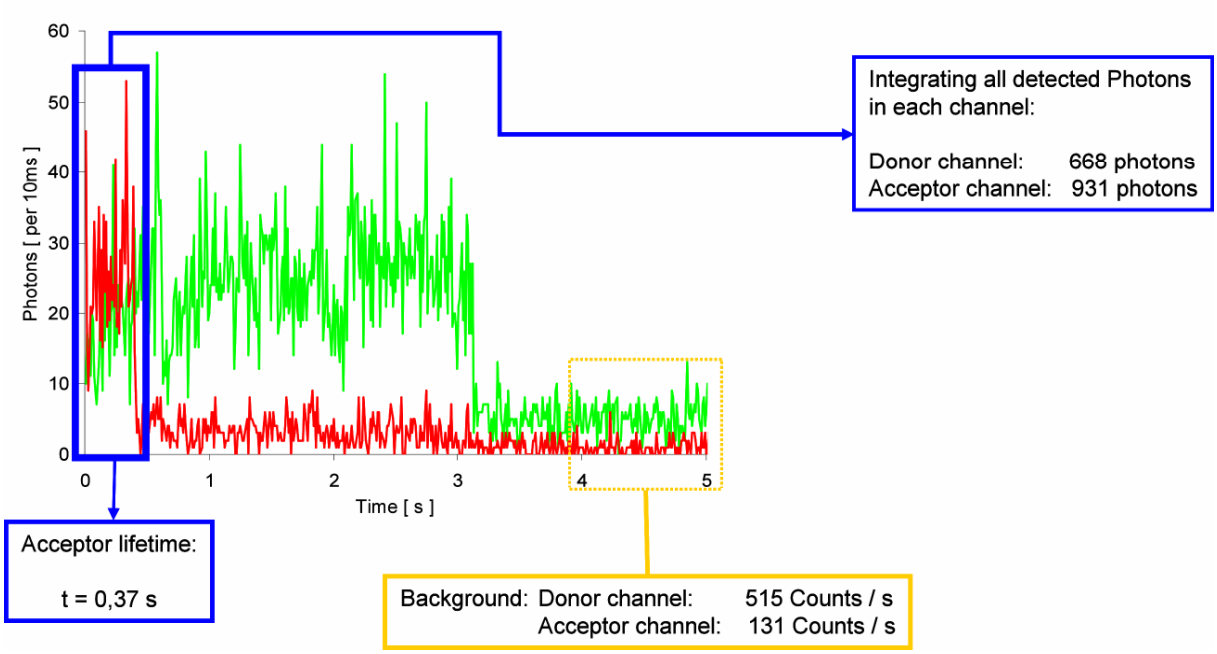

Figure 41: Fluorescence intensity trace of a typical singly donor- and acceptor-labeled coatomer complex, and scheme of data extraction that was used for subsequent calculation of E_{App}. Cross-talk was measured in independent experiments.

The FRET efficiency E_{app} of an individual complex was approximated from the fluorescence intensity trace using the formula: $E_{app} = I_A / (I_A + I_D)$ (Ha, 2001), where $I_A = (I_{A,T} - I_{A,B}) - \beta * (I_{D,T} - I_{D,B})$ and $I_D = (I_{D,T} - I_{D,B}) + \beta * (I_{D,T} - I_{D,B})$. The term $(I_{x,T} - I_{x,B})$ subtracts background noise and the term $\beta * (I_{x,T} - I_{x,B})$ corrects for spectral cross-talk. After subtraction of background and correction for crosstalk, a minimal threshold was applied, and spots with n<200 photons in either channel were discarded.

For the above calculations, the coefficient β was calculated using a surface labeled with only Cy3-labeled coatomer (acceptor only). 20 spots were picked, photobleached and the emitted photons were recorded. The coefficient β (β = 0.1153) was estimated from the ratio of emitted photons in the donor and the acceptor channel. The correction factors for quantum yield and overall detection efficiencies in the donor and acceptor channels were omitted for the FRET pair Cy3 and Cy5, as proposed by (Ha, 2001). A scheme of the calculation of E_{App} is shown in Figure 42.

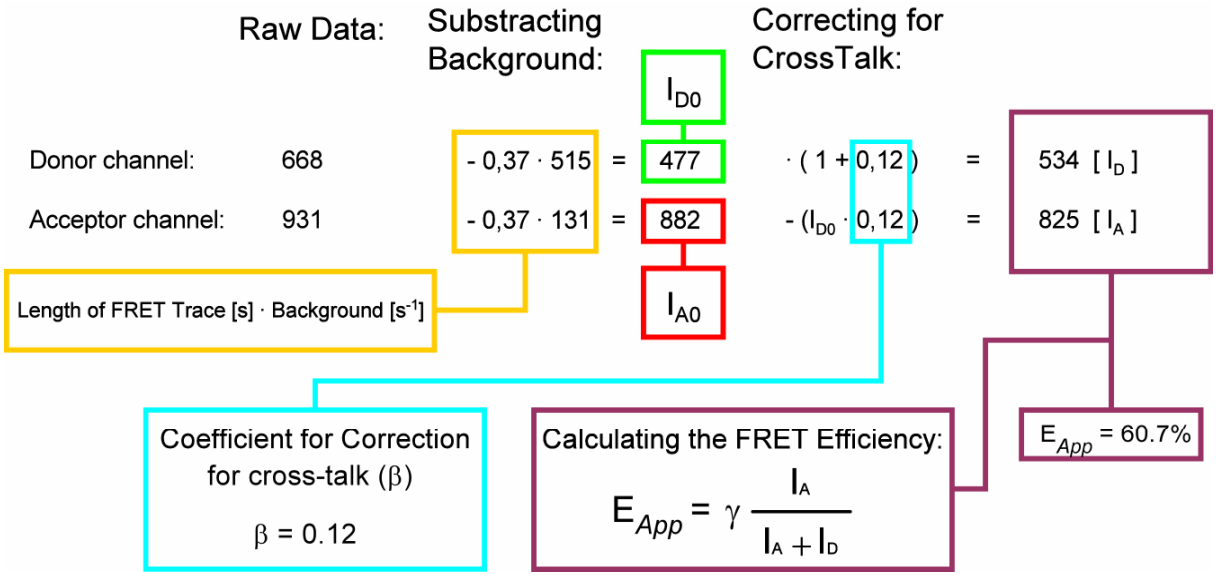

Figure 42: Schematics of steps involved in calculation of E_{App}. The coefficient for correction for cross-talk was measured in an independent set of experiments using only Cy3-labeled coatomer.

Each coatomer molecule evaluated was subsequently sorted according to its energy transfer efficiency E_{app} in a histogram with a class size of 5%. The major populations present in the histogram were assumed to be normally distributed and their mean values and standard deviations were determined by fitting one or two Gaussian functions with a chi-squared ranging between 0.90 and 1.22 using Microcal Origin 7.5. The discrepancy between fitted and measured values is attributed to the assumption that random labeling generates homogenous background. However, this deviation has no effect on the determination of the centre of the major peaks.

4.3.20. ELISA-like binding assay

The protocol this assay was described previously (Bethune et al., 2006). Coatomer was immobilized on 96-well microtiter plates pre-coated with protein A (Perbio science, Bonn). First, the plates were incubated with 300 µL of PBS-T containing 5% BSA overnight at 4°C each. Then, the wells were washed twice with PBS-T and incubated with 100 µL per well of CM1 antibody (from a hybridoma cells supernatant) for 30 min. Subsequently, the plates were washed with binding buffer, and then incubated for 1h at room temperature with a solution of 0.1 µM coatomer in PBS-T containing 1% BSA (100 µL per well). Subsequently, the plates were incubated with different dilutions of fusion proteins in binding buffer (50 mM Hepes, 90 mM KCl, 300 mM NaCl, 1 mM EDTA, 1% BSA, 0.5% Triton X-100) for 1h at RT at concentrations of 0 nM, 1 nM, 10 nM, 30 nM, 100 nM, 300 nM, 1 µM, 3 µM, 10 µM and 20

μM. Then, the plates were washed 5 times with binding buffer followed by incubation with 100 μl of a 1:4000 dilution of S-protein HRP Conjugate (Novagen, Bad Soden) in binding buffer for 30 min at room temperature. The plates were then washed 3 times with binding buffer and once with binding buffer containing no BSA and Triton X-100. Fusion proteins were detected using a solution of tetramethylbenzidin (5 mg in 100 μL of DMSO added to 50 mL of 0.1M sodium carbonate buffer at pH 6 and containing 0.02% HO). The coloration was stopped by adding 50 μL of a 0.5 M sulfuric acid solution in each well. For quantification, the absorbance at 450 nm was measured with a microplate reader (Rosys Anthos)

.

4.3.21. Electron microscopy and tomography

The following microscopes were used to screen and image both negative stain grids and cryo specimens: A Philips CM120 transmission electron microscope (Philips, FEI Philips, Hillsboro, USA) operated at 120kV, a Tecnai G2 Spirit (FEI, Hillsboro, USA) transmission electron microscope operated at 120kV and a Polara G2 Tecnai field emission transmission electron microscope (FEI, Hillsboro, USA) operated at 300kV. All electron microscopes were cooled to liquid nitrogen temperature. For cryo samples, low dose conditions were strictly followed. Screening and imaging of selected areas was performed using Digital Micrograph (Gatan Inc., Pleasanton, USA) coupled to a 1k x 1k CCD (on the CM120), a 1k x 1k CCD (on the Spirit) and a Tridiem XXX 30 Gatan Imaging Filter with a 2k x 2k CCD sensor (on the Polara; Gatan Inc., Pleasanton, USA).

4.3.21.1. Aquisition of tilt series

Tilt series were recorded using FEI tomography software (FEI Company, Hillsboro, USA). Typically, samples were tilted from -60° to +60° in steps of 1 – 2°. Higher tilting angles were achieved occasionally, depending on the of the imaged area in the grid square and on the grid.

4.3.21.2. Tomographic reconstruction

The IMOD software package was employed for tomographic reconstructions (Kremer et al., 1996). Using digital image processing steps, spurious bright pixels caused by x-rays detected by the CCD were removed, the individual images of a tilt series were aligned using high-contrast fiducial markers to generate a volume using weighted back-projection.

4.3.21.3. Segmentation of tomograms

To visualize information contained in the tomograms, volumes of interest were segmented using Amira 4.1.1 (Visage Imaging GmbH, Fürth, Germany). Features of interest were labeled with different colors, with the segmentation done partly by hand and partly by thresholding.

5. References

Ahle, S., A. Mann, U. Eichelsbacher, and E. Ungewickell. 1988. Structural relationships between clathrin assembly proteins from the Golgi and the plasma membrane. *Embo J*. 7:919-29.

Antonny, B., I. Huber, S. Paris, M. Chabre, and D. Cassel. 1997. Activation of ADP-ribosylation factor 1 GTPase-activating protein by phosphatidylcholine-derived diacylglycerols. *J Biol Chem*. 272:30848-51.

Antonny, B., D. Madden, S. Hamamoto, L. Orci, and R. Schekman. 2001. Dynamics of the COPII coat with GTP and stable analogues. *Nat Cell Biol*. 3:531-7.

Austin, C., I. Hinners, and S.A. Tooze. 2000. Direct and GTP-dependent interaction of ADP-ribosylation factor 1 with clathrin adaptor protein AP-1 on immature secretory granules. *J Biol Chem*. 275:21862-9.

Bannykh, S.I., and W.E. Balch. 1998. Selective transport of cargo between the endoplasmic reticulum and Golgi compartments. *Histochem Cell Biol*. 109:463-75.

Bannykh, S.I., N. Nishimura, and W.E. Balch. 1998. Getting into the Golgi. *Trends Cell Biol*. 8:21-5.

Barlowe, C. 2003. Molecular recognition of cargo by the COPII complex: a most accommodating coat. *Cell*. 114:395-7.

Barlowe, C., C. d'Enfert, and R. Schekman. 1993. Purification and characterization of SAR1p, a small GTP-binding protein required for transport vesicle formation from the endoplasmic reticulum. *J Biol Chem*. 268:873-9.

Barlowe, C., L. Orci, T. Yeung, M. Hosobuchi, S. Hamamoto, N. Salama, M.F. Rexach, M. Ravazzola, M. Amherdt, and R. Schekman. 1994. COPII: a membrane coat formed by Sec proteins that drive vesicle budding from the endoplasmic reticulum. *Cell*. 77:895-907.

Barlowe, C., and R. Schekman. 1993. SEC12 encodes a guanine-nucleotide-exchange factor essential for transport vesicle budding from the ER. *Nature*. 365:347-9.

Barr, F.A., and B. Short. 2003. Golgins in the structure and dynamics of the Golgi apparatus. *Curr Opin Cell Biol*. 15:405-13.

Beck, K.A., and J.H. Keen. 1991. Interaction of phosphoinositide cycle intermediates with the plasma membrane-associated clathrin assembly protein AP-2. *J Biol Chem*. 266:4442-7.

Beck, R., Z. Sun, F. Adolf, C. Rutz, J. Bassler, C. Wild, I. Sinning, E. Hurt, B. Bruegger, J. Béthune, and F. Wieland. 2008. Membrane curvature induced by Arf1-GTP is essential for vesicle formation. *Proc Natl Acad Sci U S A*. In press.

Ben-Tekaya, H., K. Miura, R. Pepperkok, and H.P. Hauri. 2005. Live imaging of bidirectional traffic from the ERGIC. *J Cell Sci*. 118:357-67.

Bethune, J., M. Kol, J. Hoffmann, I. Reckmann, B. Brugger, and F. Wieland. 2006. Coatomer, the Coat Protein of COPI Transport Vesicles, Discriminates Endoplasmic Reticulum Residents from p24 Proteins. *Mol Cell Biol*. 26:8011-21.

Bi, X., R.A. Corpina, and J. Goldberg. 2002. Structure of the Sec23/24-Sar1 pre-budding complex of the COPII vesicle coat. *Nature*. 419:271-7.

Blagitko, N., U. Schulz, A.A. Schinzel, H.H. Ropers, and V.M. Kalscheuer. 1999. gamma2-COP, a novel imprinted gene on chromosome 7q32, defines a new imprinting cluster in the human genome. *Hum Mol Genet*. 8:2387-96.

Blobel, G., and B. Dobberstein. 1975a. Transfer of proteins across membranes. I. Presence of proteolytically processed and unprocessed nascent immunoglobulin light chains on membrane-bound ribosomes of murine myeloma. *J Cell Biol*. 67:835-51.

Blobel, G., and B. Dobberstein. 1975b. Transfer to proteins across membranes. II. Reconstitution of functional rough microsomes from heterologous components. *J Cell Biol*. 67:852-62.

Blum, R., F. Pfeiffer, P. Feick, W. Nastainczyk, B. Kohler, K.H. Schafer, and I. Schulz. 1999. Intracellular localization and in vivo trafficking of p24A and p23. *J Cell Sci*. 112 (Pt 4):537-48.

Boehm, M., R.C. Aguilar, and J.S. Bonifacino. 2001. Functional and physical interactions of the adaptor protein complex AP-4 with ADP-ribosylation factors (ARFs). *Embo J*. 20:6265-76.

Boll, W., I. Rapoport, C. Brunner, Y. Modis, S. Prehn, and T. Kirchhausen. 2002. The mu2 subunit of the clathrin adaptor AP-2 binds to FDNPVY and YppO sorting signals at distinct sites. *Traffic*. 3:590-600.

Boman, A.L. 2001. GGA proteins: new players in the sorting game. *J Cell Sci*. 114:3413-8.

Boman, A.L., C. Zhang, X. Zhu, and R.A. Kahn. 2000. A family of ADP-ribosylation factor effectors that can alter membrane transport through the trans-Golgi. *Mol Biol Cell*. 11:1241-55.

Bouchet-Marquis, C., V. Starkuviene, and M. Grabenbauer. 2008. Golgi apparatus studied in vitreous sections. *J Microsc*. 230:308-16.

Bremser, M., W. Nickel, M. Schweikert, M. Ravazzola, M. Amherdt, C.A. Hughes, T.H. Sollner, J.E. Rothman, and F.T. Wieland. 1999. Coupling of coat assembly and vesicle budding to packaging of putative cargo receptors. *Cell*. 96:495-506.

Cabrera, M., M. Muniz, J. Hidalgo, L. Vega, M.E. Martin, and A. Velasco. 2003. The retrieval function of the KDEL receptor requires PKA phosphorylation of its C-terminus. *Mol Biol Cell*. 14:4114-25.

Caras, I.W., and G.N. Weddell. 1989. Signal peptide for protein secretion directing glycophospholipid membrane anchor attachment. *Science*. 243:1196-8.

Caro, L.G., and G.E. Palade. 1964. Protein Synthesis, Storage, and Discharge in the Pancreatic Exocrine Cell. an Autoradiographic Study. *J Cell Biol*. 20:473-95.

Chardin, P., S. Paris, B. Antonny, S. Robineau, S. Beraud-Dufour, C.L. Jackson, and M. Chabre. 1996. A human exchange factor for ARF contains Sec7- and pleckstrin-homology domains. *Nature*. 384:481-4.

Cheng, Y., W. Boll, T. Kirchhausen, S.C. Harrison, and T. Walz. 2007. Cryo-electron tomography of clathrin-coated vesicles: structural implications for coat assembly. *J Mol Biol*. 365:892-9.

Claing, A., S.A. Laporte, M.G. Caron, and R.J. Lefkowitz. 2002. Endocytosis of G protein-coupled receptors: roles of G protein-coupled receptor kinases and beta-arrestin proteins. *Prog Neurobiol*. 66:61-79.

Collins, B.M., A.J. McCoy, H.M. Kent, P.R. Evans, and D.J. Owen. 2002. Molecular architecture and functional model of the endocytic AP2 complex. *Cell*. 109:523-35.

Contreras, I., E. Ortiz-Zapater, and F. Aniento. 2004. Sorting signals in the cytosolic tail of membrane proteins involved in the interaction with plant ARF1 and coatomer. *Plant J*. 38:685-98.

Cosson, P., Y. Lefkir, C. Demolliere, and F. Letourneur. 1998. New COP1-binding motifs involved in ER retrieval. *Embo J*. 17:6863-70.

Cosson, P., and F. Letourneur. 1994. Coatomer interaction with di-lysine endoplasmic reticulum retention motifs. *Science*. 263:1629-31.

Crottet, P., D.M. Meyer, J. Rohrer, and M. Spiess. 2002. ARF1.GTP, tyrosine-based signals, and phosphatidylinositol 4,5-bisphosphate constitute a minimal machinery to recruit the AP-1 clathrin adaptor to membranes. *Mol Biol Cell*. 13:3672-82.

Crowther, R.A., J.T. Finch, and B.M. Pearse. 1976. On the structure of coated vesicles. *J Mol Biol*. 103:785-98.

Dell'Angelica, E.C., C. Mullins, and J.S. Bonifacino. 1999. AP-4, a novel protein complex related to clathrin adaptors. *J Biol Chem*. 274:7278-85.

Dell'Angelica, E.C., H. Ohno, C.E. Ooi, E. Rabinovich, K.W. Roche, and J.S. Bonifacino. 1997. AP-3: an adaptor-like protein complex with ubiquitous expression. *Embo J*. 16:917-28.

Dell'Angelica, E.C., R. Puertollano, C. Mullins, R.C. Aguilar, J.D. Vargas, L.M. Hartnell, and J.S. Bonifacino. 2000. GGAs: a family of ADP ribosylation factor-binding proteins related to adaptors and associated with the Golgi complex. *J Cell Biol*. 149:81-94.

Deniz, A.A., T.A. Laurence, M. Dahan, D.S. Chemla, P.G. Schultz, and S. Weiss. 2001. Ratiometric single-molecule studies of freely diffusing biomolecules. *Annu Rev Phys Chem*. 52:233-53.

Deshaies, R.J., S.L. Sanders, D.A. Feldheim, and R. Schekman. 1991. Assembly of yeast Sec proteins involved in translocation into the endoplasmic reticulum into a membrane-bound multisubunit complex. *Nature*. 349:806-8.

Deshaies, R.J., and R. Schekman. 1989. SEC62 encodes a putative membrane protein required for protein translocation into the yeast endoplasmic reticulum. *J Cell Biol*. 109:2653-64.

Devos, D., S. Dokudovskaya, F. Alber, R. Williams, B.T. Chait, A. Sali, and M.P. Rout. 2004. Components of coated vesicles and nuclear pore complexes share a common molecular architecture. *PLoS Biol*. 2:e380.

Dominguez, M., K. Dejgaard, J. Fullekrug, S. Dahan, A. Fazel, J.P. Paccaud, D.Y. Thomas, J.J. Bergeron, and T. Nilsson. 1998. gp25L/emp24/p24 protein family members of the cis-Golgi network bind both COP I and II coatomer. *J Cell Biol*. 140:751-65.

Donaldson, J.G., D. Cassel, R.A. Kahn, and R.D. Klausner. 1992a. ADP-ribosylation factor, a small GTP-binding protein, is required for binding of the coatomer protein beta-COP to Golgi membranes. *Proc Natl Acad Sci U S A*. 89:6408-12.

Donaldson, J.G., D. Finazzi, and R.D. Klausner. 1992b. Brefeldin A inhibits Golgi membrane-catalysed exchange of guanine nucleotide onto ARF protein. *Nature*. 360:350-2.

Donohoe, B.S., B.H. Kang, and L.A. Staehelin. 2007. Identification and characterization of COPIa- and COPIb-type vesicle classes associated with plant and algal Golgi. *Proc Natl Acad Sci U S A*. 104:163-8.

Doray, B., K. Bruns, P. Ghosh, and S.A. Kornfeld. 2002. Autoinhibition of the ligand-binding site of GGA1/3 VHS domains by an internal acidic cluster-dileucine motif. *Proc Natl Acad Sci U S A*. 99:8072-7.

Duden, R., G. Griffiths, R. Frank, P. Argos, and T.E. Kreis. 1991. Beta-COP, a 110 kd protein associated with non-clathrin-coated vesicles and the Golgi complex, shows homology to beta-adaptin. *Cell*. 64:649-65.

Dunphy, W.G., E. Fries, L.J. Urbani, and J.E. Rothman. 1981. Early and late functions associated with the Golgi apparatus reside in distinct compartments. *Proc Natl Acad Sci U S A*. 78:7453-7.

Ehrlich, M., W. Boll, A. Van Oijen, R. Hariharan, K. Chandran, M.L. Nibert, and T. Kirchhausen. 2004. Endocytosis by random initiation and stabilization of clathrin-coated pits. *Cell*. 118:591-605.

Emery, G., M. Rojo, and J. Gruenberg. 2000. Coupled transport of p24 family members. *J Cell Sci*. 113 (Pt 13):2507-16.

Eugster, A., G. Frigerio, M. Dale, and R. Duden. 2000. COP I domains required for coatomer integrity, and novel interactions with ARF and ARF-GAP. *Embo J*. 19:3905-17.

Eugster, A., G. Frigerio, M. Dale, and R. Duden. 2004. The alpha- and beta'-COP WD40 domains mediate cargo-selective interactions with distinct di-lysine motifs. *Mol Biol Cell*. 15:1011-23.

Fath, S., J.D. Mancias, X. Bi, and J. Goldberg. 2007. Structure and organization of coat proteins in the COPII cage. *Cell*. 129:1325-36.

Fiedler, K., M. Veit, M.A. Stamnes, and J.E. Rothman. 1996. Bimodal interaction of coatomer with the p24 family of putative cargo receptors. *Science*. 273:1396-9.

Fingerhut, A., K. von Figura, and S. Honing. 2001. Binding of AP2 to sorting signals is modulated by AP2 phosphorylation. *J Biol Chem*. 276:5476-82.

Fotin, A., Y. Cheng, N. Grigorieff, T. Walz, S.C. Harrison, and T. Kirchhausen. 2004a. Structure of an auxilin-bound clathrin coat and its implications for the mechanism of uncoating. *Nature*. 432:649-53.

Fotin, A., Y. Cheng, P. Sliz, N. Grigorieff, S.C. Harrison, T. Kirchhausen, and T. Walz. 2004b. Molecular model for a complete clathrin lattice from electron cryomicroscopy. *Nature*. 432:573-9.

Fotin, A., T. Kirchhausen, N. Grigorieff, S.C. Harrison, T. Walz, and Y. Cheng. 2006. Structure determination of clathrin coats to subnanometer resolution by single particle cryo-electron microscopy. *J Struct Biol*. 156:453-60.

Franco, M., P. Chardin, M. Chabre, and S. Paris. 1995. Myristoylation of ADP-ribosylation factor 1 facilitates nucleotide exchange at physiological Mg2+ levels. *J Biol Chem*. 270:1337-41.

Franco, M., P. Chardin, M. Chabre, and S. Paris. 1996. Myristoylation-facilitated binding of the G protein ARF1GDP to membrane phospholipids is required for its activation by a soluble nucleotide exchange factor. *J Biol Chem*. 271:1573-8.

Freedman, R.B. 1989. Protein disulfide isomerase: multiple roles in the modification of nascent secretory proteins. *Cell*. 57:1069-72.

Friedlander, R., E. Jarosch, J. Urban, C. Volkwein, and T. Sommer. 2000. A regulatory link between ER-associated protein degradation and the unfolded-protein response. *Nat Cell Biol*. 2:379-84.

Fullekrug, J., T. Suganuma, B.L. Tang, W. Hong, B. Storrie, and T. Nilsson. 1999. Localization and recycling of gp27 (hp24gamma3): complex formation with other p24 family members. *Mol Biol Cell*. 10:1939-55.

Futatsumori, M., K. Kasai, H. Takatsu, H.W. Shin, and K. Nakayama. 2000. Identification and characterization of novel isoforms of COP I subunits. *J Biochem*. 128:793-801.

Gaidarov, I., and J.H. Keen. 1999. Phosphoinositide-AP-2 interactions required for targeting to plasma membrane clathrin-coated pits. *J Cell Biol*. 146:755-64.

Ganoth, D., E. Leshinsky, E. Eytan, and A. Hershko. 1988. A multicomponent system that degrades proteins conjugated to ubiquitin. Resolution of factors and evidence for ATP-dependent complex formation. *J Biol Chem*. 263:12412-9.

Ghosh, P., and S. Kornfeld. 2003a. AP-1 binding to sorting signals and release from clathrin-coated vesicles is regulated by phosphorylation. *J Cell Biol*. 160:699-708.

Ghosh, P., and S. Kornfeld. 2003b. Phosphorylation-induced conformational changes regulate GGAs 1 and 3 function at the trans-Golgi network. *J Biol Chem*. 278:14543-9.

Gilmore, R., G. Blobel, and P. Walter. 1982a. Protein translocation across the endoplasmic reticulum. I. Detection in the microsomal membrane of a receptor for the signal recognition particle. *J Cell Biol*. 95:463-9.

Gilmore, R., P. Walter, and G. Blobel. 1982b. Protein translocation across the endoplasmic reticulum. II. Isolation and characterization of the signal recognition particle receptor. *J Cell Biol*. 95:470-7.

Glickman, J.N., E. Conibear, and B.M. Pearse. 1989. Specificity of binding of clathrin adaptors to signals on the mannose-6-phosphate/insulin-like growth factor II receptor. *Embo J*. 8:1041-7.

Goldberg, J. 2000. Decoding of sorting signals by coatomer through a GTPase switch in the COPI coat complex. *Cell*. 100:671-9.

Gommel, D.U., A.R. Memon, A. Heiss, F. Lottspeich, J. Pfannstiel, J. Lechner, C. Reinhard, J.B. Helms, W. Nickel, and F.T. Wieland. 2001. Recruitment to Golgi membranes of ADP-ribosylation factor 1 is mediated by the cytoplasmic domain of p23. *Embo J*. 20:6751-60.

Griffiths, G., and K. Simons. 1986. The trans Golgi network: sorting at the exit site of the Golgi complex. *Science*. 234:438-43.

Gurkan, C., S.M. Stagg, P. Lapointe, and W.E. Balch. 2006. The COPII cage: unifying principles of vesicle coat assembly. *Nat Rev Mol Cell Biol*. 7:727-38.

Ha, T. 2001. Single-molecule fluorescence resonance energy transfer. *Methods*. 25:78-86.

Haass, C., and P.M. Kloetzel. 1989. The Drosophila proteasome undergoes changes in its subunit pattern during development. *Exp Cell Res*. 180:243-52.

Hara-Kuge, S., O. Kuge, L. Orci, M. Amherdt, M. Ravazzola, F.T. Wieland, and J.E. Rothman. 1994. En bloc incorporation of coatomer subunits during the assembly of COP-coated vesicles. *J Cell Biol*. 124:883-92.

Haucke, V., and P. De Camilli. 1999. AP-2 recruitment to synaptotagmin stimulated by tyrosine-based endocytic motifs. *Science*. 285:1268-71.

Haucke, V., and M. Krauss. 2002. Tyrosine-based endocytic motifs stimulate oligomerization of AP-2 adaptor complexes. *Eur J Cell Biol*. 81:647-53.

Haucke, V., M.R. Wenk, E.R. Chapman, K. Farsad, and P. De Camilli. 2000. Dual interaction of synaptotagmin with mu2- and alpha-adaptin facilitates clathrin-coated pit nucleation. *Embo J*. 19:6011-9.

Hauri, H.P., F. Kappeler, H. Andersson, and C. Appenzeller. 2000. ERGIC-53 and traffic in the secretory pathway. *J Cell Sci*. 113 (Pt 4):587-96.

Heldwein, E.E., E. Macia, J. Wang, H.L. Yin, T. Kirchhausen, and S.C. Harrison. 2004. Crystal structure of the clathrin adaptor protein 1 core. *Proc Natl Acad Sci U S A*. 101:14108-13.

Hershko, A., A. Ciechanover, and I.A. Rose. 1979. Resolution of the ATP-dependent proteolytic system from reticulocytes: a component that interacts with ATP. *Proc Natl Acad Sci U S A*. 76:3107-10.

Holstein, S.E., H. Ungewickell, and E. Ungewickell. 1996. Mechanism of clathrin basket dissociation: separate functions of protein domains of the DnaJ homologue auxilin. *J Cell Biol*. 135:925-37.

Honda, A., O.S. Al-Awar, J.C. Hay, and J.G. Donaldson. 2005. Targeting of Arf-1 to the early Golgi by membrin, an ER-Golgi SNARE. *J Cell Biol*. 168:1039-51.

Itoh, T., and P. De Camilli. 2004. Membrane trafficking: dual-key strategy. *Nature*. 429:141-3.

Jha, A., N.R. Agostinelli, S.K. Mishra, P.A. Keyel, M.J. Hawryluk, and L.M. Traub. 2004. A novel AP-2 adaptor interaction motif initially identified in the long-splice isoform of synaptojanin 1, SJ170. *J Biol Chem*. 279:2281-90.

Jorgensen, E.M., E. Hartwieg, K. Schuske, M.L. Nonet, Y. Jin, and H.R. Horvitz. 1995. Defective recycling of synaptic vesicles in synaptotagmin mutants of Caenorhabditis elegans. *Nature*. 378:196-9.

Kahn, R.A., F.G. Kern, J. Clark, E.P. Gelmann, and C. Rulka. 1991. Human ADP-ribosylation factors. A functionally conserved family of GTP-binding proteins. *J Biol Chem*. 266:2606-14.

Kanaseki, T., and K. Kadota. 1969. The "vesicle in a basket". A morphological study of the coated vesicle isolated from the nerve endings of the guinea pig brain, with special reference to the mechanism of membrane movements. *J Cell Biol*. 42:202-20.

Karrenbauer, A., D. Jeckel, W. Just, R. Birk, R.R. Schmidt, J.E. Rothman, and F.T. Wieland. 1990. The rate of bulk flow from the Golgi to the plasma membrane. *Cell*. 63:259-67.

Keen, J.H., M.H. Chestnut, and K.A. Beck. 1987. The clathrin coat assembly polypeptide complex. Autophosphorylation and assembly activities. *J Biol Chem*. 262:3864-71.

Keen, J.H., M.C. Willingham, and I.H. Pastan. 1979. Clathrin-coated vesicles: isolation, dissociation and factor-dependent reassociation of clathrin baskets. *Cell*. 16:303-12.

Kirchhausen, T., and S.C. Harrison. 1981. Protein organization in clathrin trimers. *Cell*. 23:755-61.

Kirchhausen, T., S.C. Harrison, and J. Heuser. 1986. Configuration of clathrin trimers: evidence from electron microscopy. *J Ultrastruct Mol Struct Res*. 94:199-208.

Kornfeld, R., and S. Kornfeld. 1985. Assembly of asparagine-linked oligosaccharides. *Annu Rev Biochem*. 54:631-64.

Kremer, J.R., D.N. Mastronarde, and J.R. McIntosh. 1996. Computer visualization of three-dimensional image data using IMOD. *J Struct Biol*. 116:71-6.

Laemmli, U.K. 1970. Cleavage of structural proteins during the assembly of the head of bacteriophage T4. *Nature*. 227:680-5.

Langer, J.D., C.M. Roth, J. Bethune, E.H. Stoops, B. Brugger, D.P. Herten, and F.T. Wieland. 2008. A conformational change in the alpha-subunit of coatomer induced by ligand binding to gamma-COP revealed by single-pair FRET. *Traffic*. 9:597-607.

Langer, J.D., E.H. Stoops, J. Bethune, and F.T. Wieland. 2007. Conformational changes of coat proteins during vesicle formation. *FEBS Lett*. 581:2083-8.

Lederkremer, G.Z., Y. Cheng, B.M. Petre, E. Vogan, S. Springer, R. Schekman, T. Walz, and T. Kirchhausen. 2001. Structure of the Sec23p/24p and Sec13p/31p complexes of COPII. *Proc Natl Acad Sci U S A*. 98:10704-9.

Lee, I., B. Doray, J. Govero, and S. Kornfeld. 2008. Binding of cargo sorting signals to AP-1 enhances its association with ADP ribosylation factor 1-GTP. *J Cell Biol*. 180:467-72.

Letourneur, F., E.C. Gaynor, S. Hennecke, C. Demolliere, R. Duden, S.D. Emr, H. Riezman, and P. Cosson. 1994. Coatomer is essential for retrieval of dilysine-tagged proteins to the endoplasmic reticulum. *Cell*. 79:1199-207.

Lewis, M.J., and H.R. Pelham. 1990. A human homologue of the yeast HDEL receptor. *Nature*. 348:162-3.

Lewis, M.J., and H.R. Pelham. 1992. Ligand-induced redistribution of a human KDEL receptor from the Golgi complex to the endoplasmic reticulum. *Cell*. 68:353-64.

Liu, X., C. Zhang, G. Xing, Q. Chen, and F. He. 2001. Functional characterization of novel human ARFGAP3. *FEBS Lett*. 490:79-83.

Lowe, M., and T.E. Kreis. 1996. In vivo assembly of coatomer, the COP-I coat precursor. *J Biol Chem*. 271:30725-30.

Majoul, I., K. Sohn, F.T. Wieland, R. Pepperkok, M. Pizza, J. Hillemann, and H.D. Soling. 1998. KDEL receptor (Erd2p)-mediated retrograde transport of the cholera toxin A subunit from the Golgi involves COPI, p23, and the COOH terminus of Erd2p. *J Cell Biol*. 143:601-12.

Majoul, I., M. Straub, S.W. Hell, R. Duden, and H.D. Soling. 2001. KDEL-cargo regulates interactions between proteins involved in COPI vesicle traffic: measurements in living cells using FRET. *Dev Cell*. 1:139-53.

Malhotra, V., T. Serafini, L. Orci, J.C. Shepherd, and J.E. Rothman. 1989. Purification of a novel class of coated vesicles mediating biosynthetic protein transport through the Golgi stack. *Cell*. 58:329-36.

Malkus, P., F. Jiang, and R. Schekman. 2002. Concentrative sorting of secretory cargo proteins into COPII-coated vesicles. *J Cell Biol*. 159:915-21.

Malsam, J., A. Satoh, L. Pelletier, and G. Warren. 2005. Golgin tethers define subpopulations of COPI vesicles. *Science*. 307:1095-8.

Martinez-Menarguez, J.A., H.J. Geuze, J.W. Slot, and J. Klumperman. 1999. Vesicular tubular clusters between the ER and Golgi mediate concentration of soluble secretory proteins by exclusion from COPI-coated vesicles. *Cell*. 98:81-90.

Mathews, P.M., J.B. Martinie, and D.M. Fambrough. 1992. The pathway and targeting signal for delivery of the integral membrane glycoprotein LEP100 to lysosomes. *J Cell Biol*. 118:1027-40.

Matsui, W., and T. Kirchhausen. 1990. Stabilization of clathrin coats by the core of the clathrin-associated protein complex AP-2. *Biochemistry*. 29:10791-8.

Matsuoka, K., L. Orci, M. Amherdt, S.Y. Bednarek, S. Hamamoto, R. Schekman, and T. Yeung. 1998. COPII-coated vesicle formation reconstituted with purified coat proteins and chemically defined liposomes. *Cell*. 93:263-75.

McMahon, H.T., and I.G. Mills. 2004. COP and clathrin-coated vesicle budding: different pathways, common approaches. *Curr Opin Cell Biol*. 16:379-91.

McNew, J.A., F. Parlati, R. Fukuda, R.J. Johnston, K. Paz, F. Paumet, T.H. Sollner, and J.E. Rothman. 2000. Compartmental specificity of cellular membrane fusion encoded in SNARE proteins. *Nature*. 407:153-9.

Meresse, S., and B. Hoflack. 1993. Phosphorylation of the cation-independent mannose 6-phosphate receptor is closely associated with its exit from the trans-Golgi network. *J Cell Biol*. 120:67-75.

Meyer, C., E.L. Eskelinen, M.R. Guruprasad, K. von Figura, and P. Schu. 2001. Mu 1A deficiency induces a profound increase in MPR300/IGF-II receptor internalization rate. *J Cell Sci*. 114:4469-76.

Meyer, C., D. Zizioli, S. Lausmann, E.L. Eskelinen, J. Hamann, P. Saftig, K. von Figura, and P. Schu. 2000. mu1A-adaptin-deficient mice: lethality, loss of AP-1 binding and rerouting of mannose 6-phosphate receptors. *Embo J*. 19:2193-203.

Meyer, D.M., P. Crottet, B. Maco, E. Degtyar, D. Cassel, and M. Spiess. 2005. Oligomerization and dissociation of AP-1 adaptors are regulated by cargo signals and by ArfGAP1-induced GTP hydrolysis. *Mol Biol Cell*. 16:4745-54.

Michelsen, K., V. Schmid, J. Metz, K. Heusser, U. Liebel, T. Schwede, A. Spang, and B. Schwappach. 2007. Novel cargo-binding site in the beta and delta subunits of coatomer. *J Cell Biol*. 179:209-17.

Miller, E.A., T.H. Beilharz, P.N. Malkus, M.C. Lee, S. Hamamoto, L. Orci, and R. Schekman. 2003. Multiple cargo binding sites on the COPII subunit Sec24p ensure capture of diverse membrane proteins into transport vesicles. *Cell*. 114:497-509.

Moelleken, J., J. Malsam, M.J. Betts, A. Movafeghi, I. Reckmann, I. Meissner, A. Hellwig, R.B. Russell, T. Sollner, B. Brugger, and F.T. Wieland. 2007. Differential localization of coatomer complex isoforms within the Golgi apparatus. *Proc Natl Acad Sci U S A*. 104:4425-30.

Mossessova, E., R.A. Corpina, and J. Goldberg. 2003. Crystal structure of ARF1*Sec7 complexed with Brefeldin A and its implications for the guanine nucleotide exchange mechanism. *Mol Cell*. 12:1403-11.

Munro, S., and H.R. Pelham. 1987. A C-terminal signal prevents secretion of luminal ER proteins. *Cell*. 48:899-907.

Musacchio, A., C.J. Smith, A.M. Roseman, S.C. Harrison, T. Kirchhausen, and B.M. Pearse. 1999. Functional organization of clathrin in coats: combining electron cryomicroscopy and X-ray crystallography. *Mol Cell*. 3:761-70.

Nakano, A., and M. Muramatsu. 1989. A novel GTP-binding protein, Sar1p, is involved in transport from the endoplasmic reticulum to the Golgi apparatus. *J Cell Biol*. 109:2677-91.

Nickel, W., K. Sohn, C. Bunning, and F.T. Wieland. 1997. p23, a major COPI-vesicle membrane protein, constitutively cycles through the early secretory pathway. *Proc Natl Acad Sci U S A*. 94:11393-8.

Nie, Z., D.S. Hirsch, and P.A. Randazzo. 2003. Arf and its many interactors. *Curr Opin Cell Biol*. 15:396-404.

Niu, T.K., A.C. Pfeifer, J. Lippincott-Schwartz, and C.L. Jackson. 2005. Dynamics of GBF1, a Brefeldin A-sensitive Arf1 exchange factor at the Golgi. *Mol Biol Cell*. 16:1213-22.

Ohno, H., J. Stewart, M.C. Fournier, H. Bosshart, I. Rhee, S. Miyatake, T. Saito, A. Gallusser, T. Kirchhausen, and J.S. Bonifacino. 1995. Interaction of tyrosine-based sorting signals with clathrin-associated proteins. *Science*. 269:1872-5.

Olusanya, O., P.D. Andrews, J.R. Swedlow, and E. Smythe. 2001. Phosphorylation of threonine 156 of the mu2 subunit of the AP2 complex is essential for endocytosis in vitro and in vivo. *Curr Biol*. 11:896-900.

Ooi, C.E., E.C. Dell'Angelica, and J.S. Bonifacino. 1998. ADP-Ribosylation factor 1 (ARF1) regulates recruitment of the AP-3 adaptor complex to membranes. *J Cell Biol*. 142:391-402.

Orci, L., A. Perrelet, and J.E. Rothman. 1998. Vesicles on strings: morphological evidence for processive transport within the Golgi stack. *Proc Natl Acad Sci U S A*. 95:2279-83.

Orci, L., M. Stamnes, M. Ravazzola, M. Amherdt, A. Perrelet, T.H. Sollner, and J.E. Rothman. 1997. Bidirectional transport by distinct populations of COPI-coated vesicles. *Cell*. 90:335-49.

Paleotti, O., E. Macia, F. Luton, S. Klein, M. Partisani, P. Chardin, T. Kirchhausen, and M. Franco. 2005. The small G-protein Arf6GTP recruits the AP-2 adaptor complex to membranes. *J Biol Chem*. 280:21661-6.

Palmer, D.J., J.B. Helms, C.J. Beckers, L. Orci, and J.E. Rothman. 1993. Binding of coatomer to Golgi membranes requires ADP-ribosylation factor. *J Biol Chem*. 268:12083-9.

Parlati, F., J.A. McNew, R. Fukuda, R. Miller, T.H. Sollner, and J.E. Rothman. 2000. Topological restriction of SNARE-dependent membrane fusion. *Nature*. 407:194-8.

Pavel, J., C. Harter, and F.T. Wieland. 1998. Reversible dissociation of coatomer: functional characterization of a beta/delta-coat protein subcomplex. *Proc Natl Acad Sci U S A*. 95:2140-5.

Pearse, B.M. 1975. Coated vesicles from pig brain: purification and biochemical characterization. *J Mol Biol*. 97:93-8.

Pelham, H.R., K.G. Hardwick, and M.J. Lewis. 1988. Sorting of soluble ER proteins in yeast. *Embo J*. 7:1757-62.

Pelham, H.R., and J.E. Rothman. 2000. The debate about transport in the Golgi--two sides of the same coin? *Cell*. 102:713-9.

Plemper, R.K., and D.H. Wolf. 1999. Endoplasmic reticulum degradation. Reverse protein transport and its end in the proteasome. *Mol Biol Rep*. 26:125-30.

Presley, J.F., N.B. Cole, T.A. Schroer, K. Hirschberg, K.J. Zaal, and J. Lippincott-Schwartz. 1997. ER-to-Golgi transport visualized in living cells. *Nature*. 389:81-5.

Puertollano, R., R.C. Aguilar, I. Gorshkova, R.J. Crouch, and J.S. Bonifacino. 2001a. Sorting of mannose 6-phosphate receptors mediated by the GGAs. *Science*. 292:1712-6.

Puertollano, R., P.A. Randazzo, J.F. Presley, L.M. Hartnell, and J.S. Bonifacino. 2001b. The GGAs promote ARF-dependent recruitment of clathrin to the TGN. *Cell*. 105:93-102.

Rambourg, A., and Y. Clermont. 1990. Three-dimensional electron microscopy: structure of the Golgi apparatus. *Eur J Cell Biol*. 51:189-200.

Randazzo, P.A. 1997. Resolution of two ADP-ribosylation factor 1 GTPase-activating proteins from rat liver. *Biochem J*. 324 (Pt 2):413-9.

Rapoport, I., M. Miyazaki, W. Boll, B. Duckworth, L.C. Cantley, S. Shoelson, and T. Kirchhausen. 1997. Regulatory interactions in the recognition of endocytic sorting signals by AP-2 complexes. *Embo J*. 16:2240-50.

Reinhard, C., C. Harter, M. Bremser, B. Brugger, K. Sohn, J.B. Helms, and F. Wieland. 1999. Receptor-induced polymerization of coatomer. *Proc Natl Acad Sci U S A*. 96:1224-8.

Reinhard, C., M. Schweikert, F.T. Wieland, and W. Nickel. 2003. Functional reconstitution of COPI coat assembly and disassembly using chemically defined components. *Proc Natl Acad Sci U S A*. 100:8253-7.

Rhinow, D., and W. Kuhlbrandt. 2008. Electron cryo-microscopy of biological specimens on conductive titanium-silicon metal glass films. *Ultramicroscopy*. 108:698-705.

Ricotta, D., S.D. Conner, S.L. Schmid, K. von Figura, and S. Honing. 2002. Phosphorylation of the AP2 mu subunit by AAK1 mediates high affinity binding to membrane protein sorting signals. *J Cell Biol*. 156:791-5.

Rohde, G., D. Wenzel, and V. Haucke. 2002. A phosphatidylinositol (4,5)-bisphosphate binding site within mu2-adaptin regulates clathrin-mediated endocytosis. *J Cell Biol*. 158:209-14.

Rojo, M., G. Emery, V. Marjomaki, A.W. McDowall, R.G. Parton, and J. Gruenberg. 2000. The transmembrane protein p23 contributes to the organization of the Golgi apparatus. *J Cell Sci*. 113 (Pt 6):1043-57.

Rojo, M., R. Pepperkok, G. Emery, R. Kellner, E. Stang, R.G. Parton, and J. Gruenberg. 1997. Involvement of the transmembrane protein p23 in biosynthetic protein transport. *J Cell Biol*. 139:1119-35.

Roth, T.F., and K.R. Porter. 1964. Yolk Protein Uptake in the Oocyte of the Mosquito Aedes Aegypti. L. *J Cell Biol*. 20:313-32.

Rothman, J.E. 1981. The golgi apparatus: two organelles in tandem. *Science*. 213:1212-9.

Salama, N.R., T. Yeung, and R.W. Schekman. 1993. The Sec13p complex and reconstitution of vesicle budding from the ER with purified cytosolic proteins. *Embo J*. 12:4073-82.

Scales, S.J., R. Pepperkok, and T.E. Kreis. 1997. Visualization of ER-to-Golgi transport in living cells reveals a sequential mode of action for COPII and COPI. *Cell*. 90:1137-48.

Scheel, A.A., and H.R. Pelham. 1998. Identification of amino acids in the binding pocket of the human KDEL receptor. *J Biol Chem*. 273:2467-72.

Schledzewski, K., H. Brinkmann, and R.R. Mendel. 1999. Phylogenetic analysis of components of the eukaryotic vesicle transport system reveals a common origin of

adaptor protein complexes 1, 2, and 3 and the F subcomplex of the coatomer COPI. *J Mol Evol*. 48:770-8.

Semenza, J.C., K.G. Hardwick, N. Dean, and H.R. Pelham. 1990. ERD2, a yeast gene required for the receptor-mediated retrieval of luminal ER proteins from the secretory pathway. *Cell*. 61:1349-57.

Serafini, T., L. Orci, M. Amherdt, M. Brunner, R.A. Kahn, and J.E. Rothman. 1991. ADP-ribosylation factor is a subunit of the coat of Golgi-derived COP-coated vesicles: a novel role for a GTP-binding protein. *Cell*. 67:239-53.

Smith, C.J., N. Grigorieff, and B.M. Pearse. 1998. Clathrin coats at 21 A resolution: a cellular assembly designed to recycle multiple membrane receptors. *Embo J*. 17:4943-53.

Sohn, K., L. Orci, M. Ravazzola, M. Amherdt, M. Bremser, F. Lottspeich, K. Fiedler, J.B. Helms, and F.T. Wieland. 1996. A major transmembrane protein of Golgi-derived COPI-coated vesicles involved in coatomer binding. *J Cell Biol*. 135:1239-48.

Sollner, T., S.W. Whiteheart, M. Brunner, H. Erdjument-Bromage, S. Geromanos, P. Tempst, and J.E. Rothman. 1993. SNAP receptors implicated in vesicle targeting and fusion. *Nature*. 362:318-24.

Sorkin, A. 2004. Cargo recognition during clathrin-mediated endocytosis: a team effort. *Curr Opin Cell Biol*. 16:392-9.

Spang, A., K. Matsuoka, S. Hamamoto, R. Schekman, and L. Orci. 1998. Coatomer, Arf1p, and nucleotide are required to bud coat protein complex I-coated vesicles from large synthetic liposomes. *Proc Natl Acad Sci U S A*. 95:11199-204.

Stagg, S.M., C. Gurkan, D.M. Fowler, P. LaPointe, T.R. Foss, C.S. Potter, B. Carragher, and W.E. Balch. 2006. Structure of the Sec13/31 COPII coat cage. *Nature*. 439:234-8.

Sun, Z., F. Anderl, K. Frohlich, L. Zhao, S. Hanke, B. Brugger, F. Wieland, and J. Bethune. 2007a. Multiple and stepwise interactions between coatomer and ADP-ribosylation factor-1 (Arf1)-GTP. *Traffic*. 8:582-93.

Sun, Z., F. Anderl, K. Fröhlich, L. Zhao, S. Hanke, B. Brügger, F. Wieland, and J. Bethune. 2007b. Multiple and stepwise interactions between coatomer and ADP-ribosylation factor-1 (Arf1)-GTP. *Traffic*. In press.

Tanigawa, G., L. Orci, M. Amherdt, M. Ravazzola, J.B. Helms, and J.E. Rothman. 1993. Hydrolysis of bound GTP by ARF protein triggers uncoating of Golgi-derived COP-coated vesicles. *J Cell Biol*. 123:1365-71.

Terui, T., R.A. Kahn, and P.A. Randazzo. 1994. Effects of acid phospholipids on nucleotide exchange properties of ADP-ribosylation factor 1. Evidence for specific interaction with phosphatidylinositol 4,5-bisphosphate. *J Biol Chem*. 269:28130-5.

Tooze, S.A., G.J. Martens, and W.B. Huttner. 2001. Secretory granule biogenesis: rafting to the SNARE. *Trends Cell Biol*. 11:116-22.

Traub, L.M., and S. Kornfeld. 1997. The trans-Golgi network: a late secretory sorting station. *Curr Opin Cell Biol*. 9:527-33.

Travers, K.J., C.K. Patil, L. Wodicka, D.J. Lockhart, J.S. Weissman, and P. Walter. 2000. Functional and genomic analyses reveal an essential coordination between the unfolded protein response and ER-associated degradation. *Cell*. 101:249-58.

Umeda, A., A. Meyerholz, and E. Ungewickell. 2000. Identification of the universal cofactor (auxilin 2) in clathrin coat dissociation. *Eur J Cell Biol*. 79:336-42.

Ungewickell, E., and D. Branton. 1981. Assembly units of clathrin coats. *Nature*. 289:420-2.

Vigers, G.P., R.A. Crowther, and B.M. Pearse. 1986a. Location of the 100 kd-50 kd accessory proteins in clathrin coats. *Embo J*. 5:2079-85.

Vigers, G.P., R.A. Crowther, and B.M. Pearse. 1986b. Three-dimensional structure of clathrin cages in ice. *Embo J*. 5:529-34.

Wada, I., D. Rindress, P.H. Cameron, W.J. Ou, J.J. Doherty, 2nd, D. Louvard, A.W. Bell, D. Dignard, D.Y. Thomas, and J.J. Bergeron. 1991. SSR alpha and associated calnexin are major calcium binding proteins of the endoplasmic reticulum membrane. *J Biol Chem*. 266:19599-610.

Walter, P., and G. Blobel. 1980. Purification of a membrane-associated protein complex required for protein translocation across the endoplasmic reticulum. *Proc Natl Acad Sci U S A*. 77:7112-6.

Walter, P., and G. Blobel. 1981a. Translocation of proteins across the endoplasmic reticulum III. Signal recognition protein (SRP) causes signal sequence-dependent and site-specific arrest of chain elongation that is released by microsomal membranes. *J Cell Biol*. 91:557-61.

Walter, P., and G. Blobel. 1981b. Translocation of proteins across the endoplasmic reticulum. II. Signal recognition protein (SRP) mediates the selective binding to microsomal membranes of in-vitro-assembled polysomes synthesizing secretory protein. *J Cell Biol*. 91:551-6.

Walter, P., I. Ibrahimi, and G. Blobel. 1981. Translocation of proteins across the endoplasmic reticulum. I. Signal recognition protein (SRP) binds to in-vitro-assembled polysomes synthesizing secretory protein. *J Cell Biol*. 91:545-50.

Wang, Y.J., J. Wang, H.Q. Sun, M. Martinez, Y.X. Sun, E. Macia, T. Kirchhausen, J.P. Albanesi, M.G. Roth, and H.L. Yin. 2003. Phosphatidylinositol 4 phosphate regulates targeting of clathrin adaptor AP-1 complexes to the Golgi. *Cell*. 114:299-310.

Waters, M.G., T. Serafini, and J.E. Rothman. 1991. 'Coatomer': a cytosolic protein complex containing subunits of non-clathrin-coated Golgi transport vesicles. *Nature*. 349:248-51.

Watson, P.J., G. Frigerio, B.M. Collins, R. Duden, and D.J. Owen. 2004. Gamma-COP appendage domain - structure and function. *Traffic*. 5:79-88.

Weber, T., B.V. Zemelman, J.A. McNew, B. Westermann, M. Gmachl, F. Parlati, T.H. Sollner, and J.E. Rothman. 1998. SNAREpins: minimal machinery for membrane fusion. *Cell*. 92:759-72.

Wegmann, D., P. Hess, C. Baier, F.T. Wieland, and C. Reinhard. 2004. Novel isotypic gamma/zeta subunits reveal three coatomer complexes in mammals. *Mol Cell Biol*. 24:1070-80.

Whyte, J.R., and S. Munro. 2002. Vesicle tethering complexes in membrane traffic. *J Cell Sci*. 115:2627-37.

Wieland, F.T., M.L. Gleason, T.A. Serafini, and J.E. Rothman. 1987. The rate of bulk flow from the endoplasmic reticulum to the cell surface. *Cell*. 50:289-300.

Wilde, A., and F.M. Brodsky. 1996. In vivo phosphorylation of adaptors regulates their interaction with clathrin. *J Cell Biol*. 135:635-45.

Wilson, D.W., M.J. Lewis, and H.R. Pelham. 1993. pH-dependent binding of KDEL to its receptor in vitro. *J Biol Chem*. 268:7465-8.

Yoshihisa, T., C. Barlowe, and R. Schekman. 1993. Requirement for a GTPase-activating protein in vesicle budding from the endoplasmic reticulum. *Science*. 259:1466-8.

Yuan, H., K. Michelsen, and B. Schwappach. 2003. 14-3-3 dimers probe the assembly status of multimeric membrane proteins. *Curr Biol*. 13:638-46.

Zaremba, S., and J.H. Keen. 1983. Assembly polypeptides from coated vesicles mediate reassembly of unique clathrin coats. *J Cell Biol*. 97:1339-47.

Zerangue, N., B. Schwappach, Y.N. Jan, and L.Y. Jan. 1999. A new ER trafficking signal regulates the subunit stoichiometry of plasma membrane K(ATP) channels. *Neuron*. 22:537-48.

Zhang, J.Z., B.A. Davletov, T.C. Sudhof, and R.G. Anderson. 1994. Synaptotagmin I is a high affinity receptor for clathrin AP-2: implications for membrane recycling. *Cell*. 78:751-60.

Zhao, L., J.B. Helms, B. Brugger, C. Harter, B. Martoglio, R. Graf, J. Brunner, and F.T. Wieland. 1997. Direct and GTP-dependent interaction of ADP ribosylation factor 1 with coatomer subunit beta. *Proc Natl Acad Sci U S A*. 94:4418-23.

Zhao, L., J.B. Helms, J. Brunner, and F.T. Wieland. 1999. GTP-dependent binding of ADP-ribosylation factor to coatomer in close proximity to the binding site for dilysine retrieval motifs and p23. *J Biol Chem*. 274:14198-203.

Zhao, X., T.K. Lasell, and P. Melancon. 2002. Localization of large ADP-ribosylation factor-guanine nucleotide exchange factors to different Golgi compartments: evidence for distinct functions in protein traffic. *Mol Biol Cell*. 13:119-33.

Zhu, Y., B. Doray, A. Poussu, V.P. Lehto, and S. Kornfeld. 2001. Binding of GGA2 to the lysosomal enzyme sorting motif of the mannose 6-phosphate receptor. *Science*. 292:1716-8.

Acknowledgments

First, I want to thank Professor Felix Wieland for giving me the opportunity to work in his lab, and for offering me these projects. I want to express my gratitude for his supervision and patience, constant support and inspiring discussions. He opened up the fascinating and challenging field of biochemistry for me.
Second, I would like to thank Professor Irmgard Sinning for being my second advisor.
I also want to thank Dr. Viktor Sourjik and Dr. Hans-Michael Müller for being in my examination committee.

My thanks go to Dr. Dirk-Peter Herten for introducing me to single-molecule spectroscopy, and allowing me to use the facilites in his lab.

Furthermore, I would like to thank Professor Werner Kühlbrandt for giving me the opportunity to use his electron microscope facilites at the Max-Planck-Institute of Biophysics, Frankfurt.

I am obliged to all members of the Wieland group in Heidelberg, especially Julien Bethune, Jörg Moelleken, Rainer Beck, Stefanie Hubich, Carolin Weimer, Priska Eckert, Michael Geiling, Emily Stoops and Britta Brügger. Only rarely could one hope to find a group of people that are scientifically as critical and encouraging, and form a community that reached far beyond the lab.

I would also like to thank the members of the Herten group for introducing me to single-molecule spectroscopy, especially Christian Roth, Thomas Heinlein and Alexander Kiel.

In my second project, I spent a lot of time at the Max-Planck-Institute in Frankfurt. Here I want to thank Deryck Mills, Janet Vonck and Mike Strauss for teaching me electron microscopy, for their patience and encouragement even when my samples proved to be challenging.

Finally, and most of all, I want to thank my parents.